INSTITUTO SUPERIOR DE ENGENHARIA DE LISBOA

Departamento de Engenharia em Engenharia Mecânica

ISEL

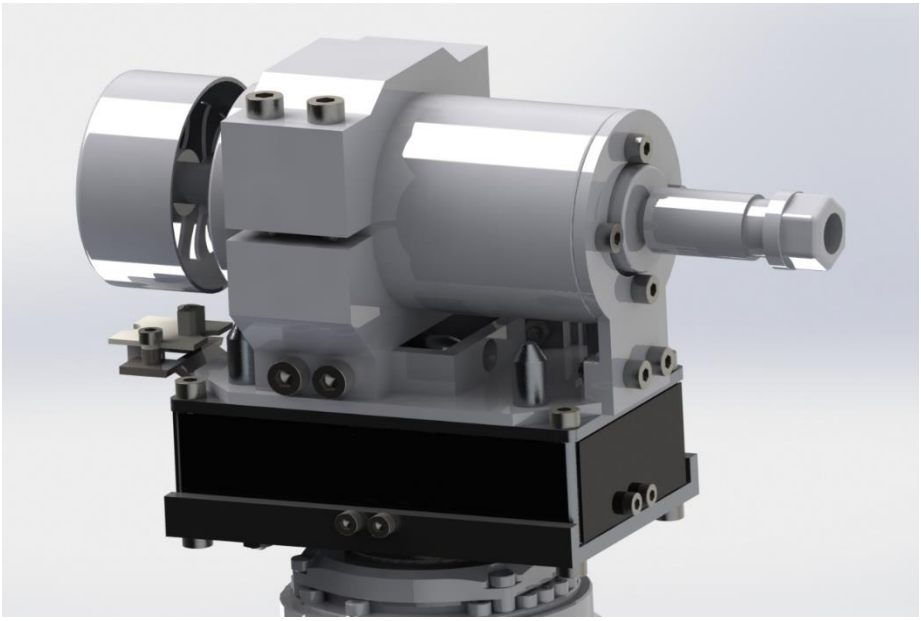

Desenvolvimento de uma Cabeça de Maquinagem para uma Impressora 3D FDM de 5 eixos

VOLODYMYR KOLYUDA
(Licenciado em Engenharia Mecânica)

Trabalho Final de Mestrado para obtenção do grau de Mestre
em Engenharia Mecânica

Orientadores:
Doutor André Rui Dantas Carvalho
Doutor Ivo Ferreira Bragança

Júri:
Presidente: Doutor Silvério João Crespo Marques
Vogais:
Doutor João Filipe de Almeida Milho
Doutor André Rui Dantas Carvalho

Janeiro de 2021

INSTITUTO SUPERIOR DE ENGENHARIA DE LISBOA

Departamento de Engenharia em Engenharia Mecânica

ISEL

Development of a Machining Head for a 5-axis 3D FFF Printer

VOLODYMYR KOLYUDA
(Mechanical Engineering Graduate)

Final Work for master's degree
in Mechanical Engineering

Supervisors:
Doutor André Rui Dantas Carvalho
Doutor Ivo Ferreira Bragança

Jury:
President: Silvério João Crespo Marques PhD
Elements:
João Filipe de Almeida Milho PhD
Doutor André Rui Dantas Carvalho PhD

January 2021

Acknowledgments

I would like to thank my two supervisors André Dantas Carvalho and Ivo Bragança for helping me accomplish this project and teaching me several important concepts for my professional life, my parents who helped me and provided conditions for my studies and finally, my friends which gave me good memories and support during the development of this thesis.

Also, I thank ISEL and the teachers that developed my interest in engineering.

Resumo

Atualmente as tecnologias de manufatura aditiva estão em crescente desenvolvimento e aplicadas em diversas áreas. Esta rápida expansão requer numerosas abordagens de produção e adaptação quanto à taxa de produção das peças.

Dentro das diferentes tecnologias de manufatura aditiva a que possui um maior relevo atualmente, é a deposição de filamentos fundidos devido à disponibilidade de máquinas compatíveis, custo e simplicidade de conceito.

Muitas vezes os requisitos para este tipo de fabrico consistem em grande qualidade dimensional para aplicações específicas. Por exemplo, algumas marcas de automóveis utilizam peças impressas com deposição de filamentos fundidos para segurar e centrar os logótipos e encaixes das matrículas. Esta tarefa requer tolerâncias apertadas para que as peças manipuladas encaixem nas peças de centragem.

Foi proposto um projeto para uma célula robótica com a função de deposição de filamentos fundidos e maquinação a partir de qualquer orientação e com tolerâncias dimensionais e de superfície requeridas. Esta célula é composta por um robô de 5-eixos com uma cabeça removível.

Este robô necessita de trocar automaticamente a cabeça entre as funções de impressão e maquinação, ou seja, esta tarefa tem de ser efetuada sem intervenção humana.

Este projeto tem o foco na cabeça de maquinagem para o robô e o mecanismo que vai permitir a troca automática entre maquinagem e impressão.

Palavras-chave: Robótica, Prototipagem, Maquinação, Impressão 3D, Ferramenta robótica automática, Simulação, Projeto, Pós-processamento, ABS, PLA, Acrilonitrila butadieno estireno, Poliácido láctico, Célula Robótica

Abstract

Currently, the Additive Manufacturing (AM) technologies are rapidly developing and being applied in various fields. This rapid expansion to so many different branches of manufacturing requires different production approaches and rates at which parts are produced.

Currently, one of the most used AM techniques is the Fused Filament Fabrication (FFF) due to hardware availability, cost and concept simplicity.

Many times, requirements demand high dimensional fidelity for specific applications. For example, some car manufacturers use FFF printed parts for holding and positioning of brand and model badges and registration plates. This requires a higher dimensional tolerance for fitting the said parts in the printed part.

Knowing this, it was proposed a project for an FFF printing robotic cell which could print desired part from any orientation and machine accordingly to the required dimensional and surface finish tolerances. This cell is mainly composed of a 5-axis robot with an exchangeable head. This robot must have the ability to autonomously exchange its head between printing and machining applications, or in other words, change productive capabilities without physical human intervention.

This project focuses on the machining head for the robot and the mechanism that will allow the robot to meet the set requirements.

Keywords: Robotics, Rapid Prototyping, Machining, 3D Printing, Autonomous Robot Tool, Simulation, Project, Post Processing, ABS, PLA, Acrylonitrile-Butadiene-Styrene, Polylactic Acid, Robot Cell.

Abbreviation List

3D	Three Dimensional
5D	Five Dimensional
ABS	Acrylonitrile butadiene styrene
AM	Additive Manufacturing
CAD	Computer Aided Design
CAM	Computer Aided Manufacturing
DOF	Degree of Freedom
FDA	Federal Drug Administration
FFF	Fused Filament Fabrication
FRP	Fiber Reinforced Plastic
HDPE	High-density polyethylene
LM	Lower Mechanism
LSM	Linear Stepped Motor
MH	Machining Head
NC	Numerical control
PLA	Polylactic acid
PMMA	Polymethylmethacrylate
PVA	Polyvinyl alcohol
RP	Rapid Prototyping
SCARA	Selective compliance assembly robot arm
SLA	Stereolithography
SLS	Selective Laser Sintering
STL	Stereolithographic File
Tg	Glass Transition Temperature

Contents

Figure Index

Table Index

1. Introduction

This chapter describes the motivation for this dissertation, defines objectives that were previously selected and others that came during development and explains the structure of this dissertation.

1.1 Motivation

While having many advantages, 3D-printing has some challenges to overcome. Specifically, fused filament fabrication that consists on the deposition of fused material layer by layer until the final geometry is achieved, has difficulty in replicating computer aided design (CAD) files with enough quality for demanding applications as the piling of layers creates sway in the surface of printed parts and temperature variations leave irregularities on the part. Also, the post-processing of printed parts can be time demanding.

To face these challenges, it was proposed a hybrid manufacturing station which consists on a medium sized robot with printing and machining capabilities. This dissertation focuses on the machining mode of this robot.

With a successful application of this dissertation, it is pretended to create a viable solution that retains many 3D printing advantages, harnesses some strong points of machining for an optimal dimensional accuracy and provides finished parts at a higher rate.

1.2 Objectives

With this dissertation it is pretended to design a viable solution for a machining head of a given robot with hybrid 3D printing/machining capabilities. This robot will be installed in a robot cell for the purpose of creating finished and ready to be installed parts from scratch.

The robot must be able to automatically attach to the mentioned machining head and the functionality and safety must be guaranteed while the robot and the head are docked. The robot cell mentioned before is for Acrylonitrile butadiene styrene (ABS) and Polylactic acid (PLA) part manufacturing, so the machining head must be capable of cutting these materials.

While in operation, the head must withstand different solicitations such as forces originated from rapid robot movement and cutting.

To assure functionality the components should provide reliable operation and maintain their purpose for multiple cycles.

The construction design, function and possibility of future modifications for further applications will be analyzed.

Successful results could be used for further 3D printing technology development and place this solution as a competitive manufacturing process for a variety of different industries and applications.

1.3 Structure

This dissertation is divided in to six main chapters. The Introduction will give an initial insight in the subject and define objectives. Literature Review has some relevant information on similar work, relevant technology topics and enlightenment on different topics. Methods will explain the development of the project. The Results chapter has the product of the adapted methods and some improvements on the initial concept. Discussion chapter will provide critical interpretation of the results and an evaluation of proposed objectives. And finally, the Conclusion will resume all the information mentioned in previous chapters and give some advice for further improvement and future work.

2. Literature Review

This chapter will address relevant topics for this dissertation according to their scientific value, actuality and other criteria. Some of the mentioned topics will be more developed that others depending on their connection to the focus of this dissertation.

2.1 Historic Notes for 3D Printing

Three-dimensional printing (3D printing) or additive manufacturing (AM) is a continuous developing technology that has been around for decades. The first 3D printer was created in 1984 by Charles W. Hull. The equipment was named "Apparatus for Production of Three-Dimensional Objects by Stereolithography" on March 11, 1986. And it was the precursor for the Stereolithographic printing (SLA). Mr. Hull was also one of the first to develop a way of CAD parts communicate with rapid prototyping (RP) systems to create computer generated parts. For this purpose, CAD models would be sliced into multiple layers and replicated by the printing apparatus [1].

SLA consists in the photosensitive resin solidification recurring to a laser. It uses a computer-controlled mirror to direct a laser in order to create successive cross sections, obtained through CAD of a desired part. When a section is complete the resin container lowers to allow the deposition of additional resin over a finished section [2].

During the same time period, Carl Deckard and Dr. Joe Beaman started working on a technology known as selective lase sintering (SLS). This process uses powder from different materials as resource to crate parts. The powder is selectively sintered by a laser. Deckard and Dr. Beaman started to work on SLS in 1984 and build the first printer by 1986. In 1989 they made the first commercial SLS printers called Mod A and Mod B. They continued to improve their creation until their company was sold to 3D Systems in 2001 [1].

Other types of 3D printing started appearing in the world as the processes that existed developed. One of them had Scott and Lisa Crump as creators. This process was designated as fused filament fabrication (FFF). It works by heating filaments to a semi-liquid state and extruding it to a surface, layer by layer. Both started a company Stratasys, Inc. that is still growing while having a large range of printer models in lineup [1].

This technology is rapidly developing and nowadays reached new standards. Some printing technologies can print at a molecular level (two-photon polymerization, which

uses femtosecond pulsed lasers to fuse a powder) and others can even build concrete houses and structures.

2.2 Additive Manufacturing

AM consists in the continuous addition of layers of a given material by a 3D Printer until a final product is formed [3]. The concept of adding layers is transversal to all 3D printers but the technology used to deposit layers differs according to the used material and AM type. The most common types of AM are FFF, SLS and SLA.

In most AM types, the part geometry is defined using 3D modeling software (CAD) and saved as a stereolithographic file (STL). Then this file is read by a 3D Printer and it starts the construction of each layer until the final geometry is achieved [4].

2.3 Types of AM technologies

This subchapter will develop the basis behind the mentioned AM types. To simplify reading, the explanation and concepts will be narrowed to the three main AM types.

2.3.1 Selective Laser Sinthering

SLS is an AM process in which a laser is used to heat powder (sinter) in order to consolidate it layer by layer until a final shape is formed. The SLS printer uses code from the CAD of the desired part to create slices of it. The laser follows a specific path to join the powder to create a cross section of the part. When a layer is finished, the powder tray is lowered, depositing more powder over the finished layer, and the process continues until the part is complete [5].

This technology has many uses like the production of a hydrophobic membrane [6]. In this study coated polyamide-12 particles were used in a SLS process to obtain super oleophobic and hydrophobic membranes. This material maintains the hydrophobic properties even after 7-day solvent treatment and abrasive cycles with sandpaper.

One other application consisted in the use of SLS Nylon (PA12) to print knit structures [7]. This study proved that is possible to SLS print tubular knit-based structures that possess stretch and extensibility of tradition made knitted textile structures while having properties of the base material.

A micro SLS process to manufacture metal three dimensional parts with micro features while controlling the microstructure of materials [8]. With the use of micro-mirror array, it is possible to micron scale details with a theoretical build speed of up to 2 cm3/hr.

2.3.2 Stereolithography

Stereolithographic manufacturing consists in the photosensitive resin solidification recurring to a laser. It uses a computer-controlled mirror to direct a laser in order to create successive cross sections, obtained through CAD, of a desired part. When a section is complete, the resin container lowers to allow the deposition of additional resin over a finished section [9].

There are a lot of implementations for this technology like the fabrication of lead-free KNN piezoceramics using the principle of photopolymerization of high solid loading ceramic suspensions [10]. According to their research further improvement can be made to the properties of obtained piezoceramics for their integration in different devices.

There are also several instances of using SLA to conduct tissue reconstruction and other medical applications [11] like:

- Rapid orthosis and prosthesis preparations
- Anatomical modeling
- Inert implants
- Biofabrication

Instances of digital light processing in SLA has been used in the manufacturing of tricalcium phosphate for bone regeneration [12]. The resulting tricalcium phosphate is biocompatible and has a high relative compressive strength when in Grid structure.

2.3.3 Fused Filament Fabrication

FFF differs from other additive manufacturing processes in the way it uses filaments that are pushed through a heated extrusion nozzle in order to melt them and selectively deposit the material, creating cross sectional layers of the final part. The different layers are created due to the coordinated movement of the extrusion head and the building plate. Some FFF printers have extrusion heads with multiple nozzles, allowing the deposition of multiple types of materials simultaneously [13].

Depending on the part geometry, the part can be printed with supports. These supports can even be water soluble and have little to no one impact on the part overall quality [14]. Furthermore, these supports are usually made with Polyvinyl Alcohol that can be made with low energy consumption and pollution, after degrading is nontoxic and splits in to carbon dioxide and water [15].

The quality of products produced by FFF depends on the various printing parameters like layer thickness, slice height, tip diameter and air gap [13].

Different types of improvements were made to FFF during the years if its development. A study demonstrated that is possible to print full lithium ion batteries with low cost filaments by modifying the used polymer of PLA [16]. According to them, with further improvement it is possible to print materials that have better conductive properties than the current ion lithium batteries.

Other study showed that it is possible to create filaments for medical drugs [17]. In this study the authors discovered that FFF has the capability to achieve active pharmaceutical ingredients loadings like other traditional oral solid dosage methods like wet granulation.

Research demonstrated that FFF methods can be used to manufacture thermoelectric materials for energy conversion applications thanks to low cost, easy of application and thermoelectric properties [18]. Alongside these advantages there are also the possibility to create complex geometrical shapes that are difficult to replicate by the traditional methods. Complex form can be applied to new types of heat exchange applications, opening new possibilities.

As the focus of this project FFF will be explained in greater detail to explain all relevant additional information regarding printing.

2.3.3.1 Materials in FFF

There is a wide variety of materials used in FFF. The material selection highly depends on the application of the part. Mostly, the used materials are ABS, polyamide, polyesters, polycarbonate, polyethylene, and polypropylene. There are other materials used for special applications like silicon nitrate, lead zirconate titanate aluminum oxide and stainless steel [19].

As the main materials used for printing for this project will be ABS and PLA, they will be focused in more detail.

ABS is thermoplastic which means that this material can be heated, melted, and cooled several times without significant properties degradation. These properties make recycling ABS very easy [20].

The most common way of making ABS is through the process of emulsion. Emulsion is mixture of two or more liquids that are normally immiscible [21]. There is also another way of producing ABS designated by continuous mass polymerization. Due to its recyclable nature, ABS can come from other used ABS parts that were melted [22].

For some applications, attention must be given to the glass transition temperature (Tg). This temperature is found bellow the melting temperature of the material and between them, the material is in a viscous liquid state with different properties [23].

PLA is a polymer fabricated with renewable sources. Raw materials for PLA include starch, tapioca roots and sugarcane. Even though it has no petroleum in its composition, it has similar properties to other commonly used petroleum-based plastics.

Some of the advantages of PLA include being biodegradable because it goes through a transformation into water, carbon dioxide and composite, it is a thermoplastic like ABS so it can be melted and reshaped without property loss as well. When it burns it does not release toxic fumes and it is FDA approved for food applications [24].

The following table shows some relevant ABS and PLA average properties:

Table 1 - ABS [22] and PLA [23] properties

Properties	ABS	PLA
Density [g/cm3]	1.08	1.29
Tensile Strength [MPa]	38	47.2
Modulus of Elasticity [GPa]	2.06	2.91
Glass Transition Temperature [ºC]	108	52
Max. Service Air Temperature [ºC]	84.3	180

2.3.3.2 Printing Parameters in FFF

One way of controlling the printing process is the modification of printing parameters that are usually imbedded in the printing software. Knowing the function of every parameter is a necessary for ideal results, because they not only can change the dimensional accuracy of the part, but also assure that it has structural rigidity.

Infill density – percentage of material inside the part volume. When this value is lower that 100%, the rest of the volume is hollow. If a part has 100% infill, it is solid and if it has 0% it is completely hollow.

Extrusion temperature – material temperature in the nozzle during extrusion.

Raster angle – angle of material orientation inside the printed part.

Layer thickness – height of each slice of deposited material. Lower values of this parameter give better finish but takes more time to accomplish the same volume as a part with higher thickness. The opposite occurs for higher thickness [25].
velocidade

2.3.3.3 Applications

This technology has various applications due to its speed and range of materials. Some of these applications include industries like aerospace, automotive, healthcare and medical, and food.

2.3.3.4 Advantages

This technology has considerable advantages over traditional production methods like subtractive manufacturing. Some of these advantages can be simplified by the following [26];

- **Highly customizable**

The printed part comes directly form CAD file, so any last-minute change in the design is far easier than in traditional methods. Usually, traditional methods require code adaptations and changes in the production steps.
Also, the material of the part can be altered in case of necessity without scrapping the whole process. Mostly, the only thing that needs change in case of material alteration in FFF is the filament extrusion temperature.

- **Fast production**

Traditional methods are limited by the production process, which needs to be rigorous and precise for optimal results. FFF does not depend on production plans, so most of the preparation time is saved allowing faster production for small batch sizes. If the desired part is standardized, traditional methods gain an advantage over the FFF, because generally cutting processes are faster when established. Also, as the manufacturing can be done near the end of production, the final part can be closer to the client and this can save time and logistic resources.

- **Material savings**

Due to the nature of FFF printing, the is less material waste compared to traditional methods. Generally, only the needed material is used in additive manufacturing. This demonstrates that FFF printing is more sustainable and environment friendly.

- **No tools needed**

Production of desired parts is done through an extruding nozzle. Having correct parameters and material is the main physical limitation. In traditional methods a single part can be obtained using multiple different tools. This fact limits the obtainability of some parts in case of missing tools and requires investment. With FFF it is only required a printer and filaments.

2.3.3.5 Limitations

Even though this technology has many advantages over the traditional methods, there are still several limitations in its current form. The most relevant are listed below [27];

- **Dimensional**

Even considering all benefits of FFF, there are some limitations to this type of printing technology. One of them is the dimensional accuracy of the part. This limitation is inherent to the printing process because not only the stacking multiple layers will always leave a characteristic sway, resembling stairs, on the side of the product, but also the temperature difference will make the cooling irregular, making the final dimensions slightly different from the ones imported via CAD file.

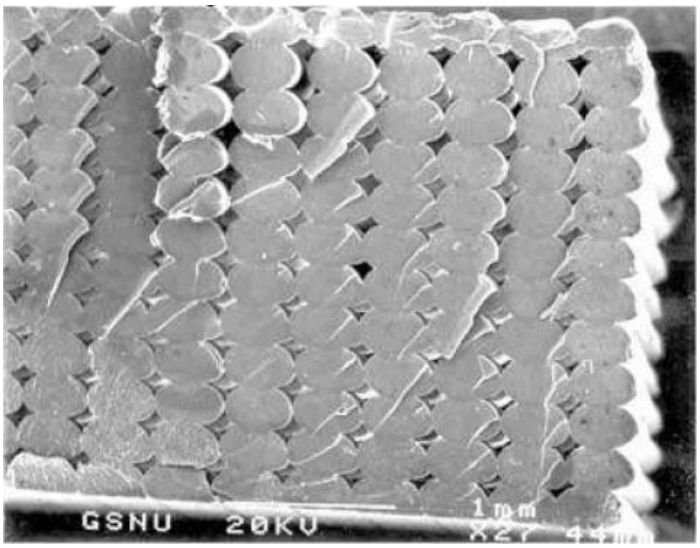

Figure 1 - Amplified structure of a printed component [28]

Usually the faces that are parallel to the printing plate have better surface roughness. This happens because the stair like geometry only appears on surfaces that are perpendicular to the printing plate.

- **Structural**

Also, this AM type needs stable and secure deposition surfaces. If the part has an overhanging feature according to the printing orientation, the part can collapse. To mitigate this fact, usually the printing software includes support functions that provide the desired fixation of the part and allows the deposition over overhanging portions.

The mentioned supports usually are created alongside the desired part and with the same material. Nowadays, some FFF printers have double extrusion nozzles and that allows the usage of two different materials simultaneously. This contributed to the use of water-soluble materials, like polyvinyl alcohol (PVA) for the material of support structures. PVA has the advantage of being soluble with water, allowing easier support removal without the risk of damaging the part.

Also, since layer orientation will influence the way the air gaps are distributed inside the printed part, FFF printed parts always have some degree of anisotropy in their mechanical properties. This is even more evident when machining is performed in infilled volumes of the part.

Other type of defect can appear due to lack of printing plate adhesion. This can cause dimensional warping in the printed part. This phenomenon occurs due to several reasons like unleveled platform, low heat platform, low heat filament and dirty platform [29] [30]. This defect can be prevented by cleaning the platform, assuring proper filament and platform temperature and usage of stick glue or decorator tape.

2.3.3.6 Overcoming Limitations

To overcome the dimensional limitation a solution was proposed. This solution consists on the application of machining for the finishing treatment of 3D printed parts. The objective is to use the dimensional precision of machining on 3D printed parts. To explain this application a brief introduction into machining is presented.

2.4 Machining

Currently, machining is defined as controlled processes, by a power tool, that cuts raw material into a desired shape with defined dimensions. In its essence, it is a material removal process. Due to the emergence of additive manufacturing, this kind of processes became known as subtractive manufacturing [31].

Under the concept of machining, according to Michigan Technological University, exist the following categories [32]:

- Cutting, involving single or multipoint tool, each with a defined geometry
- Abrasive processes, such as grinding
- Nontraditional processes (water jet cutting, other processes)

From the latter, abrasive cutting uses grinding and erosion as a method or material removal. This is accomplished using an abrasive tool with small cutting particles imbedded in it. The particles used to cut the material are worn off, exposing new particles, and maintaining a ready cutting face [33].

Other articles categorize machining in to three main classes [34]. These are turning, drilling, and milling with other operations falling on other subcategories.

Drilling (*figure 2*) consists on the use of a pointed helical cylinder to open a hole in the workpiece. The material that was in the hole location is removed to the helical design of the tool.

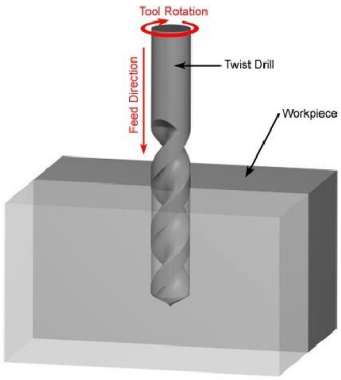

Figure 2 – Drilling process representation [35]

Turning (*figure 3*) operates by removing material with a stationary tool while the workpiece rotates. The outside diameter of the workpiece is being worked on in this type of operation. The workpiece is fixed to the spinning axis by an adjustable chuck.

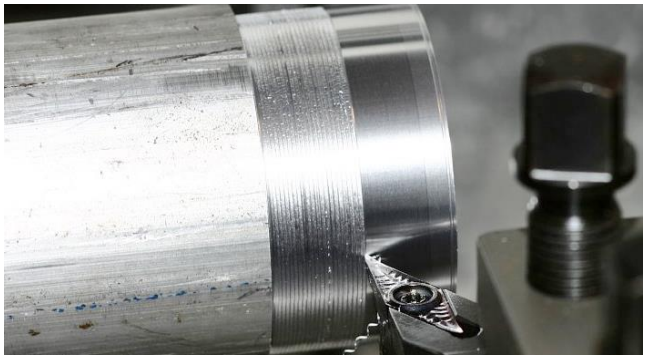

Figure 3 – Turning process representation [36]

Milling (*figure 4*) is a type of machining in which a tool with multiple sharp edges spins to remove material from the workpiece. This rotation is provided by mounting the tool on to a spindle and several complex geometries are achievable thanks to relative movement of multiple axis, normally 3 or 5. The excess material is removed in chip form and a large variety of materials can be used. Some of the materials are metals, wood, composites, and plastics [37].

Figure 4 – Milling process representation [38]

Numerically controlled (NC) milling is a category of machining, which consist in one or more tools being driven by a machine tool along a programed path, known as tool path, to obtain final geometry of the working piece [39].

During this process, the work piece transforms from initial work piece to final work piece. It differs from traditional milling through machine control. NC milling performs tasks that were programmed, so the process is automatic and repeatable. While traditional milling requires a machine operator to perform different operations.

As milling processes are the focus of this dissertation, a deeper explanation on this machining operation will be given.

2.4.1 Milling Machine Types

One form of categorization of milling machines is the number of degrees of freedom (DOF). DOF in a milling machine is defined as the number of axis that the tool can move along. The more common types of milling machines have three DOF (*figure 5*).

Figure 5 - Three-Dimensional Milling Machine [35]

The machine in the last figure represents a three-dimensional milling machine. It can operate along three paths, x, y and z, in order to create the desired part.

More complex milling machines can operate with more DOF. For example, the next machine has five DOF (*figure 6*).

Figure 6 - 5D Milling Machine [36]

This type of milling machine not only can operate in the mentioned 3 axes, but also can tilt the tool in two more, making this machine a 5-axis milling machine.

2.4.2 Types of operations in milling

Different types of operation can be performed in milling. The following operations are the ones that are supposed to be possible by the resulting machining head of this project.

Face Milling

In face milling (*figure 7*) the surface that is being cut is perpendicular to the cutter axis. This operation produces flat surfaces, and the feed is either horizontal or vertical. Generally, the peripheral teeth do most of the cutting. Like in other types of operations the cutter and the workpiece must be steadily attached to eliminate relative movement during machining [40].

Figure 7 - Face milling operation [41]

Holes/Drilling

This process (*figure 8*) uses a drill bit to cut a hole with a circular cross section in the work piece. The drill bit is attached to a rotary toll and mostly has multiple cutting surfaces. Material is removed in chip form during hole formation [40].

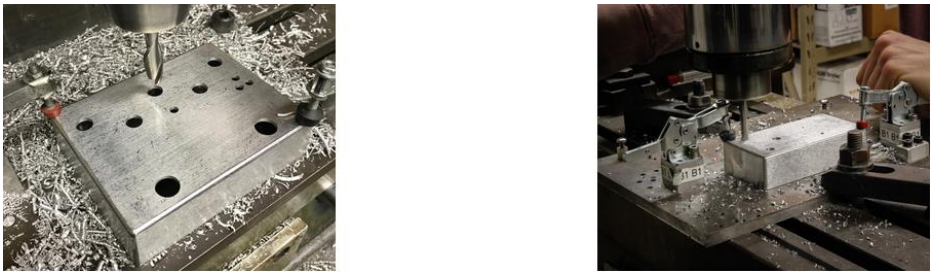

Figure 8 - Drilling operations [42]

End Milling

End milling (*figure 9*) differs from other types of milling in the fact that it uses slightly different type of tooling to cut a given material. It uses cutting teeth on the sides and on the end mill. Some of the applications for this this type of tooling are profile milling, tracer milling, shape milling and plunging [43].

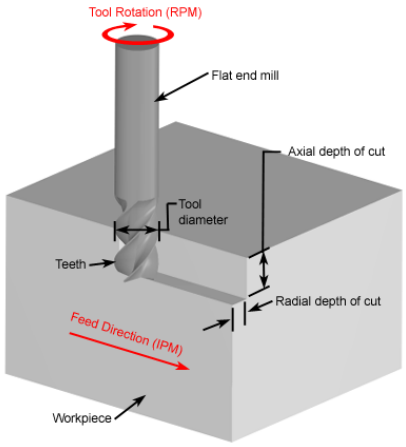

Figure 9 - End milling operation [44]

Milling requires different types of tools according to piece material and geometry and the desired operation. Usually, milling tools have multiple cutting surfaces through which, material is removed in form of chips.

Examples of these tools are roughing end mill, slab mill cutter, end mill, hollow mill, and ball mill [45].

Milling parameters are the specific values that describe how a work piece is cut. Depending on the piece material, fixation equipment, tool type and material, and other factors, each of the parameters needs to be adjusted for optimal results in part quality, time and tool wear. Some of them are:

Cutting speed (Vc)

Speed of cutting surfaces at which material is removed from a workpiece [46]. It can be represented by a vector tangential to the radius of the rotary tool.

$$v_c = \frac{\pi * CD_{depth} * n}{1000} \ (m/min) \qquad \textbf{(1)}$$

In this equation CD_{depth} represents cutting diameter at a cutting depth in mm and n represents spindle speed in rev/min.

Feed per Tooth

Used to obtain table feed and it is calculated by the maximum chip thickness for a given material and operation [46].

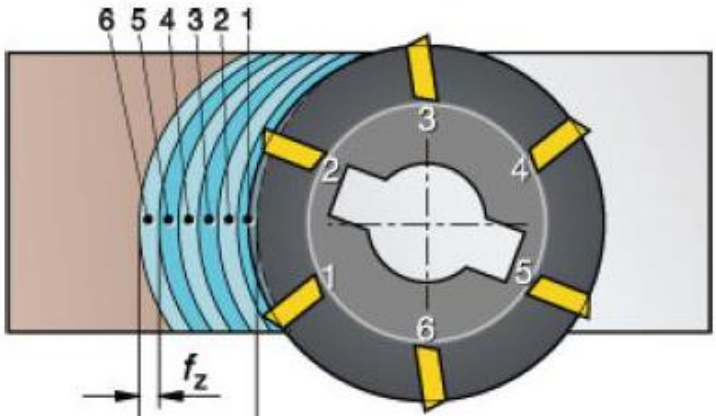

Figure 10 - Feed representation [41]

$$f_z = \frac{v_f}{n * z_c}\ (mm) \qquad \textbf{(2)}$$

Here, v_f represents table feed, z_c is the number of cutting teeth and n is the spindle speed in rpm.

Material Removal Rate

Rate of material removal from a workpiece. It is established by the table feed (v_f) in mm/min, depth of cut (ap) and width (a_e) both in mm [46].

$$Q = \frac{ap * a_e * v_f}{1000}\ (cm^3/min) \qquad \textbf{(3)}$$

Cutting Power

Effective power needed to perform a cutting operation (Pc). It depends on the depth of cut (ap), cutting width (ae), table feed (vf), specific cutting force (Kc) and machine efficiency (ɳ) [47].

$$Pc = \frac{ap * ae * vf * Kc}{60 * 10^6 * \eta}\ (kW) \qquad \textbf{(4)}$$

Ap and ae in mm, vf in mm/min, Kc in MPa and ɳ in % of machine efficiency.

Specific Cutting Pressure

This variable depends on the kc1. It is the force needed to cut a chip with an area of 1mm² and a thickness of 1mm. This value also depends on the rake angle of the tool ($\gamma 0$) that is being used. And the mc is the ratio between kc1 and chip thickness (hm) [48].

$$Kc = kc1 * hm^{-mc} * \left(1 - \frac{\gamma 0}{100}\right) (N/mm^2) \quad \textbf{(5)}$$

2.4.3 Cutting force

Cutting forces are forces originated from the machine tool removing material from a workpiece. Generally, it has two variations, the primary and secondary cutting forces. The primary cutting force is solely created by the relative movement between the cutting tool and the workpiece. The secondary cutting force are residual force originated by the primary forces; it usually manifests as vibration during machining [49].

From equation 4, a simplification can be made to obtain the cutting force Fc with the Kc of a given material. This equation can be described as follows:

$$Fc = ap * ae * Kc\ (N) \quad \textbf{(6)}$$

Where Fc is in N, ap and ae are in mm and Kc is in N/mm².

The magnitude of cutting forces in machining highly depends on the material being cut. Softer materials offer less resistance to the cut so consequently they have inferior cutting forces. As the materials that will be machined during this project are ABS and PLA, the research for cutting forces will be conducted on plastics and other with similar properties. The materials that will be machined in this project are ABS and PLA so a deeper research on forces, developed during plastics machining, is needed.

ABS and PLA are some of the most popular materials for 3D FFF printing. They are widely available, relatively cheap and have good properties for many applications. To the author's knowledge there are no records of specific studies regarding machining forces in these materials. To overcome this obstacle other materials with similar properties were evaluated, namely thermoplastics, polymers, and composites.

Patel [50] in his dissertation studied the behavior of different polymers to cutting. The main materials that were used are Polymethylmethacrylate (PMMA) and tubes of 4/6 and 6/12 Nylon. In his experiment a testing rig (*figure 11*) was built to perform cutting test on different specimen.

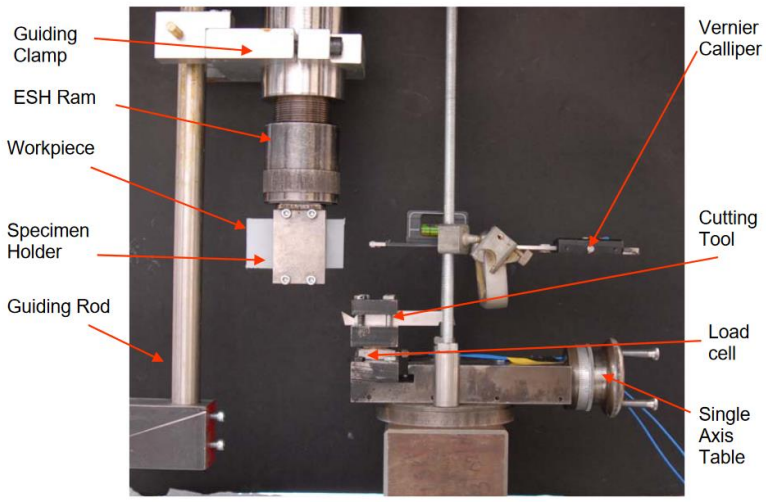

Figure 11 - Orthogonal cutting test rig [50]

For Nylon tests, the following results were obtained by the orthogonal cutting:

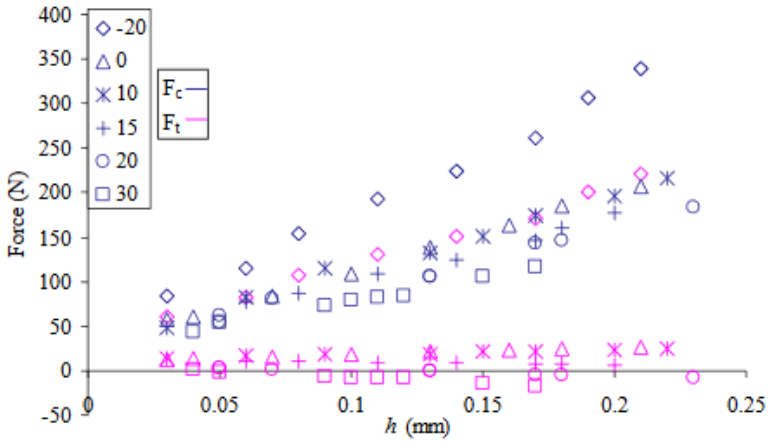

Figure 12 - Cutting (Fc) and normal (Ft) forces during the steady state cutting of Nylon 4/6 for different rake angles at a rate of 0.01m/s [50]

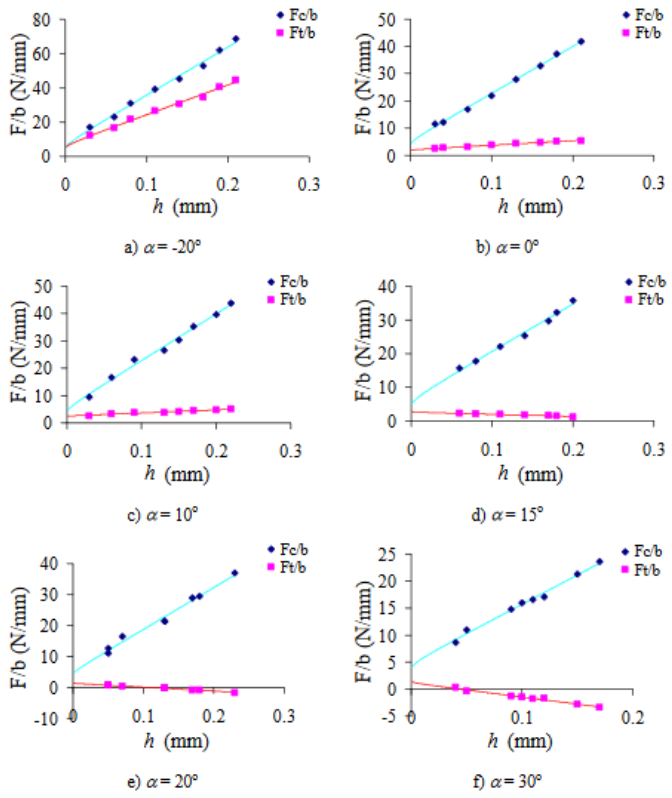

Figure 13 - Experimental data points and theoretical values of F_c/b and F_t/b for nylon 4/6 for each rake angle at a cutting speed of 0.01m/s [50]

With this study is possible to observe the behavior of a polymer, in this case Nylon, to cutting. Negative rake angle resulted in higher normal forces as the depth of cut is increased. But increasing the rake value resulted in a change of resultant force orientation from positive to negative (from pushing the specimen to pulling it) (*figure 12*). In the next plot (*figure 13)*, several forces over distance values were obtained and plotted against h that is cutting depth. The blue dots represent cutting force over distance readings and the pink dots are normal forces over distance. With these results, it is possible to obtain theoretical values for specific cutting pressure (dividing F/b values by cutting depth). Although, these values vary to milling because this study reflects orthogonal cutting, as it was mentioned.

A research for machining forces in milling of carbon fiber reinforced plastics was conducted in the University of Cassino and Southern Lazio [51]. For this, a 15 kW and 15000 rpm CNC milling machine was used. The cutting was done without lubrication and multiple cutting speeds were utilized.

The orientation of cutting forces follow the represented axis.

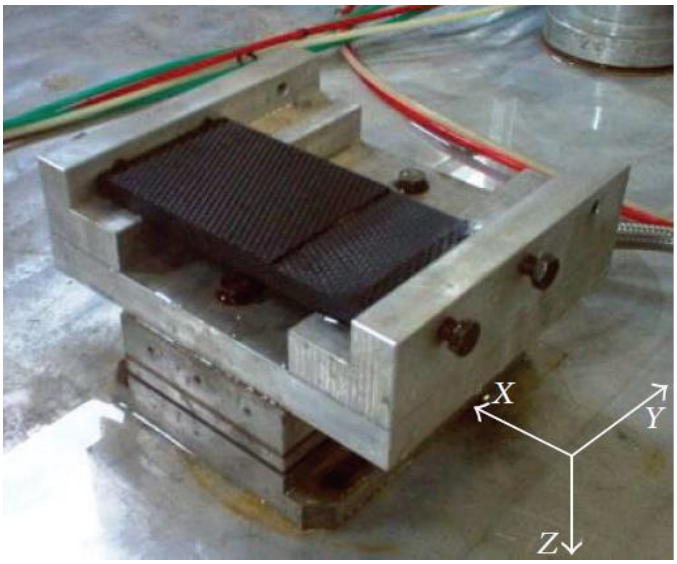

Figure 14 - Experimental setup with axis [43]

With the different parameters the following plots were obtained for the forces during machining.

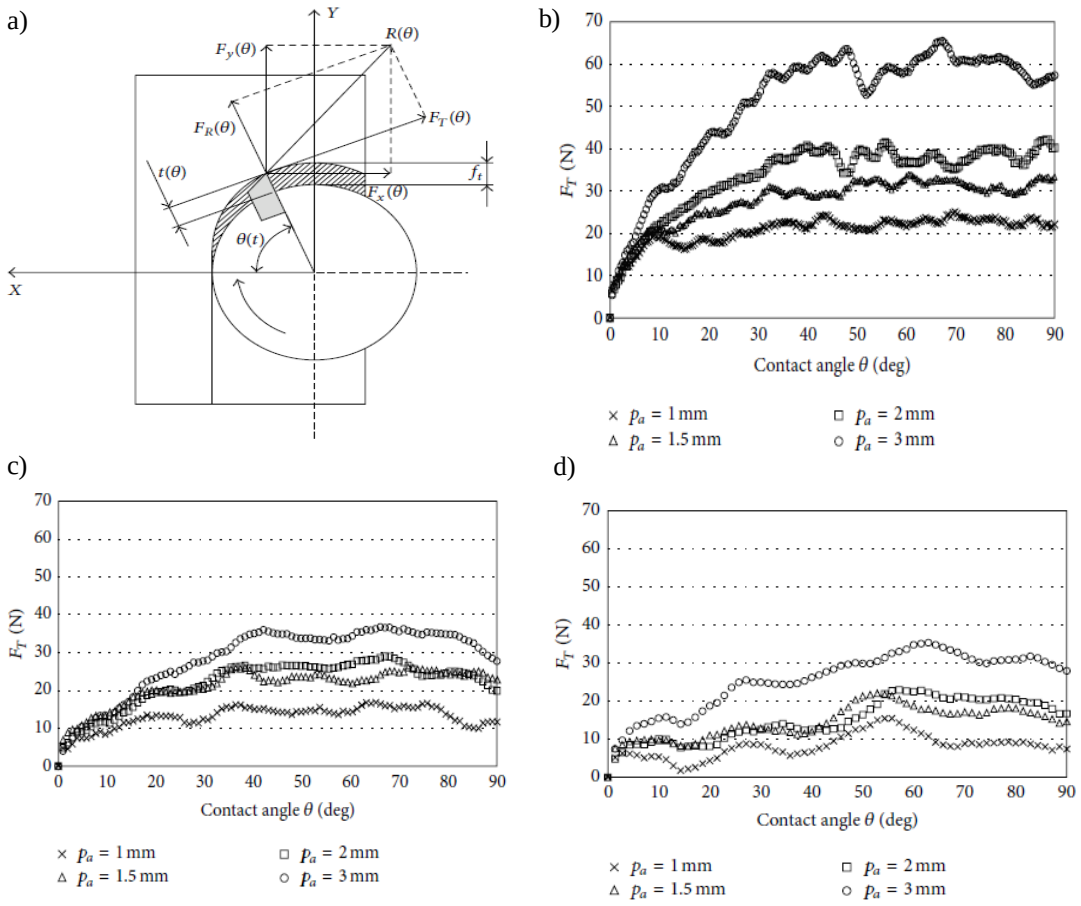

Figure 15 - a) Representation of tangential and radial force components, Tangential force vs contact angle with feed per tooth = 0.022mm and cutting speed = b) 100 m/min, c) 200 m/min, d) 300 m/min [50]

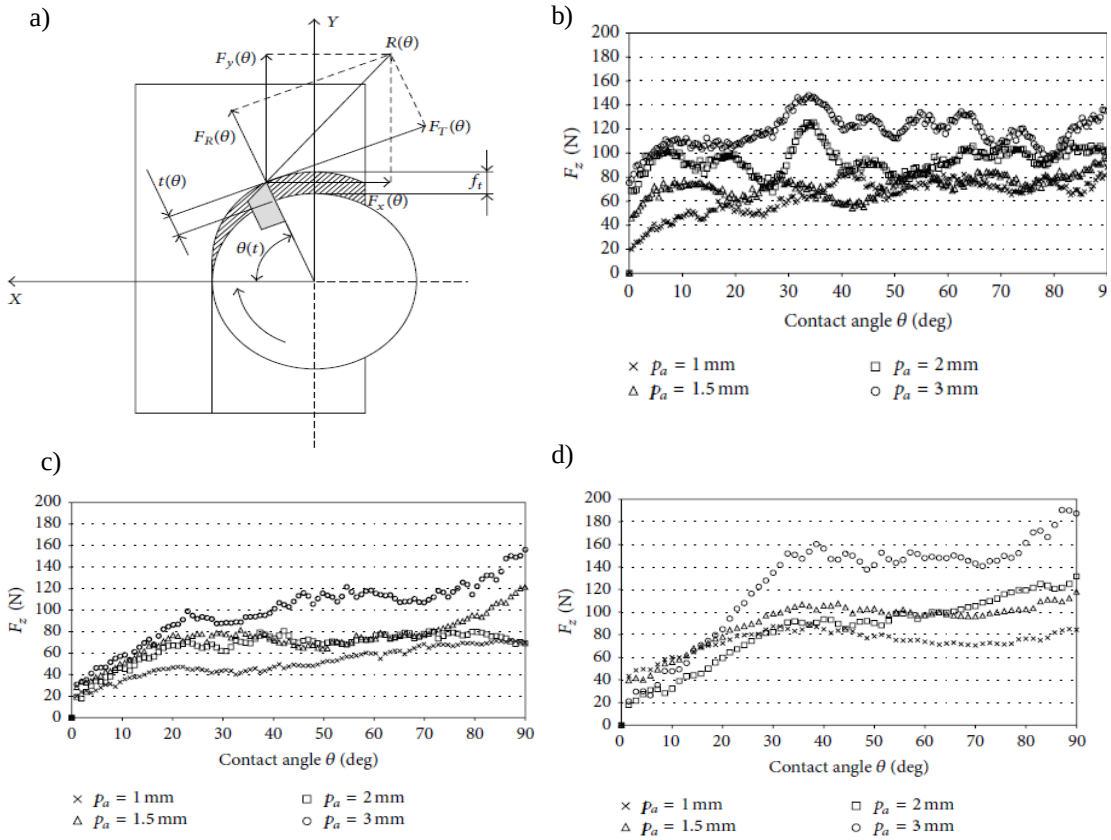

Figure 16 - a) Representation of tangential and radial force components, Fz component vs contact angle with feed per tooth = 0.044 mm and cutting speed = a) 100 m/min, b) 100 m/min, c) 100 m/min [50]

Broadly, the cutting force Ft decreases with increased cutting speed (*figure 15*). The Fz components plots (*figure 16*) shows that increasing the "pa" that is the cutting depth, increases the axial forces and that the force increases rapidly with contact angle (30º) and then tends to stabilize. After the experiments it was verified that increased axial depth increases surface roughness and a higher cutting speed decreases surface roughness. From this study is possible to use these values for this dissertation as the conditions are similar to the proposed dissertation conditions.

Another study explored the modelling of machining forces in plain woven carbon fiber-reinforced plastics [52]. They used a force coefficient approach to create an approximate model for machining forces. The experiment was performed according to the following figure (*figure 17*).

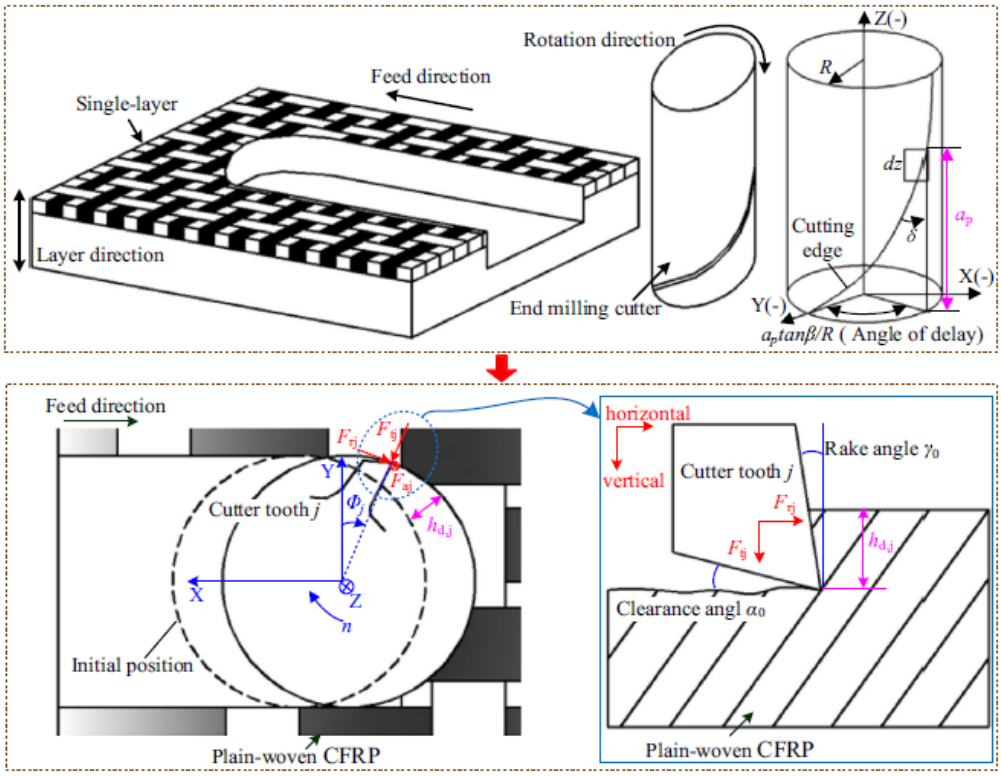

Figure 17 - Milling force model [52]

The following figures (*figure 18 and 19*) represent a comparison between theoretical model and experimental results for Fx and Fy milling forces.

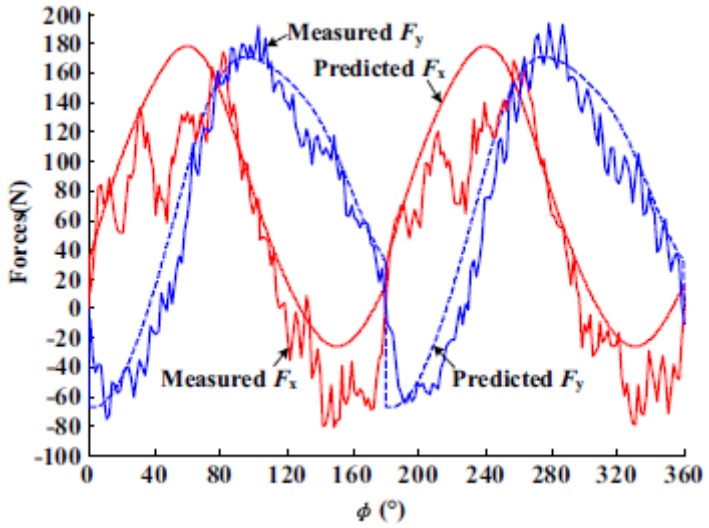

Figure 18 - Predicted milling forces in Vc=109 m/min, fz=0.18 mm/tooth, ap=2 mm [52]

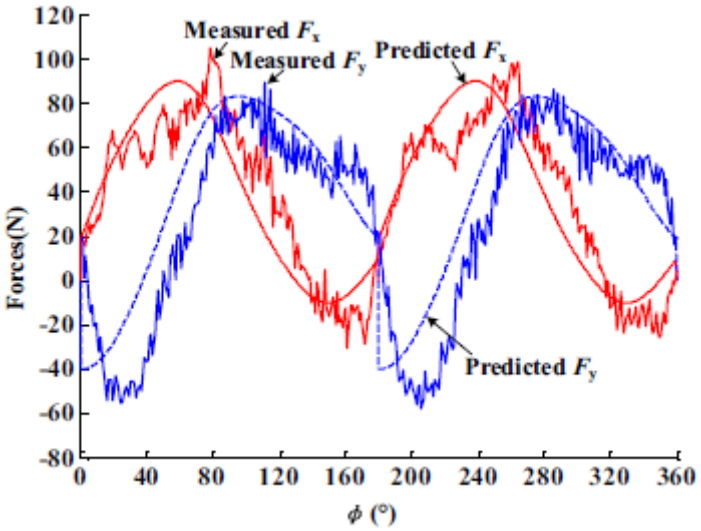

Figure 19 - Predicted milling forces in Vc=65 m/min, fz=0.14 mm/tooth, ap=1.2 mm [52]

Observing these plots (*figure 18 and 19*), it is possible to correlate an increase in force components with increased cutting depth and increased feed per tooth. The fluctuation of these values further confirms the anisotropic properties of the plain-woven carbon fiber composite with variations during different rotation angles. From the results of this experiment, it was accessed that the force prediction model is close to the experimental values and has similar maximum averages. Furthermore, the error deviation between the theoretical model and experimental is 10% [52].

The values shared between both studies are similar and coherent considering the used materials. For practical reasons, these values will be used in the development of this project and are stated in the "Methods" chapter. The properties of the materials represented in these studies are relatively better (higher rigidity and other mechanical properties) than normal ABS and PLA. Consequently, if this project is developed according to these forces, it will have a safety factor.

2.4.4 Chatter

Chatter (figure 20) in milling, is a form of cutting vibration in a machining system subjected to external non-cyclical forces. It manifests itself as a strong vibration of the tool and workpiece during cutting operation.

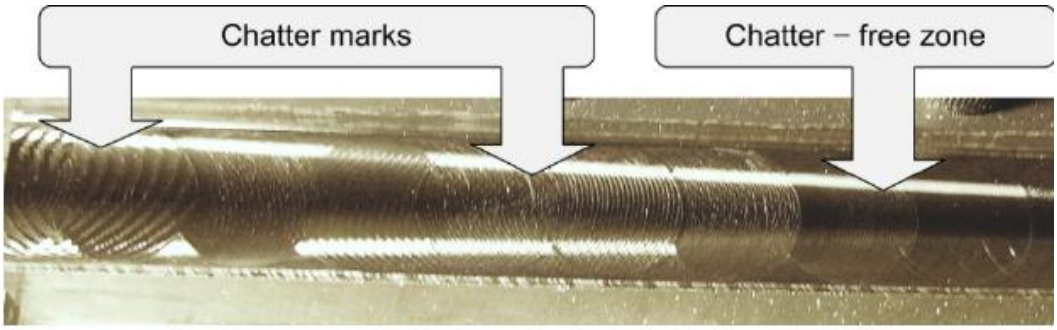

Figure 20 - Chatter in milling [53]

This phenomenon brings many limitations to a successful machining operation like workpiece surface quality, undesirable noise and increase tool wear [54].

2.5 Robotics

Even though machining can solve dimensional problems in 3D printing there is still the necessity of preparing the part for post processing after printing. This can be achieved by removing the printed part from the printer and fixing it in a machining station. The mentioned process can be time consuming and it goes against the speed advantage of AM. To save time and financial resources it was decided to use a robot with both printing and machining capabilities. This robot also must switch autonomously between both modes. For the development of this concept a brief introduction of robots is presented. Here are included some concepts that are important to the project development.

2.5.1 Definition

The word robot is originated from the Czech word for “forced labor”. As time passed it changed definitions and as of today, as is defined by the Robotics Institute of America, a robot must possess the following characteristics: being reprogrammable, multifunctional, manipulator designed to move materials, parts or other specialized devices through a preprogramed path and steps [55].

With that said, robotics is an engineering field which relates all the interaction with robots like conception, design, manufacture and operation. Initially the implementation of robots was intended to help workers with difficult tasks, but with increased human labor costs and increased robot availability, companies started to study the possibility of upgrading their working force [56].

2.5.2 Applications

This technology has many benefits in different industries. That is why it is used in some of the following applications [57].

Welding – different types of welding can be performed by a robot. Usually, in this application, the robot must follow a preprogrammed path to provide linear or punctual welds in a working piece. The robot is equipped with a welding tool that must be carefully placed in each desired position to perform the operation and avoid collisions.

Pick and place – this application handles parts to move their position. It is usually used for sorting, assembly or general moving of parts. Requirements are positioning precision and holding force, as the part needs to be positioned in specific positions, hold to not be dropped and not damaged.

Spray Painting – for these types of tasks, the robot must follow a path to provide an even coat thickness in every direction. Because of this, the time spent on each portion of the part is extremely important. The robot speed will dictate if the paint application is correct. Also, the robot must have flexibility to access tight spaces.

Metrology – robot usage for measuring products. Usually made by slow moving robots that verify the coordinates of preprogrammed points or it can be made by part digitalization.

Machining – different tasks like milling, deburring, drilling, grinding, and polishing can be performed by robots. For this application, the applied resultant forces must be considered to ensure dimensional reliability.

2.5.3 Robot Configurations

There are different types of robot configurations and iterations. According to development and usage, the geometry of the robot can be very different. Some of the most used robot types are Cartesian, selective compliance assembly robot arm (SCARA), delta and articulated. What distinguishes these robot types is the joint configuration [58].

Cartesian robots possess three linear joint, giving them the ability to works in 3 axis, x, y and z.

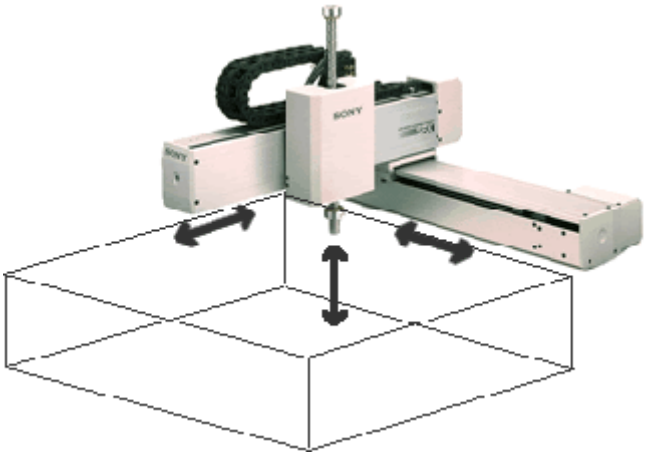

Figure 21 - Cartesian robot [59]

SCARA robots have two parallel axis that gives them ease of operation in one selected plane.

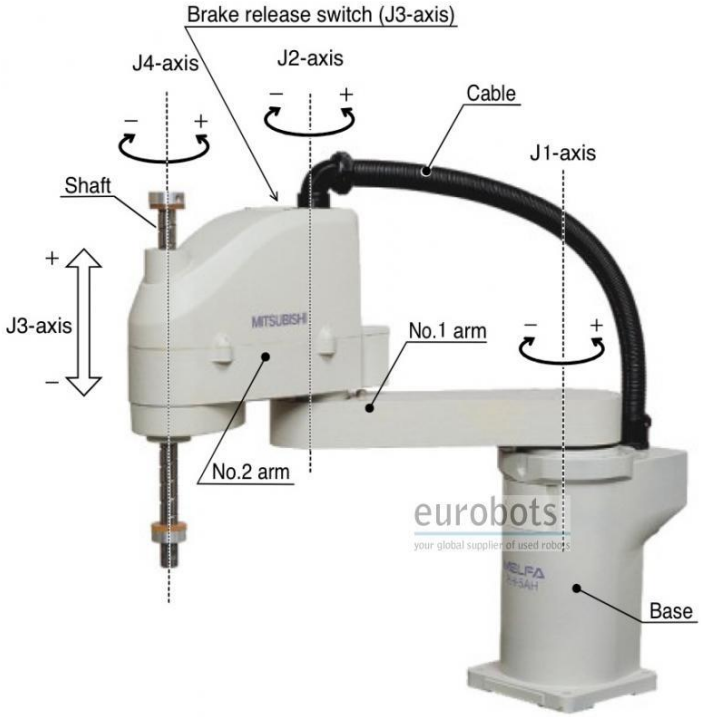

Figure 22 - SCARA robot [60]

Delta robots, that look like spiders, have precise movements because of the joined arms resembling parallelograms.

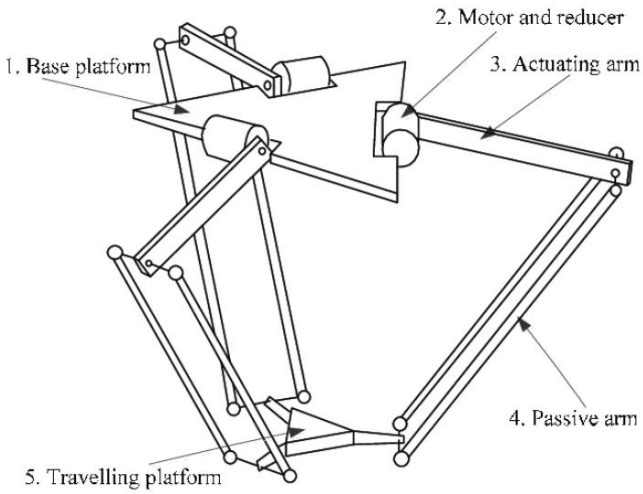

Figure 23 - Delta robot [61]

Articulated robots have multiple joints. The base has a twisting joint and additional joints are rotational. Typically, robots for industrial applications have four or six joints. The number of joints will influence the freedom of movements of the robot, but the actual number usually is limited by the application.

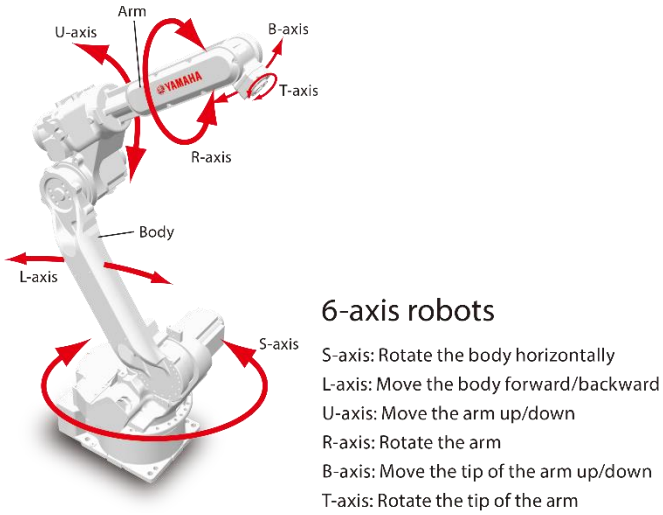

Figure 24 - 6 axis articulated robot [62]

This thesis focuses on the articulated type of robot, so the next topics are based on information regarding this type.

2.5.4 Robotic Axis

Robots are composed of several joints. These joints give the robot the possibility to move along axis. The number of joints dictates the number of axis, and in consequence degrees of freedom (DOF). The selected robot for a chosen task must have enough DOF to allow

the operation. One of the most common types of operation is pick and place, represented by the following figure.

Figure 25 - Representation of a pick and place operation performed by a robot [63]

Robotic joints can be categorized in the following groups [64]:

Linear joints – relative movement between input and output link is translational sliding motion, with parallel axes between them.

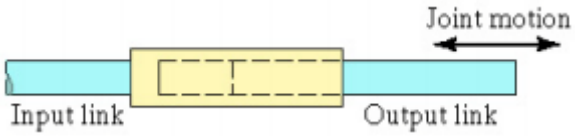

Figure 26 - Linear joint representation [64]

Orthogonal joints – relative movement between input and output link is translational sliding motion, with perpendicular axes.

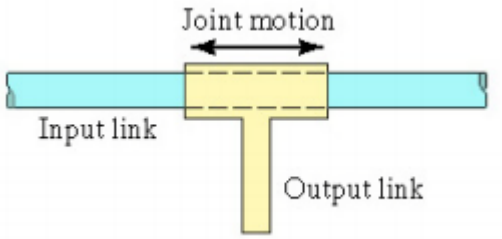

Figure 27 - Orthogonal joint representation [64]

Rotational joint – rotational relative movement between input and output, while rotation axis is perpendicular to both links.

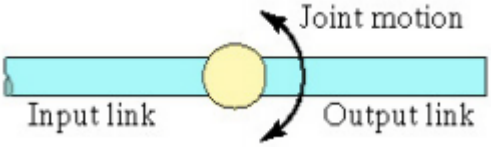

Figure 28 - Rotational joint representation [64]

Twisting joint – rotary relative motion between two links with parallel axes between each link

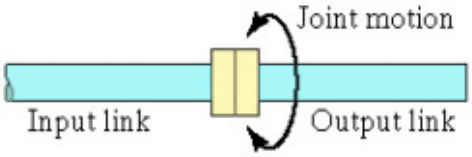

Figure 29 - Twisting joint representation. [64]

Revolving joint – rotational relative movement with axis of the input link parallel to axis of rotation, while axis of the output link is perpendicular to rotational axis.

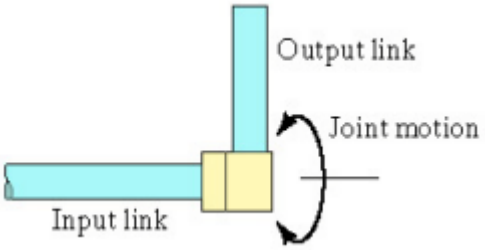

Figure 30 - Revolving joint representation [64]

2.5.5 Accuracy

Accuracy is defined as the maximum position or orientation error obtained when moving to a point located in the Cartesian space. This error quantity depends on a defined frame of reference, like the point which intersects the first axis with the base plate. Accuracy depends on the repeatability of the robot [65].

2.5.6 Repeatability

Ability of the robot to return successively to a certain point. Usually, this point can be defined in the Cartesian space and achieved with specific joint orientations. Robot manufactures provide this information in the robot specification [66]. This concept is important for the reliability of the mechanism throughout many cycles of operation.

2.5.7 Robot Rigidity

One of the most important concepts for robots is rigidity. During different tasks, robots experience applied forces. The transversal force is the robot weight, and it is present regardless of the task. Also, there are specific applied forces depending on the task like machining. In robotic machining the cut material provides resistance, and it is applied to the robot in form of resultant forces. Rigidity will dictate the reaction of the robot to these forces. In machining a reduced rigidity will induce chatter and vibration in the robotic system. This will affect quality, accuracy and tool wear [67].

2.5.8 Robot Cells

Robot cells consist in the use of a defined space for a specific task performed by one or several robots. Some advantages in this configuration are part quality improvement, reduced labor and productions costs, and reduction in waste. Furthermore, there are regulations regarding robot operating speed in proximity to a human and using a properly isolated working cell, removes the mentioned speed limitations allowing maximum productivity. Also, the safety factor is increased due to isolation of robots from humans. So, in case of an accident the risk area is isolated and only hardware is damaged [68].

2.5.9 Robotic Milling

Robotic milling is an increasingly relevant field in the product manufacturing industry. It gives more flexibility than traditional 3D and even 5D milling due to the number of DOF that a robot can be built. This gives robotic milling an edge over the mentioned manufacturing processes, specifically in the volume occupied by the machine, takt time and consequentially production costs.

Regarding this type of application, a project was proposed for designing a 3D printed fixture to fix a spindle motor to ABB IRB 140 robot [69]. From their results, it can be assessed that this type of configuration is very flexible in different machining operations. Also, not only using machining heads but other type of manufacturing equipment like 3D printing heads and laser cutting, would give small companies a big advantage in manufacturing flexibility.

CNC Robotics is a company which provides different solution in automation. One of them is precisely the implementation of robots in machining. According to them, this solution is more cost effective than traditional machine tools. This is more evident in applications involving large plastic parts, foam, composites, and some softer metals. This is especially true in applications which replace manual operations. CAD/CAM software companies now support the programming of robots with milling tooling designed by them. This gives the ability to create toolpaths directly from CAD models and optimize and simulate the program on the computer [70].

2.5.10 Robotic Printing

There are several instances of use of robots in 3D printing. This development is backed by the necessity to eliminate support structures existent in traditional bottom-up printing, explore multi-plane printing and a higher flexibility in manufacturing.

A robot mounted FFF printer was developed for a 6-axis robot [71]. The prototype had the capability of simultaneous printing with two materials, achieving an average dimensional error of 0.76%, 2.04% and 3.9% for three different printed components. Most of this error was due to layer thickness assumption. This solution had the advantage of a larger printing space and with an implementation of a movable base or gantry-type robot the accuracy of the printed parts can be further increased.

Another paper discussed the concept of a 6 DOF robotic printer and inherent benefits of multi-plane printing like improvement of mechanical properties, printing time and different material layout strategies [72].

Other application of robots in 3D printing is the creation of cementitious structures using a multi-robot configuration [73]. Here, the authors proved a concept of applying a system configuration with different modules; planning of robot placement to optimize workspace, mobile robot navigation and localization to reach printing location. Comparing to similar systems, their achieved better scalability and higher time efficiency due to multiple robot printers and better on-site printing capability due to mobility of the system. The result not only can be scaled for bigger projects but also be applied in difficult access areas and even other planets.

There are also systems which use a cable suspended robot for FFF printing [74]. This concept was explored using a six motor and six cable setup. Cable suspended robots have two main advantages, they are simpler because fewer motors are required for positioning and all actuators can be mounted on an overhead structure and there are less problems with collisions. The material used for this proof of concept was foam as it is inexpensive and light, therefore ideal for this application. The results were acceptable, and the printed structures had the possibility of large volumes.

2.5.11 3D Printing and Machining through robotics

In literature exist several concepts of hybrid application of 3D printing and machining. All of them share the objective of combining the advantages of dimensional accuracy of machining with the flexibility of 3D printing technologies.

One example is a hybrid machine which alternates between machining and FFF printing with a rotary head [75]. This rotation can also be used to tilt the extruder and recurring to another motor in the printing plate, effectively making this machine a 5-axis printer. In this proof of concept, the extruding nozzle and rotary machining tool axis are mounted on the same axis and a motor is responsible for the rotation of this axis and consequently the choice between modes. This solution was implemented to avoid having complexity in the head assembly with actuators and to reduce time to machine because the cutter does not have the necessity of being perpendicular in relation to the printed part surface.

The results of this proof of concept showed that this solution eliminates the necessity of support material for overhang features due to the 5-axis mechanism. This will reduce cost, time printing and possible defects by the removal of support material. There is also the possibility of printing embedded materials (printing on top of other materials like metals) to increase stiffness, reduce time and cost. The latter is possible thanks to better access of a 5-axis system relatively to a 3-axis printer. The machining capability was used for trimming of free form surfaces and tapered hole enlargement of FFF printed parts with a significant processing time reduction relative to a normal FFF printed part with same surface quality.

Massachusetts Institute of Technology also proposed an approach for hybrid fabrication [76]. This approach consisted of three types of manufacturing included in a single robotic working station. These were additive, formative, and subtractive fabrication. To achieve this, different effectors were utilized. They could be fixed to the robot or be stationary and the work piece could be moved by the robot.

For additive manufacturing three different effectors were used. The first consisted of a print head that extrudes ABS plastic and it was built based on a MakerBot MK6 Extruder. The second was a high-density polyethylene (HDPE) plastic print head and it was designed and assembled to explore the concept of printing using recycled materials. The print material was obtained via shredding of used milk containers. And finally, the third print head was developed to rapidly print larger structures with urethane foam.

Forming fabrication was explored recurring to a tool head with easily exchangeable tool holder and modeling clay was used as a material for sculpting.

For subtractive fabrication two different effectors were used. The first one consisted of a rotary tool with adjustable chuck for different cutting tools and the second one was meant for cutting of large material volumes via a large router. The latter was mounted alongside the urethane extruder.

The resulting equipment was capable of printing ABS with similar quality to a commercial MakerBot 3D printer. Multi-axis printing was achieved by fixing the printer and allowing the robot to move the building platform. This setup allowed manufacturing of different part without support material.

The urethane foam printing head functioned effectively, producing large structures rapidly and due to urethane low density and high adhesion properties, large overhang features were possible.

The formative clay sculpting utilized an indentation method where the depth of each indentation was informed by the thickness of the desired final object at any given point.

Finally, the subtractive manufacturing was successful on a large range of soft materials like foam, wood and wax. The milling mode was limited by the rigidity of the system so only soft material were used. But nonetheless, milling tasks performed by the robot were versatile due to the range of motion, ease of access to the work piece, and large working space.

2.5.12 Autonomous Head / Tool Change

One of the main concepts of this dissertation is the use of an autonomous/automatic mechanisms for the exchangeability of printing and machining capabilities. Several companies use this concept in their solutions. That is the case of the company ATI Industrial Automation which provides several models of solutions in this field [77].

Their solutions allow to automatically change tooling for robots with high reliability for millions of cycles and maintaining repeatability. Their solutions have a Master-side and a Tool-side that are built to lock or couple automatically, carry a payload and pass different types of signals like electric and pneumatic. Also, most of these solutions use pneumatic actuation for the locking mechanism. This gives a lot of security on the functionality of the mechanism but restrains this type of mechanisms in application which require less space and peripherals like pneumatic reservoirs and compressed air supply.

Other instances of use of this concept are mentioned in a dissertation by Mihail Babcinschi [78]. Babcinschi designed and manufactured 3D-printed tools for a robot, a mechanism for automatic tool change and a tool holder. The docking mechanism was pneumatic and worked well for small payloads. The purpose of this work was to facilitate tasks which required manual tool changes. With a successful implementation of this project, time and resources could be saved and profit increased.

2.6 Conclusions

Use of articulated robots for FFF printing and machining applications is widely developed and presents many advantages over traditional methods like desktop printers and CNC stations, respectively.

Literature has a similar concept to this dissertation. In which a multi-manufacturing station is implemented. The main difference is the either manual change of capabilities or making the work piece the moving part between operations. Some hybrid applications found were adaptations of traditional methods like the installation of rotary tool on a desktop FFF printer.

Automatic tool change in hybrid applications was also not found. Some applications use motors to rotate printing/machining dispositive.

Generally, automatic tool changers have robust pneumatic actuation to provide stability, repeatability, and safety. With this type of actuation, a wide variety of applications can be covered but not the one described in this dissertation because of the relatively small scale and decision to avoid added complexity.

The challenges of this project rely on the rigidity of the proposed system. This includes both the mechanism and the whole robot system during operation. Most of the instability may arrive from the forces during machining and inertia of the system during robot movements. To overcome these problems, the proposed system must be rigid enough to sustain machining forces and guarantee proper fixation of the machining head during robot movement and cutting.

Also, the system must be able to successfully perform printing and machining tasks in order to reduce production time, costs and add complexity to the PLA and ABS printed parts using robot multiple axis of the robot. Knowing that this dissertation focuses the machining head and the docking mechanism, a successful hybrid manufacturing station will expand the possible applications for 3D printing and manufacturing flexibility.

3 Methods

This chapter will explain the steps that were taken during the development of this dissertation. Each component will be discussed in function and form. Assumptions and paths taken are going to be detailed and justified.

3.1 Initial assumptions

The main objective of this project is the dimensional assurance of 3D printed (FFF) parts using a machining head for a 5-axis robot. With that said, the first assumption is the fact that the robot must be able to print the parts and machine them. The robot will be part of a work cell that will use a CAD files to print and finish a component according to desired dimensional standards. The robot also must be autonomous in switching between end effects with printing and machining properties.

Other requirements are:

- The main printing materials that will be considered for this project are PLA and ABS.
- The working space of the machining head is 200x200x200 mm and it is assumed that the tool of the machining head can reach any side of the working space.
- The maximum depth that should be machined is 1 mm.
- Maximum allowed weight of all components mounted on the robot must be under 2 kg.

To define different required operations, a benchmark part was created. This part has most of the desired features for machining and the machining capabilities of the system will be tested on it.

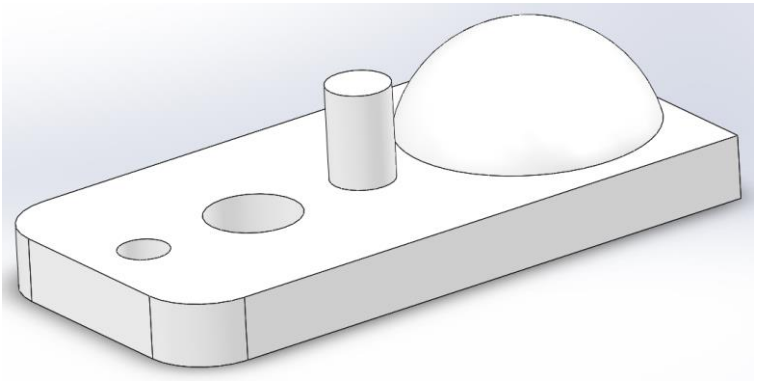

Figure 31 - CAD representation of the model part

The part has a shaft for end milling operations, holes for hole dimensioning, a curved surface for ball end milling and abrasive finishing.

3.1.1 Automatic tool change

For this project one of the most useful features for the machining head would be automatic cutting tool change. This would eliminate the necessity of multiple machining heads and reduce time and cost in various operations.

During search for components for this solution, it was discovered that adapters for spindles and complete automatic spindles are heavy and have a substantial cost increase over normal tool chucks. Also, most of them have pneumatic actuation. This meant that pneumatic hoses would be required, and this would interfere with the machining head mechanism because of the required connections.

The main limitations of the automatic cutting tool change in this project are the following:

Cost – a spindle with an automatic tool change mechanism is more expensive than normal spindles.

Weight – the lightest spindle found with this capability has the same weight as the objective weight of the project.

Pneumatic actuation – necessity of additional hardware and a compressed air source.

Designing a mechanism for automatic tool change that has electrical actuation would be a standalone project and it is not the scope of this dissertation, so due to these constraints, automatic tool change was not implemented in this project.

3.2 Introduction

According to function, this project will be divided in two groups. The development of each group will be described separately to better organize this document. Groups are designated according to function of the subcomponents.

The first group is related to all the relevant components to the lower connecting mechanism and it is named “Lower mechanism” (LM). The second group consists of components from the machining head, so it will be referred as “Machining Head” (MH). The decisions made regarding component selection, dimensions and other will be clarified and explained.

3.3 Lower Mechanism

To fulfill project requirements, the machining head must be able to the attach to and release from the robot without human intervention. This requires a connecting mechanism for them. As it was shown in the literature, there are companies that use this type of mechanism to autonomously change tools of a robot [77]. Due to the weight of these tools, the mechanism usually consists of pneumatic actuation.

For this project it was decided that pneumatic actuation is not ideal as it needs a lot of extra hardware like source of compressed air, reservoir, filters, tubing and valves. So, to save space and weight the chosen actuation was electrical.

3.3.1 Linear Stepper Motor

After researching possible solutions for electrical actuation, the most adequate type of actuator for this application was a linear stepper motor (LSM). LSM is most suitable for this because it needs to hold a connecting part and position it in two specific positions. LSM can extend a rod precisely along a path, creating more possibilities regarding available space. For comparison, pneumatic actuators have specific positions (retracted and extended) so there is no possibility of positioning the rod in an intermediate state.

Also, LSM have detent torque, which is a residual movement resistive torque after the current input is stopped. This property is also beneficial in case of power shortage as it will ensure the LM/MH connection in emergency situations.

The 15000 Series Can-Stack Stepper Motor Linear Actuator from Haydon Kerk was selected. Specifically, the captive that is represented on the right. Being captive means that the output shaft does not have rotational movement opposing the non-captive ones.

Figure 32 - Selected LSM (on the right) [79]

The following elements represent some of the relevant characteristics of this LSM;

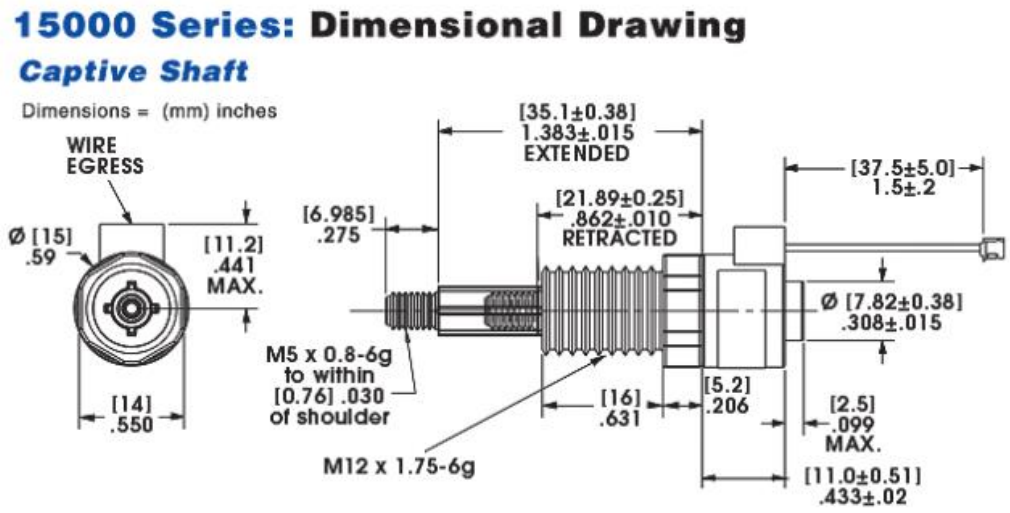

Figure 33 - Dimensional Drawing of the selected LSM [79]

Table 2 - Specification of the selected LSM [79]

Wiring		Bipolar		
Step Angle	Degree	18º		
Winding Voltage	VDC	4	5	12
Current/Phase	A rms	0.2	0.16	0.07
Resistance/Phase	ohms (Ω)	20	31	180
Inductance/Phase	mH	5.6	8.7	48.8
Power Input	Watts	1.6		
Rotor Inertia	gcm²	0.09		
Insulation Class		Class B (75º Rise)		
Weight	g	28		
Insulation Resistance	MΩ	100		

To hold this component, a specific part was designed to make use of its threaded mounting. The next figure represents the CAD of the designed stepper holder.

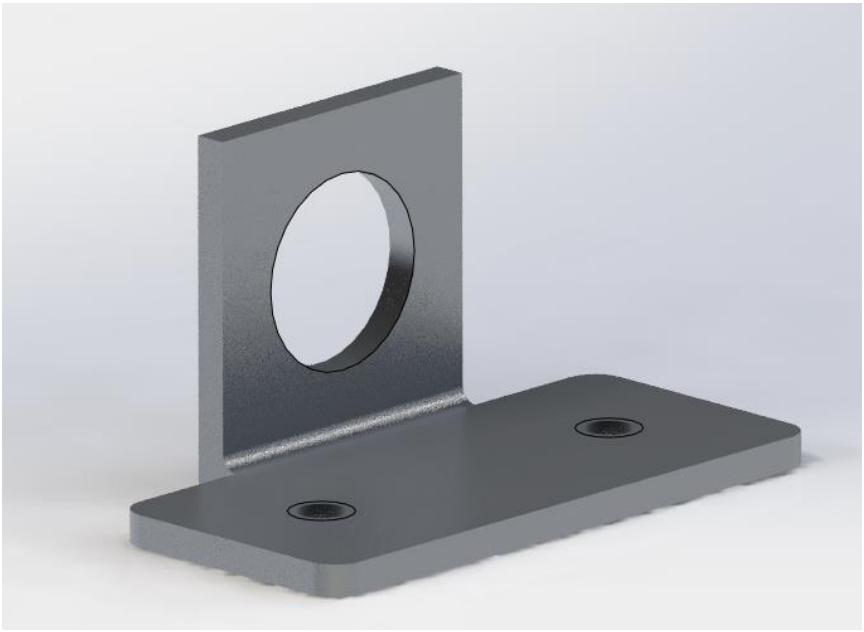

Figure 34 - Stepper Motor holder

3.3.2 Linear Stepper Motor Control

To properly position the MH/LM connector, LSM must be controlled. This control is achieved via voltage variation. To control the voltage that is supplied to the LSM, it is necessary to include a driver, to supply the adequate required voltage and a controller, to control the supply logic.

3.3.2.1 LSM Driver

For this application the main limitations for the LSM driver is weight, cost, dimensions and the possible supply voltage range. As in most controllers, the voltage and current handled by the controller must be higher than the one required by the stepper motor. A driver was selected. This driver is MP6500 Stepper Motor Driver.

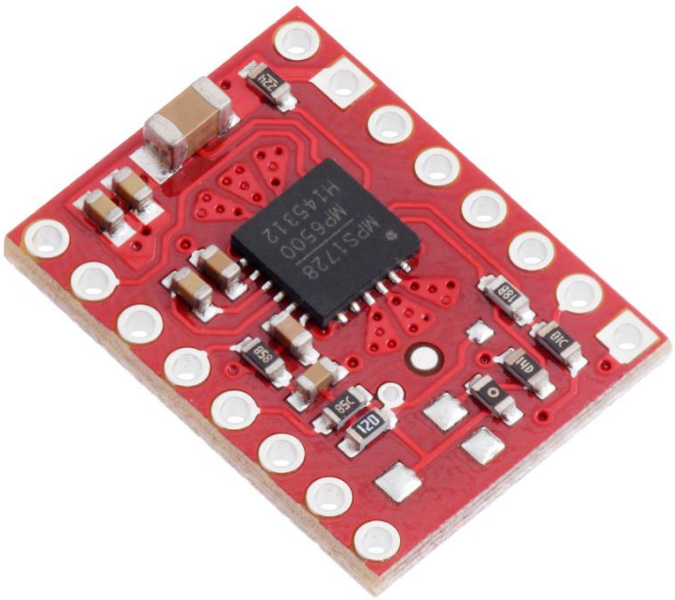

Figure 35 - MP6500 Stepper motor driver [80]

And the general specifications for this driver are the following.

Table 3 - MP6500 Stepper motor driver specifications [80]

Minimum operating voltage	4.5 V
Maximum operating voltage	35 V
Continuous current per phase	1.5 A
Maximum current per phase	2 A
Minimum logic voltage	2.1 V
Maximum logic voltage	6 V
Micro step resolutions	Full, 1/2, 1/4 and 1/8
Current limit control	digital
Size	15.24 x 20.32 mm
Weight	1.4 g

To secure this component while the assembly is in motion, a structure was designed. It consists of a supporting platform with a holding arm. The arm is fixed by a screw to the holding structure. Finally, the structure is fixed to the base of the LM by two screws.

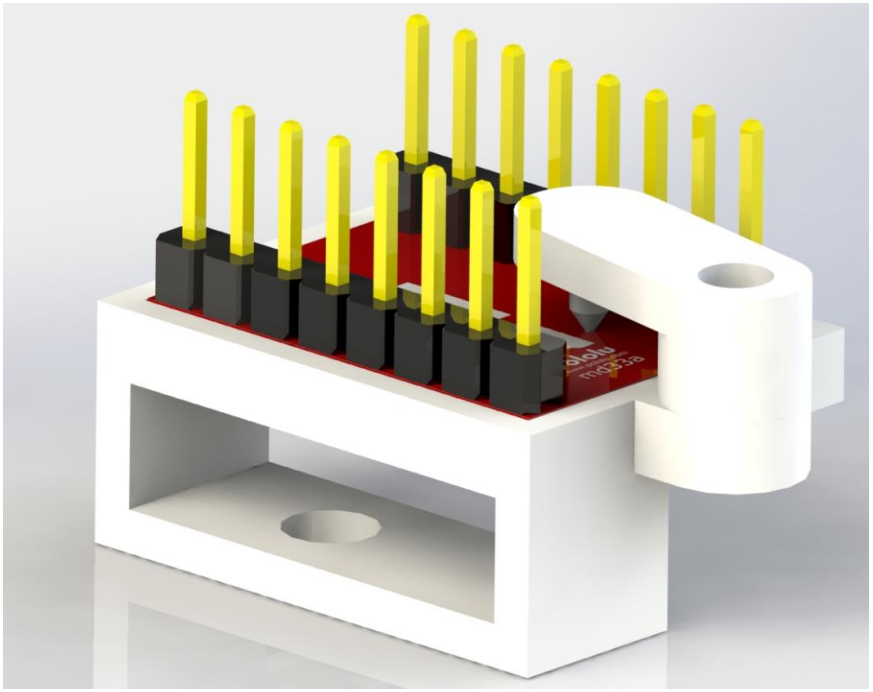

Figure 36 - Stepper Driver holding structure

3.3.4 Controller

For this application, the selected controller must be capable of handling the correct amount of information input. Mainly to save space and weight, this controller will handle the logic behind the LSM actuation and spindle motor speed and actuation control via spindle driver.

The most used type of controller for experimental projects are Arduino boards. They are widely available, cheap and bring ease of use thanks to intuitive programming.

As the logic voltage interval is 2.1V to 6V, most of the boards available could be used. The chosen product for this was Arduino Uno Rev3. Due to space constraints, it was decided to mount the controller outside the machining head assembly. So, the proposed solution for controller integration is the creation of a compartment in the robot which can house it, or it can be outside the structure of the robot and be connected via robotic wrist. The latter would require a design adaptation to allow electrical connection from the wrist to the LM.

Figure 37 - Arduino Uno Rev3 [81]

Table 4 - Arduino Uno Rev3 specifications [81]

Microcontroller	ATmega328P
Operating Voltage	5 V
Input Voltage (recommended)	7-12 V
Input Voltage (limit)	6-20 V
Digital I/O Pins	14 (of which 6 provide PWM output)
Analog Input Pins	6
LED_BUILTIN	13
Length	68.6 mm
Width	53.4 mm
Weight	25 g

3.3.5 Electrical Connections

After consulting data sheets form each motor, driver and the micro-controller, the required electrical connection chart was created.

Starting by the spindle motor driver, that is in the MH, it will have two connections. Power and Ground supplied by the spindle motor driver. To have some feedback regarding speed regulation of the spindle motor, the MH also has a mounted photoelectric infra-red sensor. It will provide feedback for the controller to control rotational speed according to the requirements. This sensor has a special connector of four signals, two for power and the remaining for information.

In the LM there are two main electrical components, LSM and corresponding driver.

The controller is supplied by a power source and has eight logic connections and an additional USB connection for computer control and programming. Four of them are from stepper driver, two are from spindle driver and one is from the speed sensor.

The stepper driver has four connections to the linear stepper motor, two for the power supply of the motor and other two for its own supply.

The following figure represents the connections established between the mentioned components.

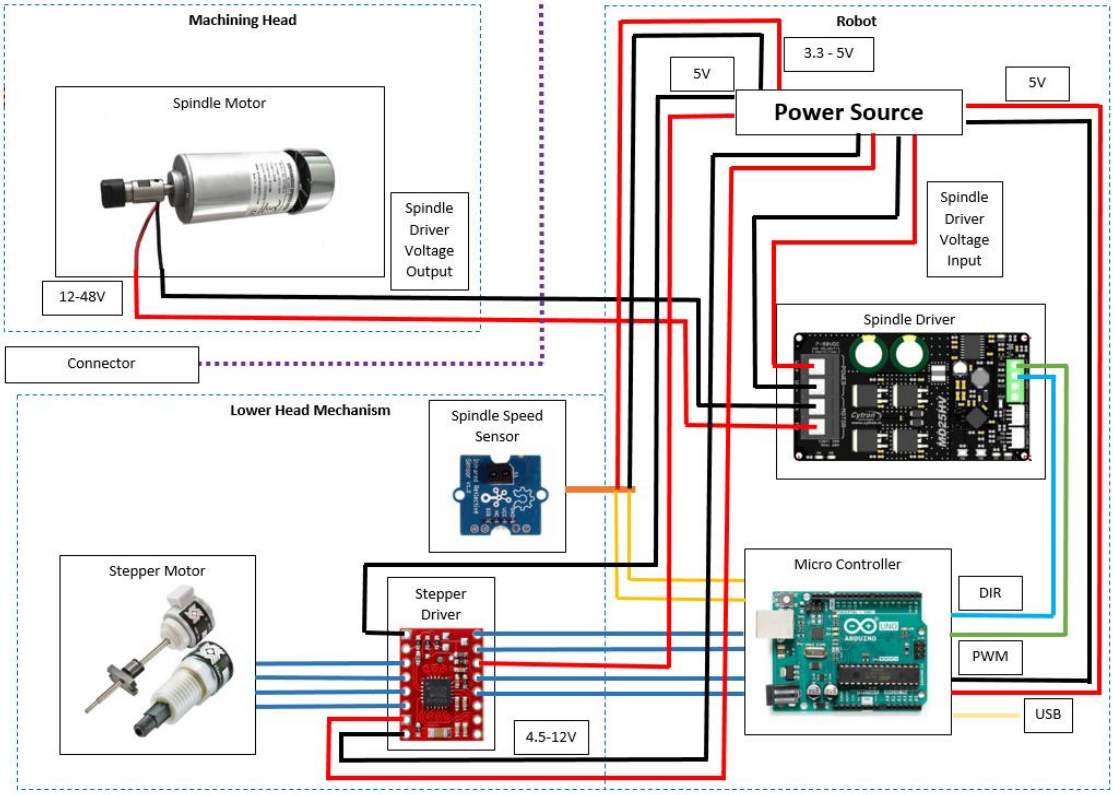

Figure 38 - Proposed Electrical Connections

To supply the spindle motor through MH/LM connection, a Molex connector was chosen. Molex connectors are largely available, relatively inexpensive and light weight due to plastic construction. The selected models are Super Saber Receptacle and Super Saber Plug. The super series was chosen due to the high current achieved by the spindle motor power supply during startup. The Super Saber Receptacle comes with a tab that clamps on the Super Saber Receptacle for securing the connection, but unplugging requires manual intervention to tilt the tab. To avoid breaking the connectors during MH/LM separation, the tab was removed, and the connection will be secured but the relative position and fixation of the MH/LM assembly.

Figure 39 - Super Sabre Receptacle [82]

Table 5 - Super Sabre Receptacle specifications [82]

Circuits (maximum)	2
Gender	Receptacle
Material	Nylon
Net Weight [g]	1.880
Current (maximum per contact) [A]	34
Maximum Mate Force	17.8 N per contact
Minimum Unmate Force	4.4 N per contact

Figure 40 - Super Saber Housing Plug [83]

The following table represents different specifications for these connectors.

Table 6 - Super Sabre Housing Plug [82]

Circuits (maximum)	2
Gender	Plug
Material	Nylon
Net Weight [g]	3.326
Current (maximum per contact) [A]	34
Maximum Mate Force	17.8 N per contact
Minimum Unmate Force	4.4 N per contact

As the highest voltage comes from the spindle supply, the correct connector must be chosen for current handling. According to the specification this connector can withstand the average calculated current for this use. Both genders of the connector are secured by 3D-printed parts that are attached to the MH and the LM.

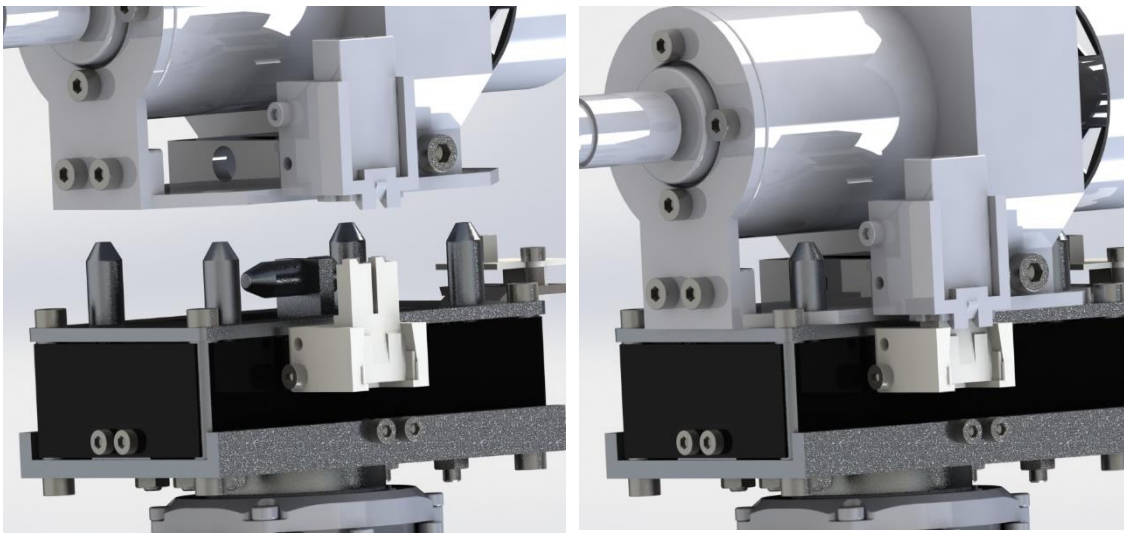

Figure 41 - Mounted Molex connectors open and closed with their respective supports

3.3.6 Structure of Lower Mechanism

Next step was the lower mechanism structure. To facilitate electrical connections, the LSM will be mounted in the lower mechanism structure. Ideally, this assembly is as compact and light as possible. To study and visualize the connection between LM and a robot, a model robot was chosen. Like it was mentioned before, the supporting robot for the machining head described in this dissertation is not build yet, so for dimensional and connection purposes, a model robot is used.

Although the model robot will not be used in the final iteration of this project, it will allow a better representation of the assembly, visualize relations between components and dimensions. The robot selected for the model is the ABB IRB 120. The CAD file used was obtained from the official ABB site [84].

Figure 42 - IRB 120 [84]

Table 7 - IRB 120 Specification [84]

Robot Version	**Reach (m)**	**Handling Capacity (kg)**	**Armload (kg)**
IRB 120-3/0.6	0.58	3	0.30
Number of axes	6		
Protection	IP30		
Mounting	Any angle		
Controller	IRC 5 Compact/IRC5 Single Cabinet		
Integrated signal supply	10 signals on wrist		
Integrated air supply	4 air on wrist (5 bar)		
Robot base	180 x 180 mm		
Robot height	700 mm		
Robot weight	25 kg		

This robot was chosen since it has a universal tool connector, several sources of technical information and an included CAD representation. The following figure illustrates the universal connector that is used by brands like KUKA and ABB in robots within similar categories.

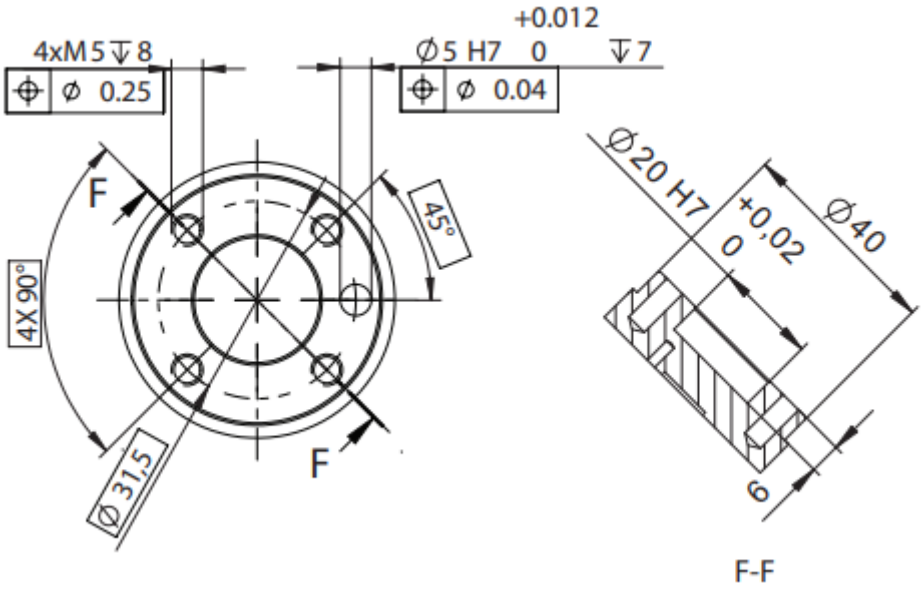

Figure 43 - IRB 120 mounting flange representation [84]

This connecting flange is the basis for the project because it will support the assembly not only in static conditions but also in dynamic ones. The assembly was built according to the dimensions of the flange and the LSM. The base of the LM has the appropriate holes to allow fixation to the flange of the robot. The part that connects the LM to the robot is the following.

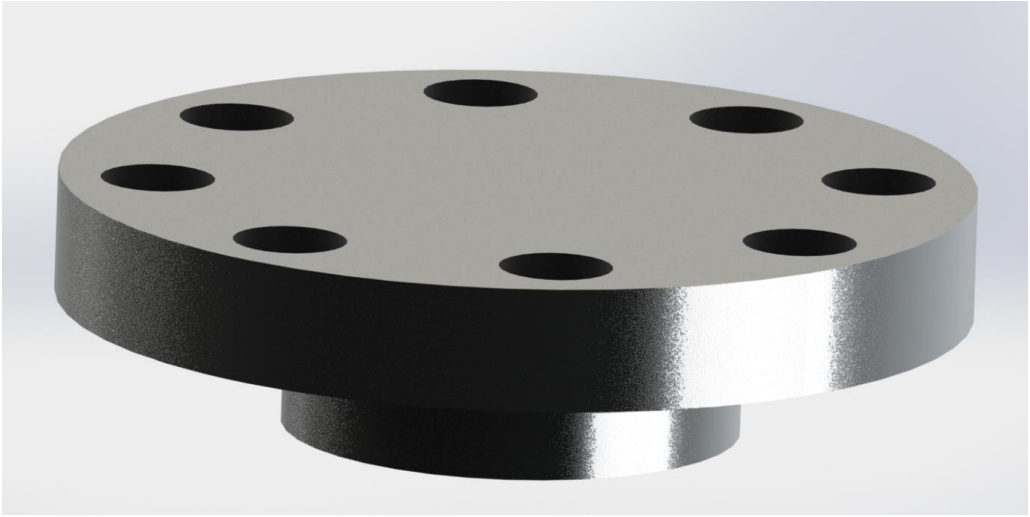

Figure 44 - Flange connector

This component mirrors the mounting holes from the flange of the robot. The holes have M5 threads and only four of them are used because of the low weight of the LM/MH assembly.

The structure of the LM consist of a cage that will support all the main axial solicitations during operation.

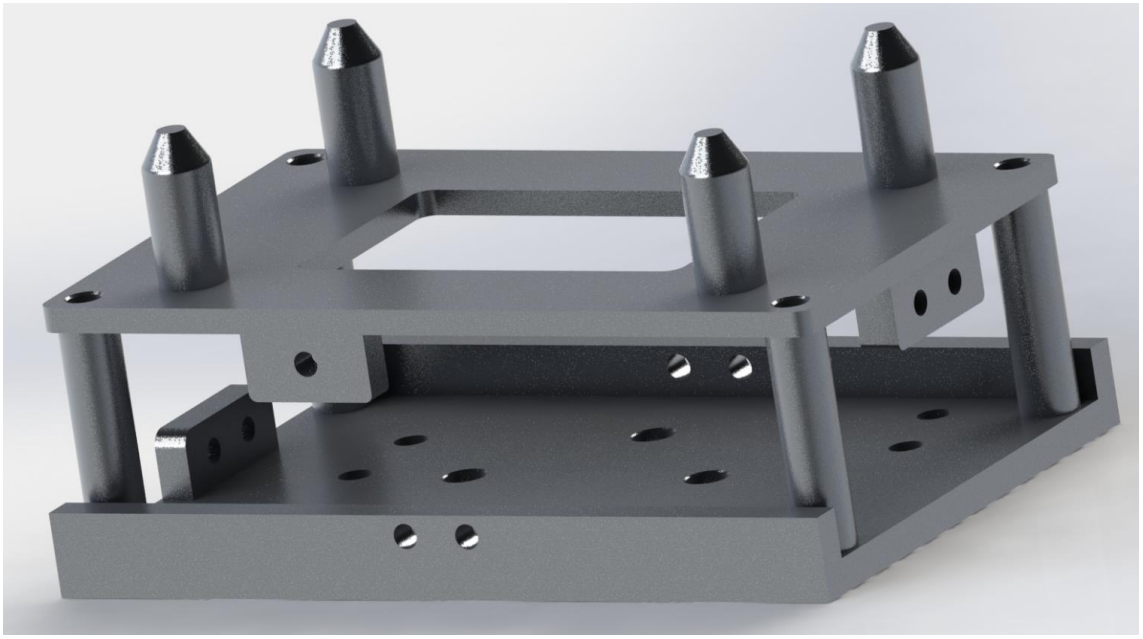

Figure 45 - LM structure cage

Later, a necessity for a sensor will be explained and as it will be mounted in the LM, the specific bracket was modelled. It is attached to the LM on the back and aligns the sensor with the fan of the spindle motor.

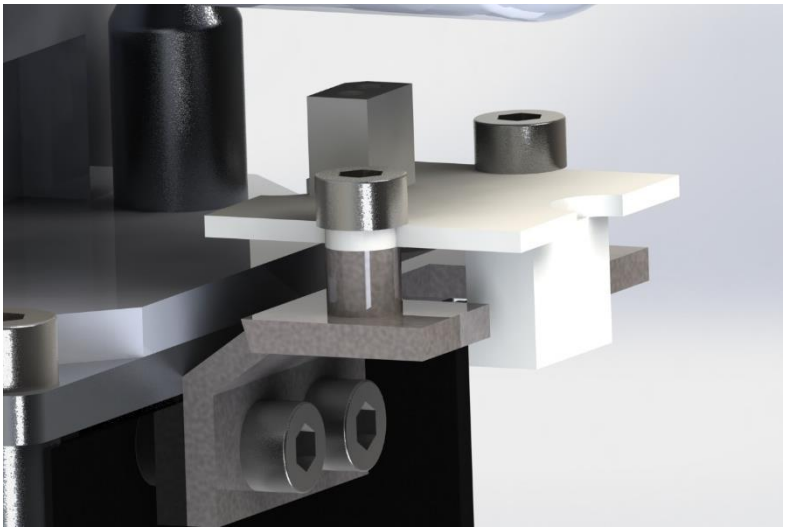

Figure 46 - Photoelectric sensor mounting bracket

3.3.7 Connection Mechanism

The connector piece consists of a metal part with several rounded shafts which will lock the lower mechanism to the machining head in the z axis. To eliminate the possibility of radially loading the LSM with the machining head's weight, both the lower mechanism and the machining head have holes for the shafts in the connector. With this, the LSM only must support the weight of the connecting part and provide the desired movement.

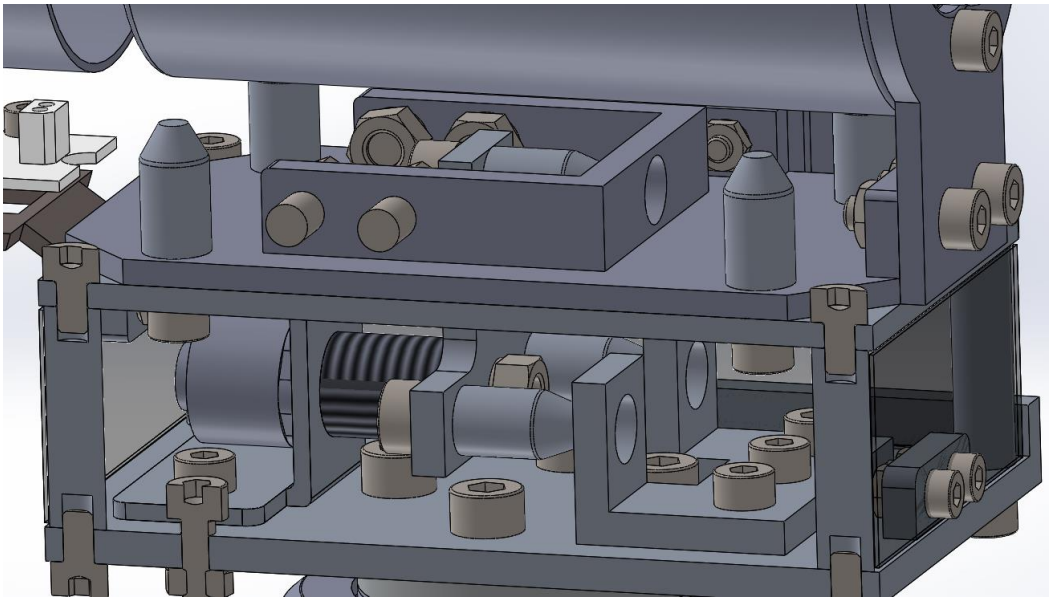

Figure 47 - Connecting claw with respective pins

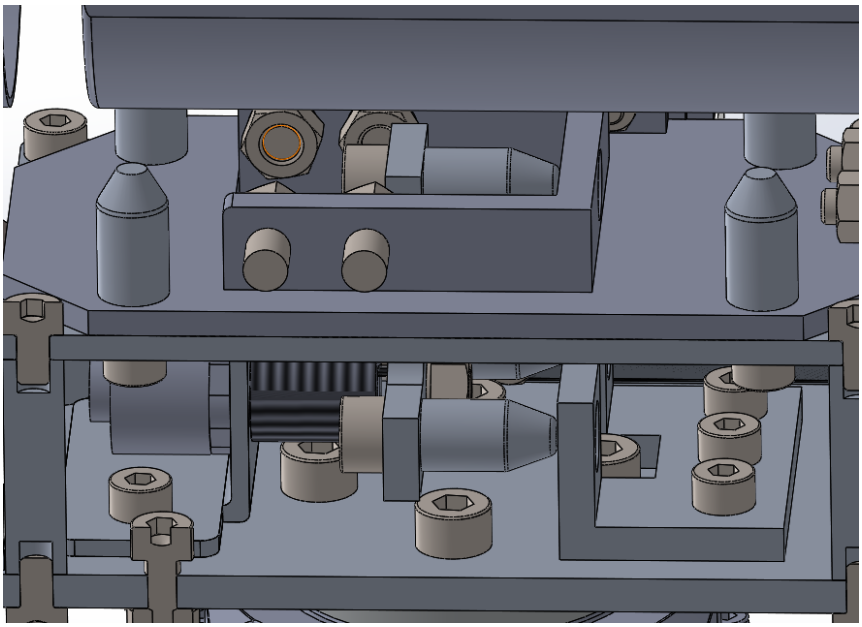

Figure 48 - Retracted connections mechanism

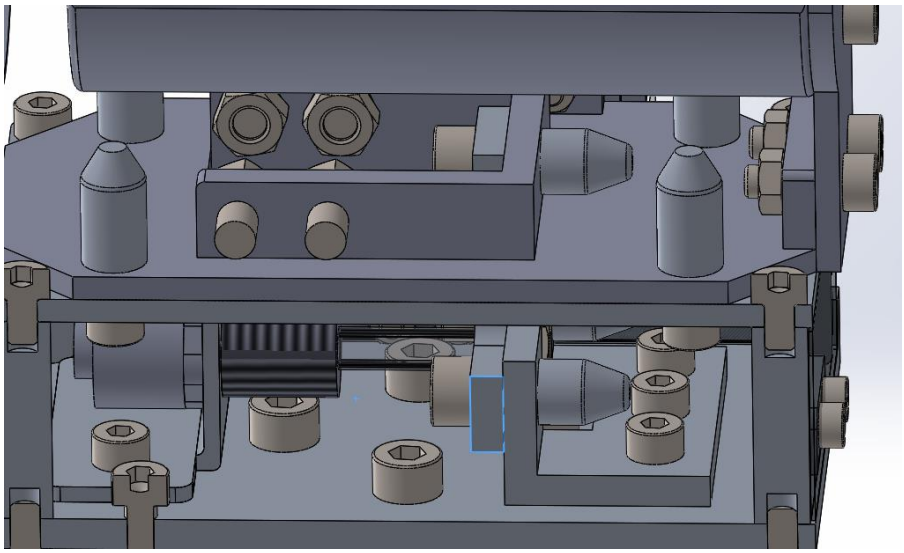

Figure 49 - Extended connection mechanism

To allow the actuation of this mechanism, the lower mechanism and the machining head must be carefully aligned and positioned. The z axis movement and positioning depend on the robot's movement. So, the remaining axis are x and y. To accomplish this, four guiding pins were implemented in the top of the lower mechanism assembly.

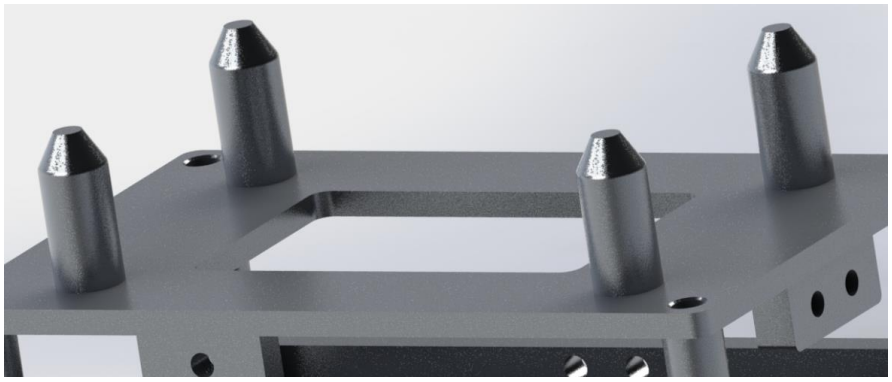

Figure 50 - Representation of the guiding pins in the LM

These guiding pins are rounded at the top to absorb some of the rotational error of the robot when he is approaching the connection position. With them, the lower mechanism will be fixed in the x and y axis to the machining head, completing the connection.

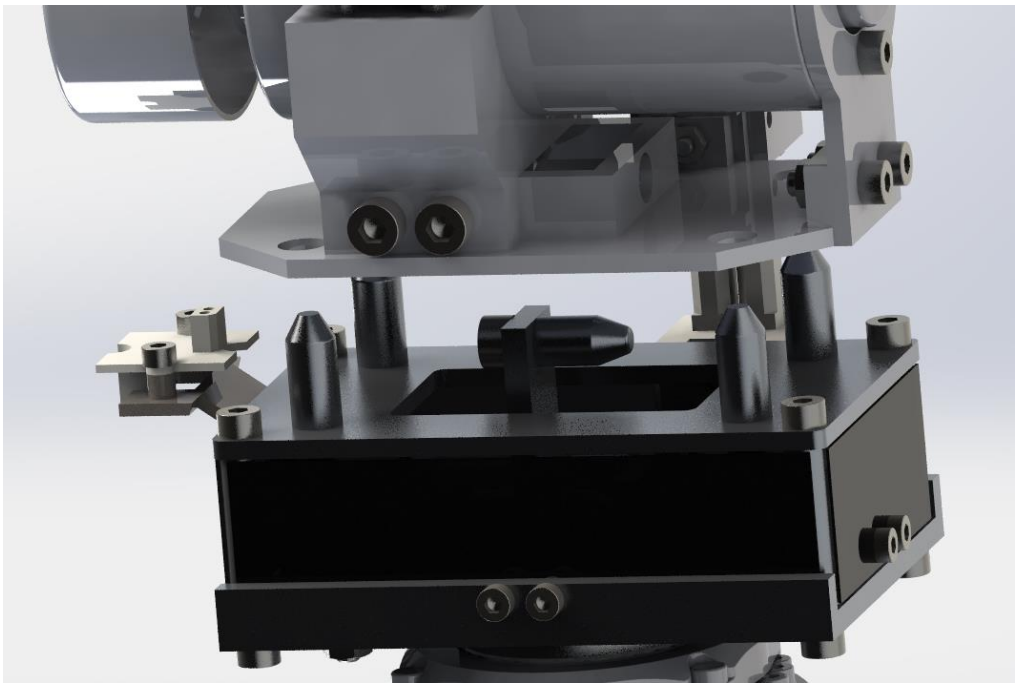

Figure 51 - LM/MH pre-docking position

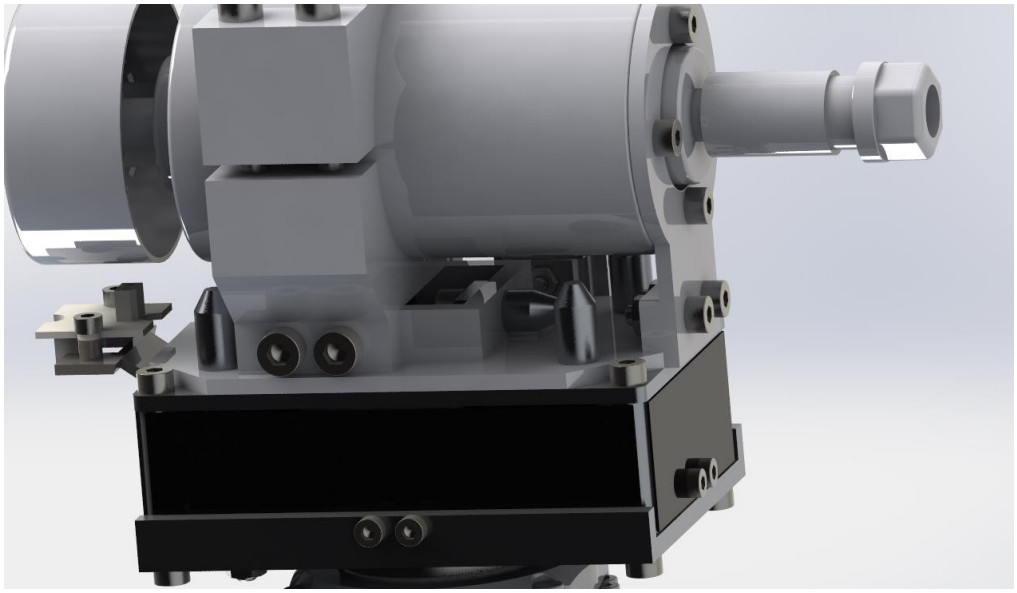

Figure 52 - LM/MH docking position

All connections between parts are made with screws. The sizes used are M3, M4 and M5. This decision allows a higher flexibility in assembling and disassembling components and easy future modification.

3.4 Machining Head

The main limitations of the machining head are weight and structural integrity while the tool is in operation.

While the concept of weight is simple, the machining head must not exceed the projected allowed weight, the structural integrity depends on multiple factors. Some of them are the forces developed during tool operation, working temperatures and resonance frequencies of the assembly.

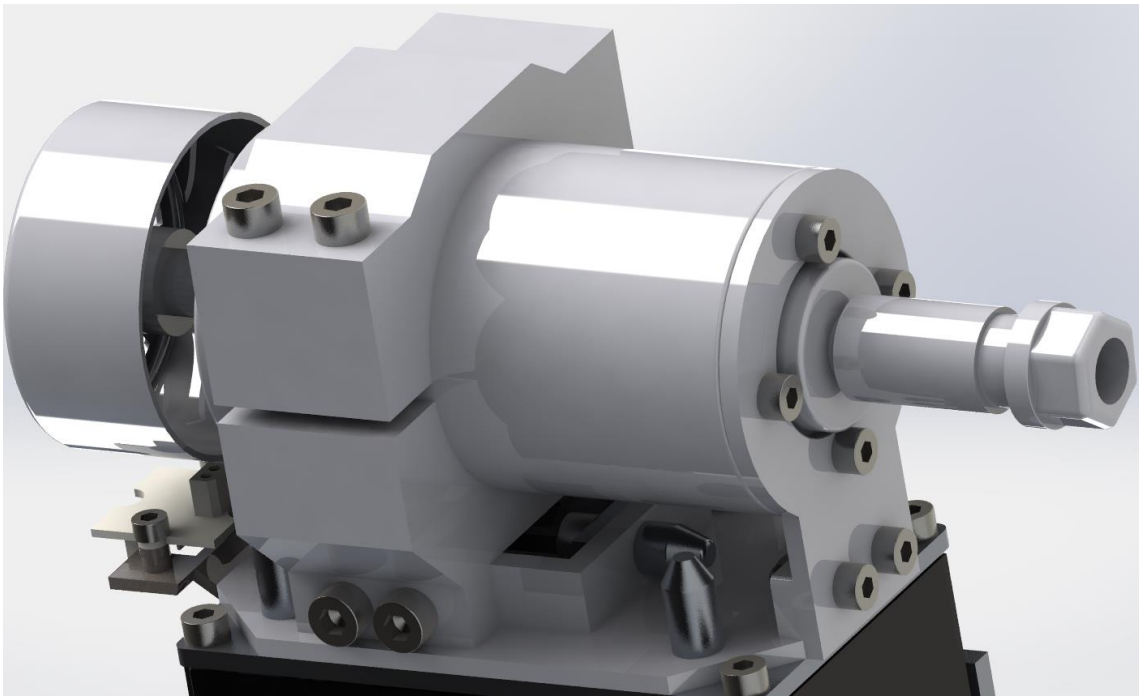

Figure 53 – Machining Head Representation

3.4.1 Spindle Motor

In order to select the most adequate spindle motor for this application it is necessary to obtain some working conditions. These are the ideal cutting parameters like cutting speed and required cutting torque, and maximum cutting forces during operation. Cutting speed will determine if the material removal rate is adequate for working temperature, cutting torque will influence the ease of material removal and cutting forces will influence the structure of MH/LM assembly and the cutting quality and precision.

Regarding the forces developed during operation, these were obtained through research of studies and articles that contemplate the milling forces of required materials. In the literature there are no direct results for these kind of forces in PLA and ABS machining, so another approach was taken. Several studies regarding the machining forces of fiber reinforced plastics (FRP) were found. They were chosen because they are the closest reference point for PLA and ABS properties and also using forces obtained with these materials will give a safety factor for this project because FRP, depending on the composition, generally have higher mechanical resistance, thus higher machining forces.

To obtain the machining forces, several plots were analyzed, and maximum values were registered.

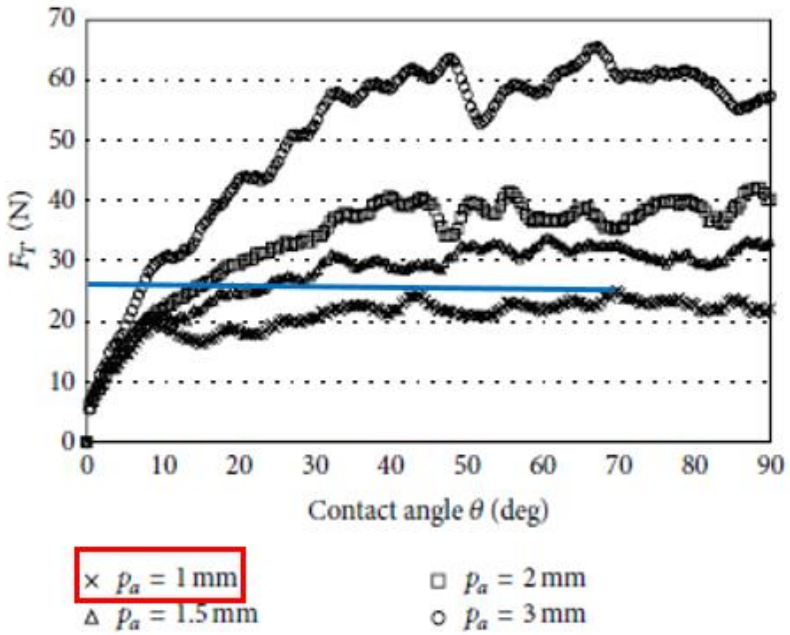

FIGURE 11: F_T component versus contact angle (cutting speed = 100 m/min; feed per tooth = 0.022 mm).

Figure 54 - Force identification process [51]

Using the maximum depth of cutting of 1 mm, the maximum tangential force is observed through the plot. The previous figure shows a maximum valor of Ft of approximately 26N. This process was repeated for the remaining graphs.

The following tables describe different types of forces developed during FRP machining according to literature review. The values were obtained for the agreed maximum machining depth of 1mm.

Table 8 - Tangential, Radial and Axial machining forces on FRP and different parameters

Cutting Speed [m/min]	Feed per Tooth [mm]	Max. Tangential Force [N]	Max. Radial Force [N]	Max. Axial Force [N]
100	0.022	26	70	-
100	0.044	-	-	82
200	0.022	18	65	-

200	0.044	-	-	75
300	0.022	16	95	-
300	0.044	-	-	85

Maximum radial forces will limit tool usage and give an idea of resultant forces during operation. Tangential forces provide means to calculate the minimum required torque for the spindle motor.

The calculations for the required torque started by deciding the maximum tool diameter. It was agreed to maintain a maximum tool diameter of 10mm. The equation for torque is the following:

$$T = \frac{Td}{2} Ft \ [Nm] \tag{7}$$

Where T is the torque [Nm], Td [m] is the tool diameter and Ft [N] is the tangential force. Using the worst-case scenario from the results of the previous table resulted in a required torque of, at least, 0.13Nm.

The literature also recommends certain cutting speeds according to the type of material [85].

Some sources suggest cutting speeds higher than 300m/min up to 480m/min for ABS [85] and lower cutting speed for PLA [86]. To achieve these values a higher speed flexibility spindle motor is needed. Cutting speed depends on the tool diameter, that is fixed according to the operation, and the spindle speed. This relation is represented by the equation:

$$Vc = \frac{\pi \ D \ n}{1000} \ [m/min] \tag{8}$$

Where Vc represents cutting speed in m/min, D is tool diameter in millimeters and n is spindle speed in rpm. Using all the requirements, namely the minimal torque, spindle speed, minimal weight and minimal dimensions, the following spindle motor was selected.

Figure 55 - Xinghuangduo 300W Spindle [87]

Table 9 - Spindle Motor Specifications

Power [W]	300
Operating Voltage [V]	12-48
Speed [RPM]	3000-12000
Torque [Nm]	0.4
Net Weight [kg]	0.8
Diameter [mm]	52
Type	Brushed DC Motor

Due to the recommended usage from the manufacturer for this motor, it will be assumed that it can withstand the required radial and axial forces. Manufacturer does not provide further information regarding this topic, but the recommended materials for this spindle are plastics, wood and light metals. Also, higher powered variations of this motor are provided with a cooling fan. The manufacturer does not supply the efficiency nor the maximum operating temperature for this motor, so it is assumed that the fan is appropriate for this motors cooling during worst case conditions.

3.4.2 Spindle Motor Mounting

The mounting structure for the motor will be like one provided by the motor manufacturer, even though it will be adapted to the machining head to optimize space, weight and mechanical resistance of the assembly. The following figures represent the manufacturers and the adapted spindle holder.

Figure 56 - Spindle holder usually used [87]

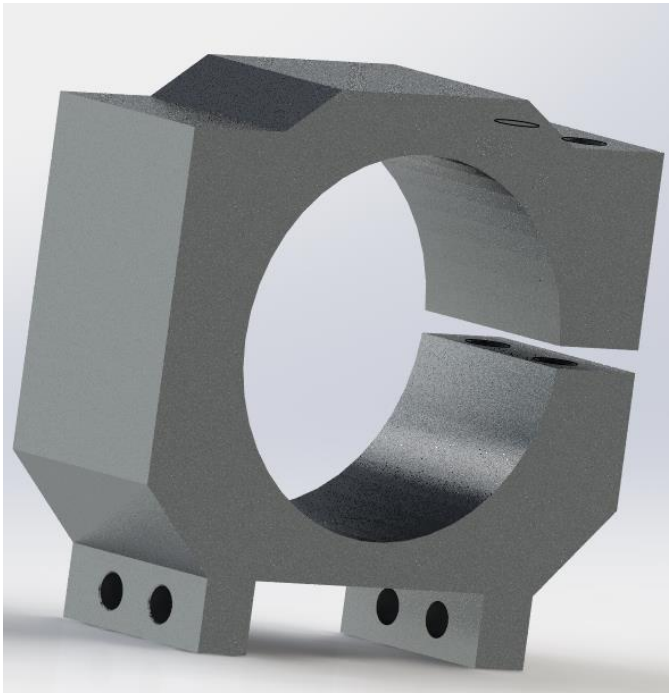

Figure 57 - Adapted spindle holder

This part will be mounted on the machining heads base, this is exemplified by the following figure:

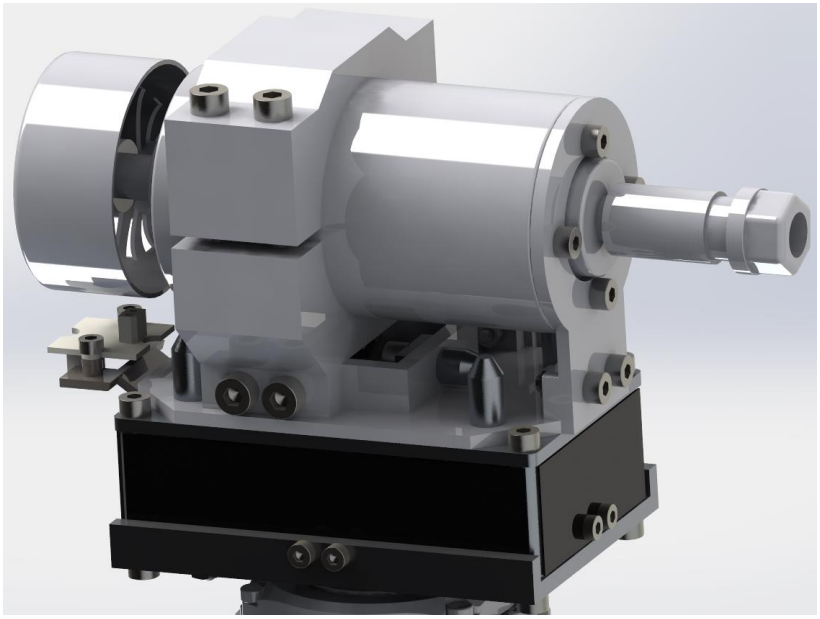

Figure 58 - Spindle mounted on the MH

With the weight of the spindle and other components, the selected material for structural applications was 2000 series Aluminum.

The machining head base has the proper holes for the guides on the lower mechanism assembly and space for the connecting part to enter.

During development of each component, the focus is to facilitate modifications in this project and for future enhancements of this dissertation to enlarge the selection of possible materials that can be worked on.

3.4.3 Spindle Motor Control

The spindle motor speed can be controlled through voltage manipulation. According to the operation and the material, the spindle speed must be adjusted. Controlling spindle speed must be done by a driver. This project requires remote control of spindle speed, so the controlling capability of the circuit must be digital. Also, the driver must have the ability to handle adequate output voltage according to motor specification and provide correct working current.

The voltage must be adequate to ensure full motor capability so the desired speed can be achieved. Current capability of the driver must be higher than the nominal motor current or even higher to account starting current spikes, otherwise the motor will burn the driver when requiring more current than the driver can provide.

The Cytron 25A 7-58V Single Brushed DC Motor Driver was selected.

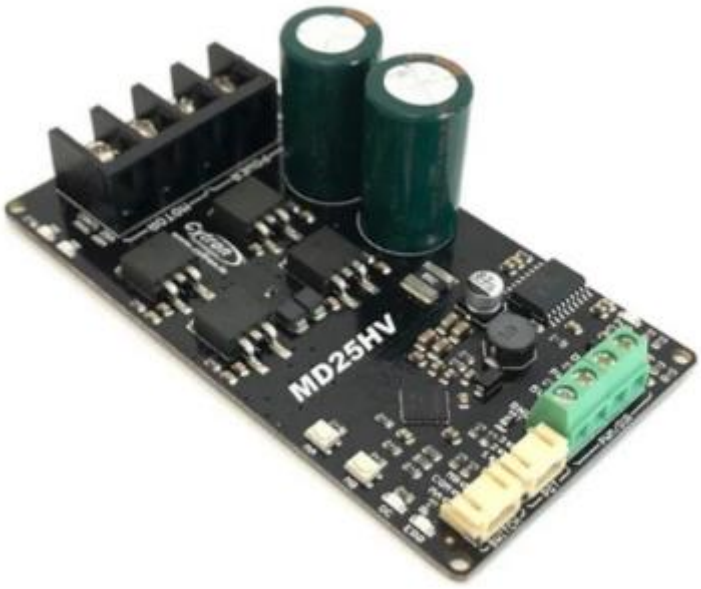

Figure 59 - Cytron 25A 7-58V Single Brushed DC Motor Driver [88]

This driver was specifically chosen for brushed direct current motor and it has the following characteristics:

Table 10 - Spindle Motor Driver Specification [88]

Operating Voltage [V]	7 - 58
Maximum Motor Current [A]	25 continuous, 60 peak
Output for the host Controller	5V (250mA max)
PWM/DIR Inputs [V]	1.8, 3.3, 5, 12 and 24 logic
PWM Frequency [kHz]	40 (output frequency fixed at 16)

This driver has the appropriate operating voltage (7 - 58V) for spindle motor control (12 – 48V) and it can handle peak current from the spindle motor.

The operational current was obtained through the following equation:

$$I[A] = \frac{P[W]}{U[V]} \quad \textbf{(9)}$$

In which the P is the spindle motor power in Watts, the U is the motor voltage in Volts, and I is the equivalent current in Amperes. This confirms that this driver can handle the required operational parameters. Not only the operational current is lower (6.25 A) than the one that can be handled by the driver (60 A peak), but also is several times higher. This provides a factor of safety in case of current peaks during start up, for example.

The driver can control the speed of the spindle motor but as it is a brushed DC motor, the spindle lacks feedback. Or in other words, there is no way of telling accurately the speed of rotation. The voltage provided can be used for the effective speed but due to material resistance, energy losses and relative movement the reading will never be accurate. So, for this purpose a sensor is needed. There are many ways to apply sensors to estimate rotational speed. Some of them use encoders, shafts with key/slots alongside a proximity sensor and others use photoelectric sensors to read specific points during rotation. For this application the latter was selected because the concept is simple, no further modifications to existing components are needed and photoelectric sensors are cheap and widely available. The Grove Infrared Reflective Sensor v1.2 photoelectric sensor was selected [89].

Figure 60 - Grove Infrared Reflective Sensor v1.2 [89]

The following table represent some of the relevant sensor specifications.

Table 11 - Grove Infrared Reflective Sensor v1.2 specifications [89]

Operating Voltage [V]	3.3-5
Operating Current [mA]	14.69 – 15.35
Effective detectable distance [mm]	4 - 15
Response time [µs]	10
Weight [g]	8.5
Dimensions [mm]	20 x 20

This sensor will be mounted in the previously mentioned holder with two screws. And will be aligned with the spindle fan. A marking will be made in the fan to identify point of rotation and consequently the rotational speed because the fan is fixed in the same axle

as the tool holder. The fan speed will correspond to the tool rotation speed. This sensor will be connected to the micro-controller and give a more accurate rotational speed reading.

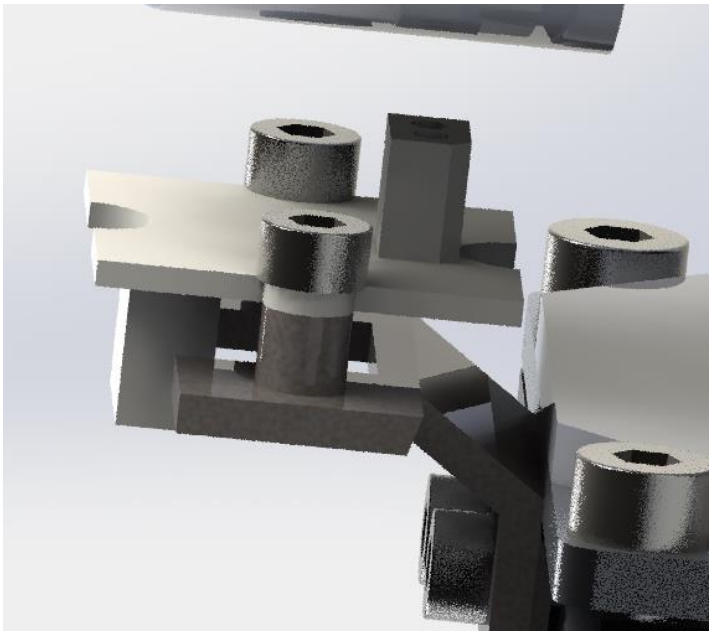

Figure 61 - Sensor mounting

3.4.4 Spindle Tools

Depending on the operation, different tools will be used. As this project requires material removal for better tolerances, two types of tools will be used. They are abrasive tools and cutting tools. Both types will be secured by the ER 11 collet that is provided with the spindle. This collet chuck has the possibility for 1 to 7 mm diameter tools. Considering the projects initial requirements, this collet chuck covers most of the pretended applications. Eventually, other collets can be used to adapt the spindle to different tools. It works by pressing the cutter against tapered teeth by fastening the collet.

Figure 62 - ER11 Collet [90]

3.4.4.1 Abrasive Tools

Some part features and defects require a different approach from cutting. For these instances abrasive tools will be used. A component was designed to fix abrasive discs. The ER collet from the spindle will be utilized to clamp an abrasive disc holder.

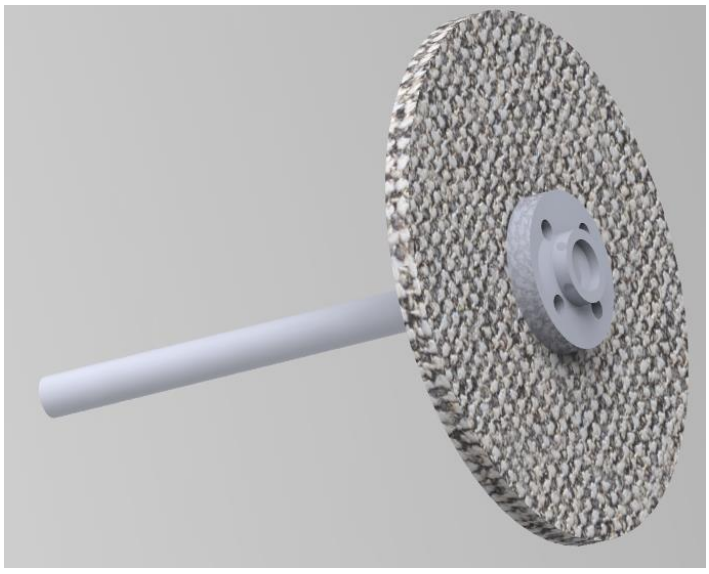

Figure 63 - Abrasive Disc Assembly

For ABS and PLA, the represented abrasive disc types were selected.

Figure 64 - Selected abrasive disc for plastics [91]

Different finishes require different abrasive disc roughness, so according to the desired task the appropriate disc is required.

3.4.4.2 Cutting Tools

Tools will be selected according to material requirements and the available chuck. The selected spindle comes with an ER11 collet.

As mentioned, the type of material, feature and desired finish, will dictate the required tool for the machining head. The following tools were selected through the Dormer Selector using the required cutter diameters and material set to thermoplastics.

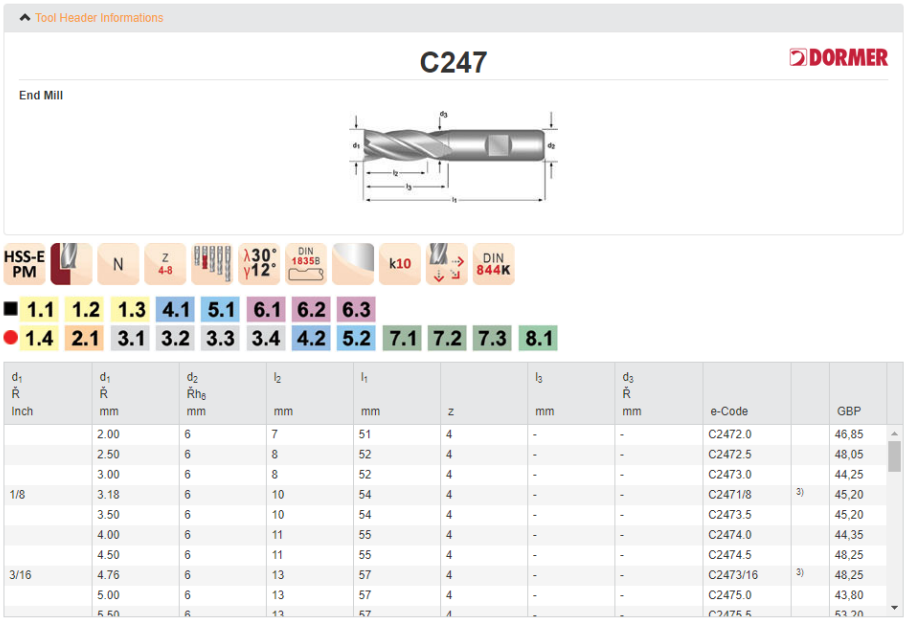

d_1 R inch	d_1 R mm	d_2 Rh_6 mm	l_2 mm	l_1 mm	z	l_3 mm	d_3 R mm	e-Code		GBP
	2.00	6	7	51	4	-	-	C2472.0		46,85
	2.50	6	8	52	4	-	-	C2472.5		48,05
	3.00	6	8	52	4	-	-	C2473.0		44,25
1/8	3.18	6	10	54	4	-	-	C2471/8	3)	45,20
	3.50	6	10	54	4	-	-	C2473.5		45,20
	4.00	6	11	55	4	-	-	C2474.0		44,35
	4.50	6	11	55	4	-	-	C2474.5		48,25
3/16	4.76	6	13	57	4	-	-	C2473/16	3)	48,25
	5.00	6	13	57	4	-	-	C2475.0		43,80

Figure 65 - End mill cutter for PLA [92]

This end mill cutter is ideal for PLA because it has 4 cutting teeth. This will accelerate operations and maintain low machining temperature, avoiding reaching the Tg.
For ABS the ideal cutter needs fewer teeth, so the following milling cutter was selected.

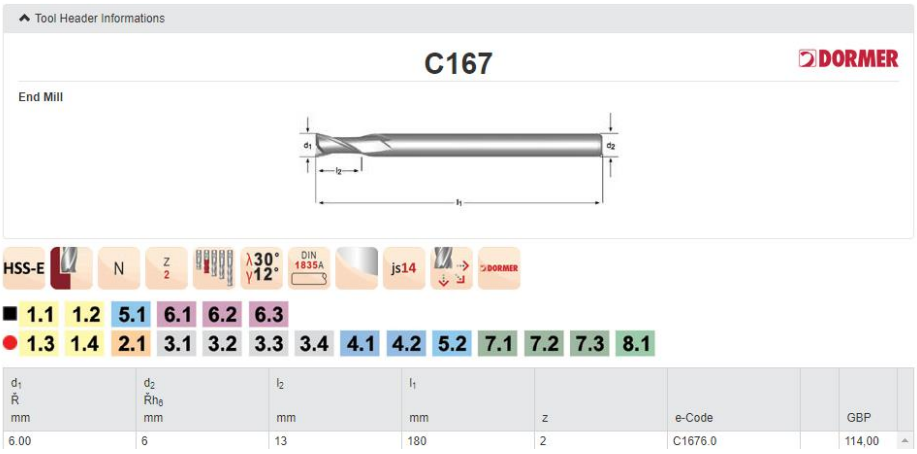

d_1 R mm	d_2 Rh_6 mm	l_2 mm	l_1 mm	z	e-Code		GBP
6.00	6	13	180	2	C1676.0		114,00

Figure 66 - End mill cutter for ABS [92]

These end mill cutters will be used for finishing operations in ABS and PLA. For other types of operations like ball nose end milling the following cutters were selected.

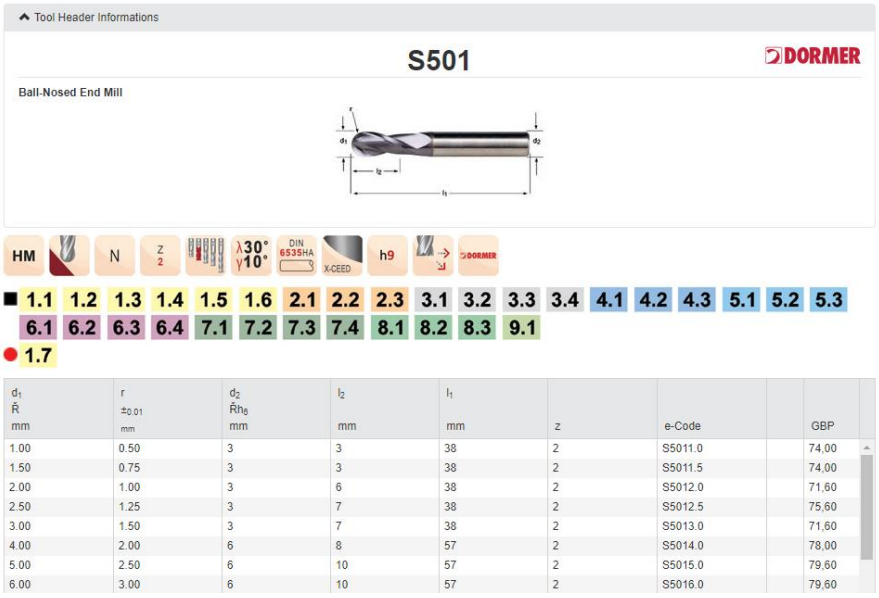

d_1 R mm	r ±0.01 mm	d_2 Rh8 mm	l_2 mm	l_1 mm	z	e-Code		GBP
1.00	0.50	3	3	38	2	S5011.0		74,00
1.50	0.75	3	3	38	2	S5011.5		74,00
2.00	1.00	3	6	38	2	S5012.0		71,60
2.50	1.25	3	7	38	2	S5012.5		75,60
3.00	1.50	3	7	38	2	S5013.0		71,60
4.00	2.00	6	8	57	2	S5014.0		78,00
5.00	2.50	6	10	57	2	S5015.0		79,60
6.00	3.00	6	10	57	2	S5016.0		79,60

Figure 67 - Ball End Mill cutter for ABS [92]

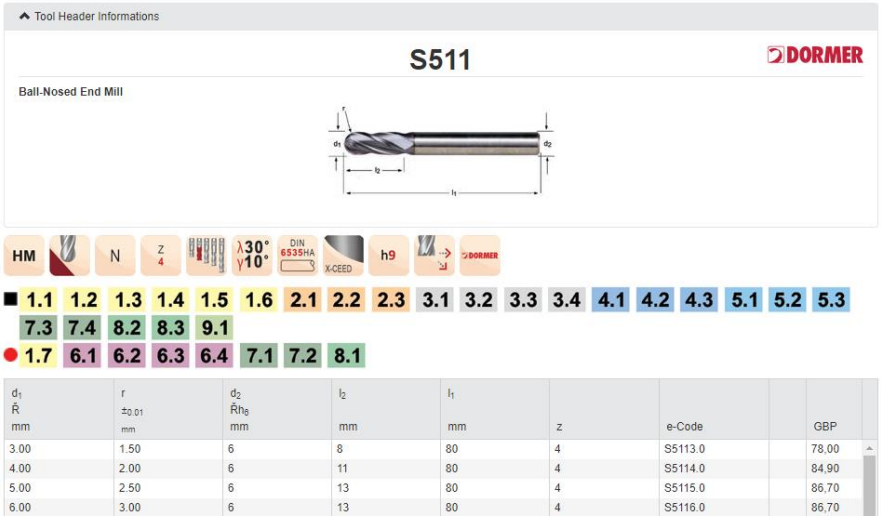

d_1 R mm	r ±0.01 mm	d_2 Rh8 mm	l_2 mm	l_1 mm	z	e-Code		GBP
3.00	1.50	6	8	80	4	S5113.0		78,00
4.00	2.00	6	11	80	4	S5114.0		84,90
5.00	2.50	6	13	80	4	S5115.0		86,70
6.00	3.00	6	13	80	4	S5116.0		86,70

Figure 68 - Ball End Mill cutter for PLA [92]

With these main cutters most of the operations can be performed. With original chuck any tool with maximum 7mm diameter can be used. For larger cutters, other chuck must be manually mounted.

4 Analysis

This chapter will describe different types of analysis that were made to ensure the integrity of the model during different types of solicitations. The first one is the static analysis and the second is the frequency analysis. The results obtained through these tasks will be used to validate and improve the model.

4.1 Static Analysis

This analysis focuses on the response of the assembly during the machining head connection to the robot. The study is conducted with the components in the connection position and the maximum loads are included along with different assembly orientations relative to the ground. Only the structural parts were analyzed as these are the ones subjected to larger loads. To optimize calculations and save time, the components were simplified and unnecessary features for the analysis were removed.

4.1.1 Components

Only the structural components were used it this analysis because they support the most load when the whole system is solicited. The more complex components were simplified to facilitate calculations and save time. This reduction in complexity is achieved mostly by removal of certain cosmetic and not relevant features for this study like fixation points for non-structural components.

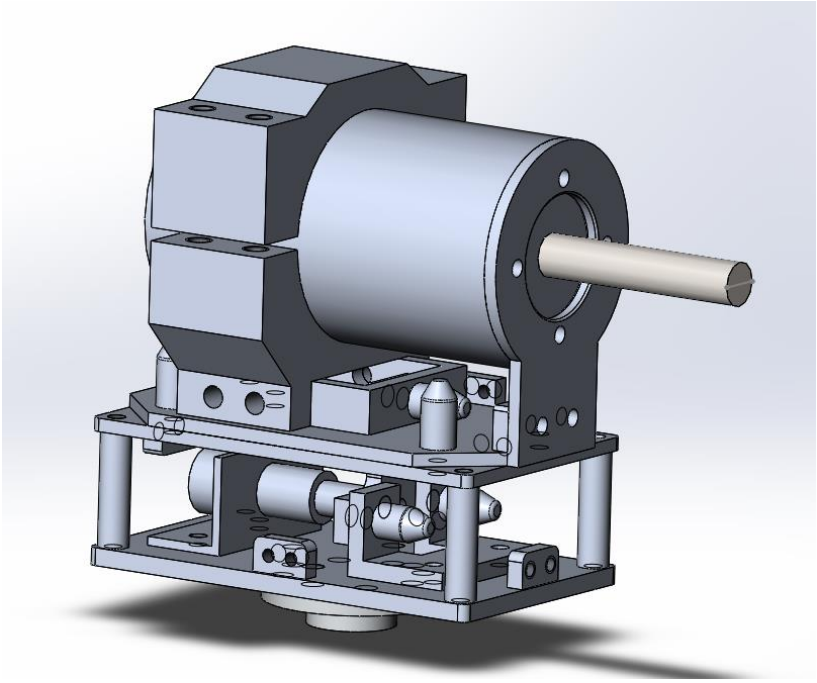

Figure 69 - Simplified Representation

Figure 70 - Complete Representation

4.1.2 Static analysis setup

For the fixation of the LM, fixed geometry was used in the bolt holes and the cylindrical face of the flange connector. As the robot model has a maximum payload of 3 kg, it is assumed that the standardized flange is enough to lock the LM to the robot without residual movement.

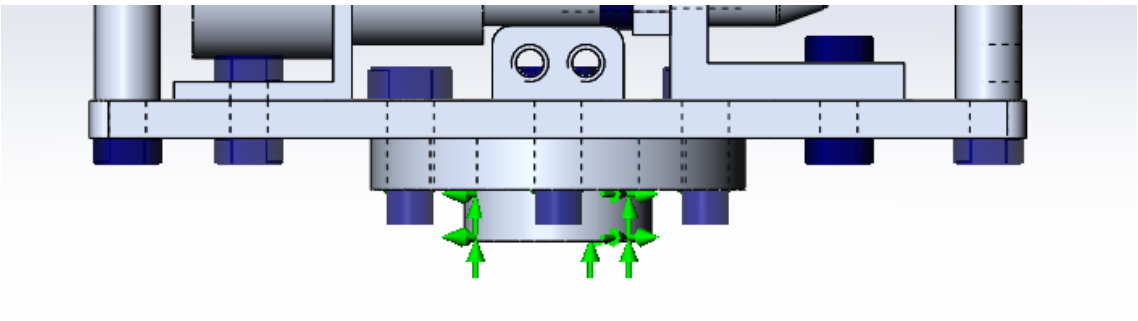

Figure 71 - Fixtures in Static Study

As for the general connections between components, all connections consist on a bolt or a bolt and nut set. The bolts used are the ones present in the CAD software analysis tool. Real bolt models can make the calculations more complex so, this approach was used. According to bolt size, the correct pre-load torque was applied.

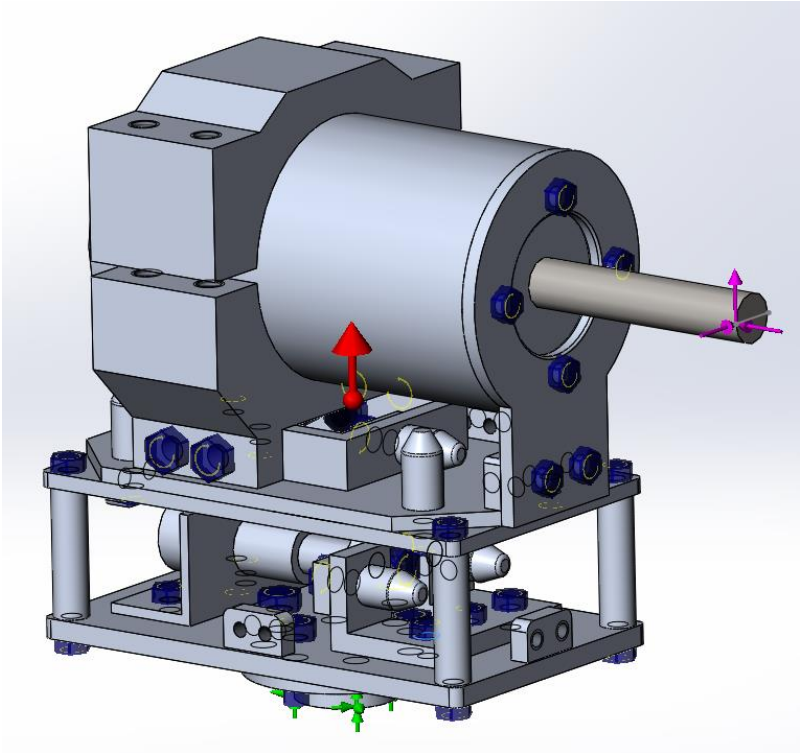

Figure 72 - Connections between components in Static Study

Using a 4.6 class bolt, the recommended tightening torque for M4 is 0.84 Nm, so this is the value that was used.

Threads	Friction coeff. $\mu_K = \mu_G$	Maximum preload $F_{M\,max}$ [kN]							Maximum tightening torque $M_{A\,max}$ [Nm]							Conversion factor X
		Property class based on ISO 898/1							Property class based on ISO 898/1							
		3.6	4.6	5.6/4.8	6.8	8.8	10.9	12.9	3.6	4.6	5.6/4.8	6.8	8.8	10.9	12.9	
M4	0,08	1,3	1,74	2,17	3,48	4,6	6,8	8,0	0,63	0,84	1,05	1,68	2,3	3,3	3,9	0,50
	0,10	1,26	1,68	2,10	3,36	4,5	6,7	7,8	0,73	0,97	1,21	1,94	2,6	3,9	4,5	0,58
	0,12	1,22	1,63	2,04	3,26	4,4	6,5	7,6	0,82	1,09	1,37	2,19	3,0	4,6	5,1	0,67
	0,14	1,19	1,58	1,98	3,17	4,3	6,3	7,4	0,91	1,21	1,51	2,42	3,3	4,8	5,6	0,76
M5	0,08	2,12	2,83	3,54	5,67	7,6	11,1	13,0	1,2	1,65	2,06	3,3	4,4	6,5	7,6	0,58
	0,10	2,06	2,74	3,43	5,48	7,4	10,8	12,7	1,4	1,9	2,4	3,8	5,2	7,6	8,9	0,70
	0,12	2,00	2,67	3,33	5,33	7,2	10,6	12,4	1,6	2,2	2,7	4,3	5,9	8,6	10,0	0,81
	0,14	1,94	2,59	3,23	5,18	7,0	10,3	12,0	1,8	2,4	3,0	4,8	6,5	9,5	11,2	0,93
M6	0,08	3,00	4,01	5,01	8,02	10,7	15,7	18,4	2,1	2,8	3,6	5,7	7,7	11,3	13,2	0,72
	0,10	2,90	3,87	4,84	7,74	10,4	15,3	17,9	2,5	3,3	4,1	6,6	9,0	13,2	15,4	0,86
	0,12	2,82	3,76	4,71	7,53	10,2	14,9	17,5	2,8	3,7	4,7	7,5	10,1	14,9	17,4	0,99
	0,14	2,74	3,65	4,57	7,31	9,9	14,5	17,0	3,1	4,1	5,2	8,3	11,3	16,5	19,3	1,14
M8	0,08	5,4	7,3	9,1	14,6	19,5	28,7	33,6	5,2	6,9	8,6	13,8	18,5	27,2	31,8	0,95
	0,10	5,3	7,1	8,8	14,2	19,1	28,0	32,8	6,0	8,0	10,0	16,1	21,6	31,8	37,2	1,13
	0,12	5,15	6,9	8,6	13,8	18,6	27,3	32,0	6,8	9,1	11,3	18,2	24,6	36,1	42,2	1,32
	0,14	5,0	6,7	8,3	13,4	18,1	26,6	31,1	7,5	10,1	12,6	20,1	27,3	40,1	46,9	1,51

Figure 73 - Bolt Preloads according to Class [93]

The global contact is set to “no penetration” as it is mandatory when using bolts and nuts, but some component contacts are set to “bonded” to simulate their real function. This applies to the motor holder /motor, because they are clamped together and tool / motor to balance the model (marked with red in the following figure). Shaft movement in case of “no penetration” causes imbalance in the simulation.

For the mesh used in these analysis a curvature-based mesh was used as it delivers good results with a significant reduction in calculation time. Using the curvature-based mesh reduced the simulation time from 25 minutes to 18 minutes in relation to the default type of mesh.

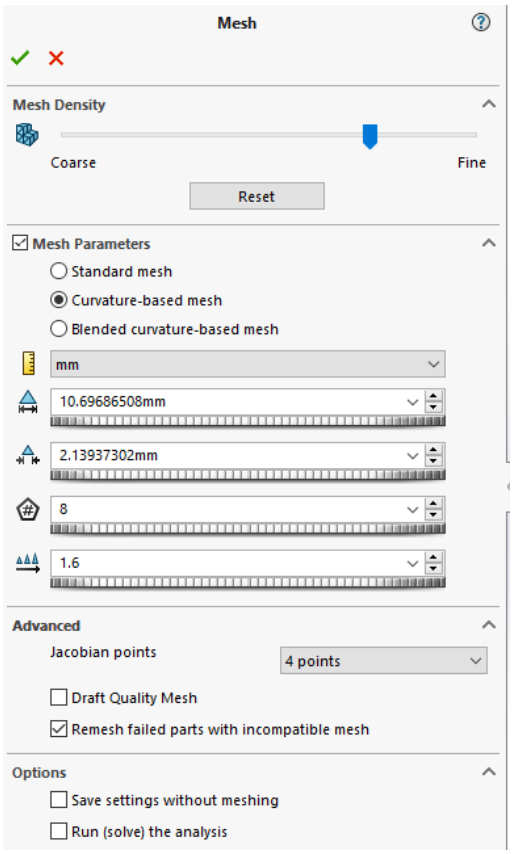

Figure 74 - General mesh parameters used for the studies

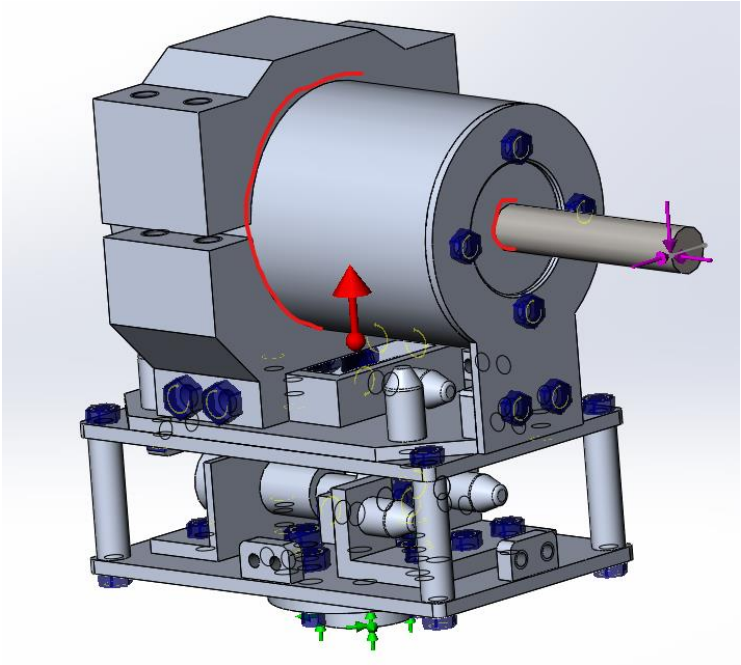

Figure 75 - Contact Representation

The final step was the application of solicitations. These solicitations are the maximum machining forces applied on the cutting tool and gravitational acceleration. Different orientations for both solicitations were tested to simulate different orientations and cutting

conditions. These solicitations were obtained from the plots of carbon fiber reinforced plastics machining studies. After reaching the conclusion that the orientation of these solicitations had little impact on the results, only one set of directions was used.

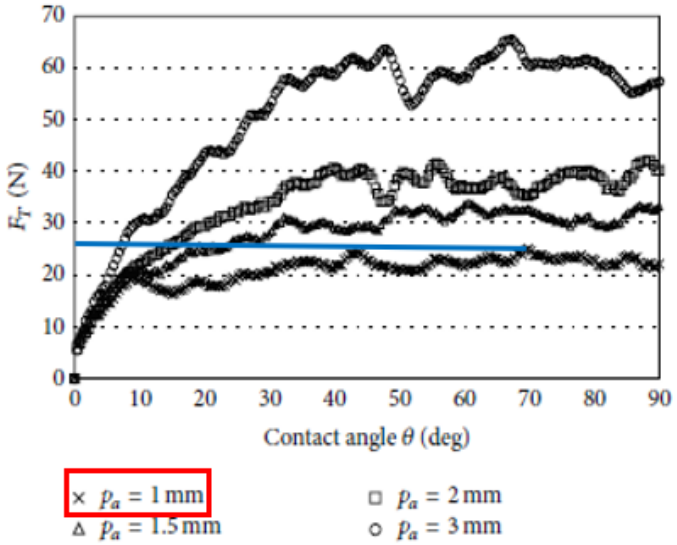

FIGURE 11: F_T component versus contact angle (cutting speed = 100 m/min; feed per tooth = 0.022 mm).

Figure 76 - Minimal forces tested [51]

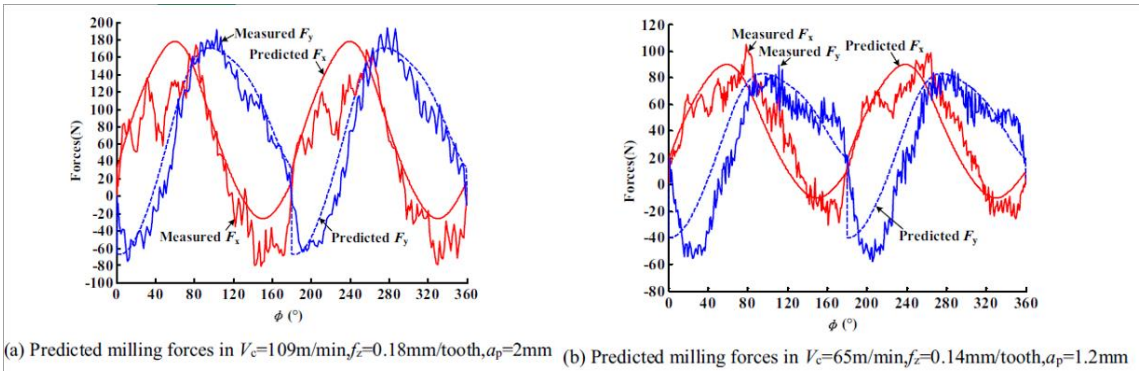

(a) Predicted milling forces in V_c=109m/min,f_z=0.18mm/tooth,a_p=2mm (b) Predicted milling forces in V_c=65m/min,f_z=0.14mm/tooth,a_p=1.2mm

Figure 77 – Maximal forces tested [52]

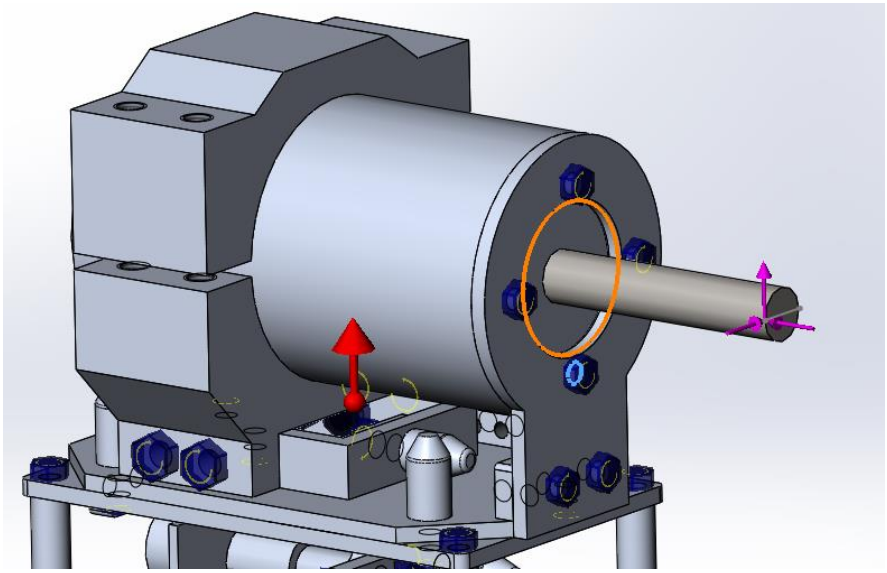

Figure 78 - Representation of the solicitations

The following table represents the 3 different sets of force used in the studies:

Table 12 - Sets of force used in studies

Forces [N]	Fx	Fy	Fz
1	30	30	80
2	100	100	150
3	300	300	450

4.1.3 Results

For the first set of solicitations, the weaker forces were utilized. These forces are aimed at the proposed use of this system, ABS and PLA. The second and third set of forces will determine the possible use of this system to other materials.

During assessments it was decided to aim for a von Mises Stress safety factor of 2, or in other words, all the components are subjected to a maximum stress of half of the Yield Stress of the material.

Results for the first set of forces (1)

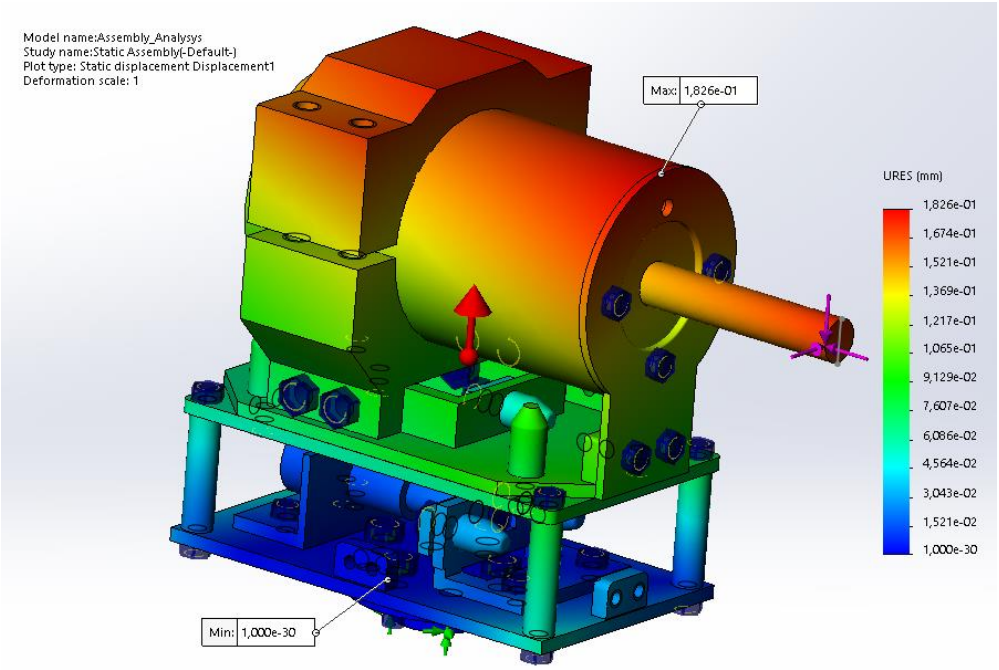

Figure 79 - Normal displacement plot (Force 1)

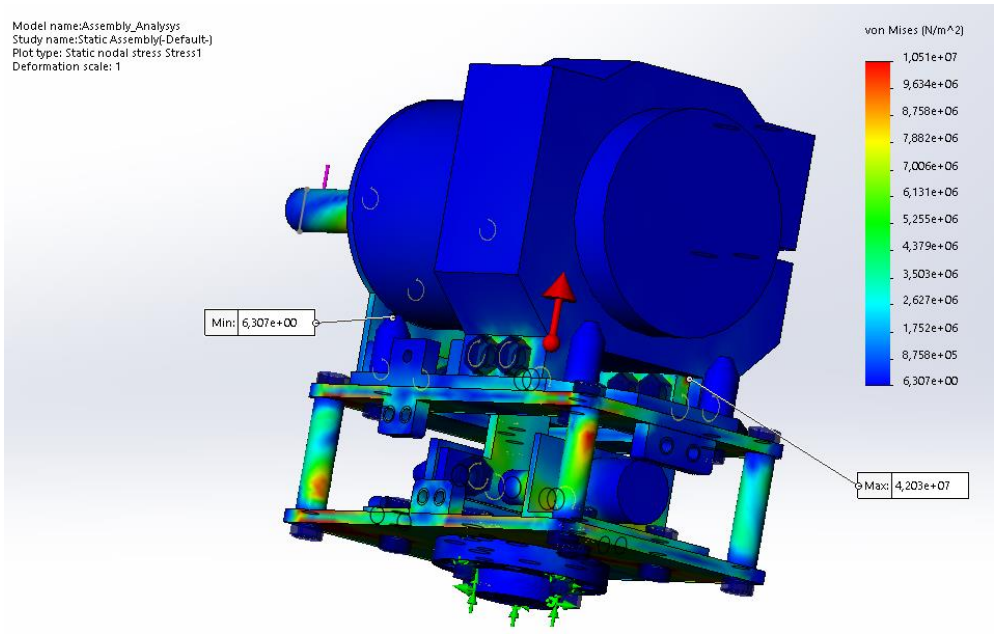

Figure 80 - von Mises Stress Plot (Force 1)

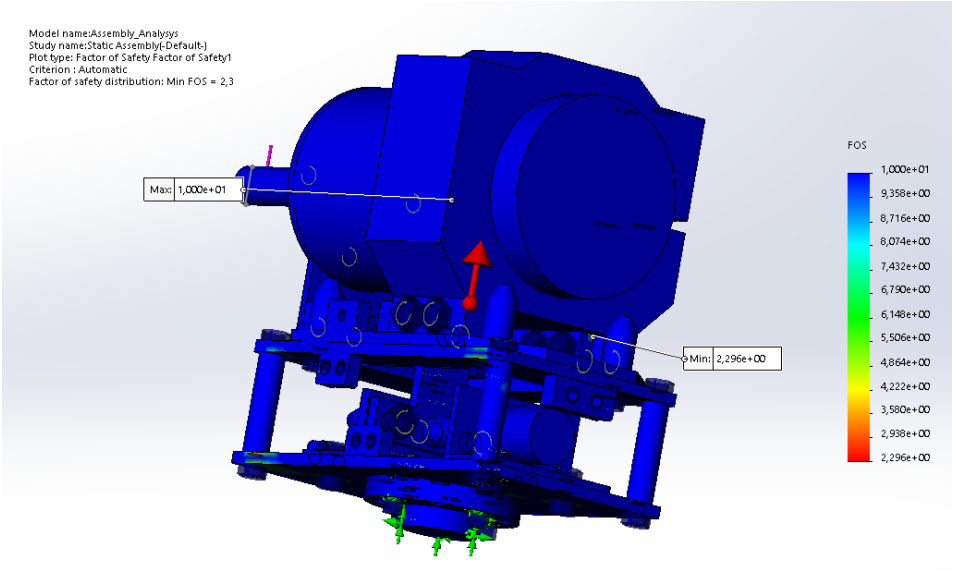

Figure 81 - von Mises factor of safety plot (Force 1)

The first set of forces provide an adequate result which gives a von Mises safety factor of 2.2 along with a cutting shaft displacement of 0.18mm.

Results for the second set of forces (2)

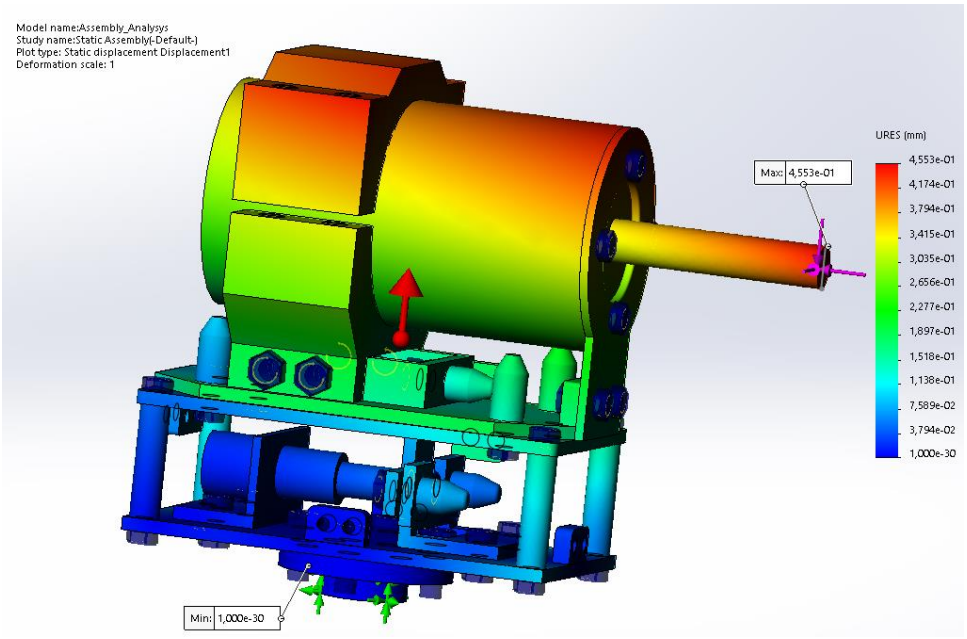

Figure 82 - Normal displacement plot (Force 2)

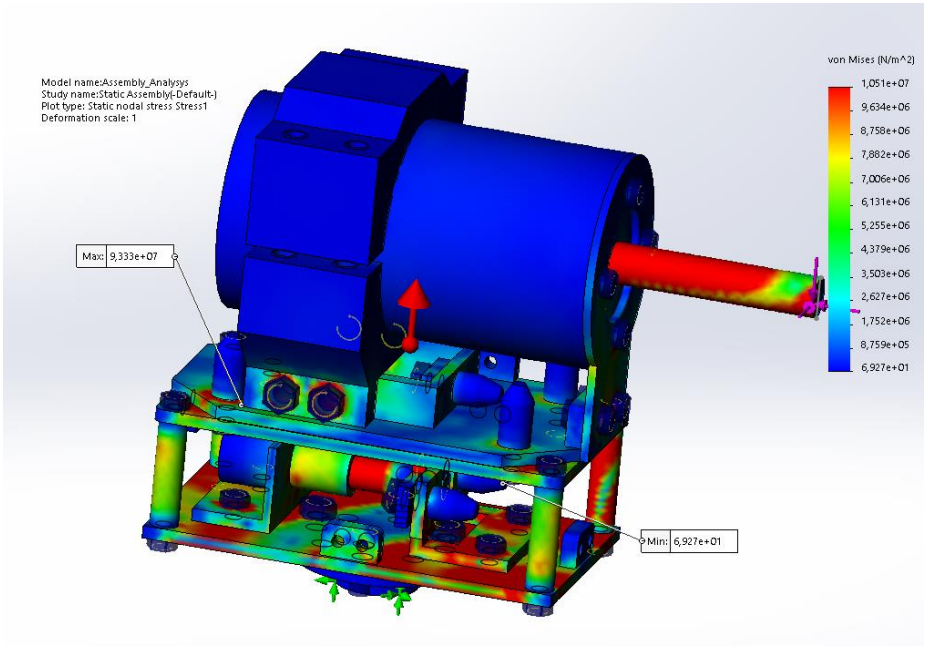

Figure 83 - von Mises stress plot (Force 2)

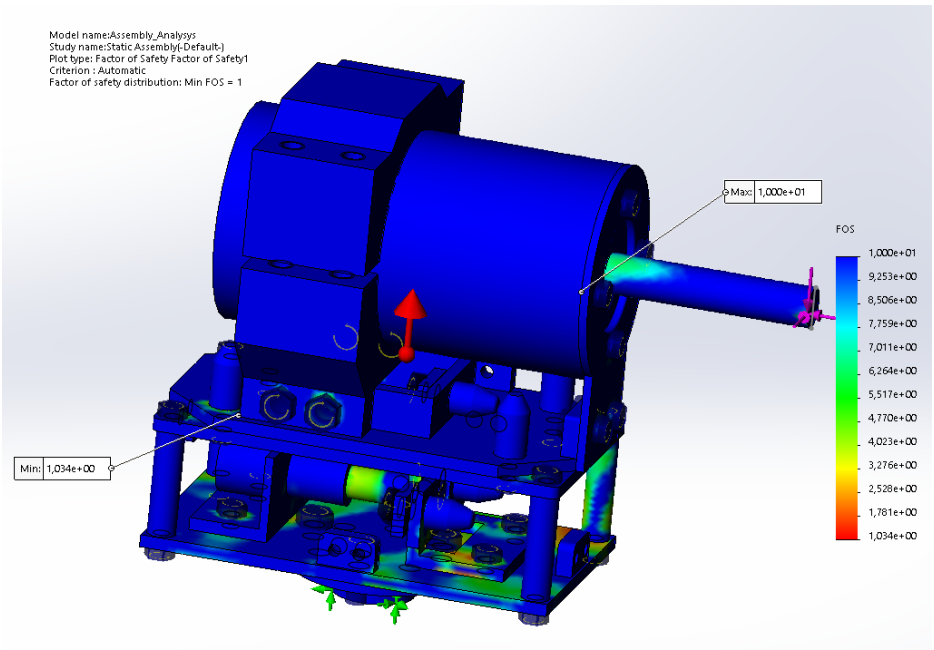

Figure 84 - von Mises factor of safety plot (Force 2)

Results for the third set of forces (3)

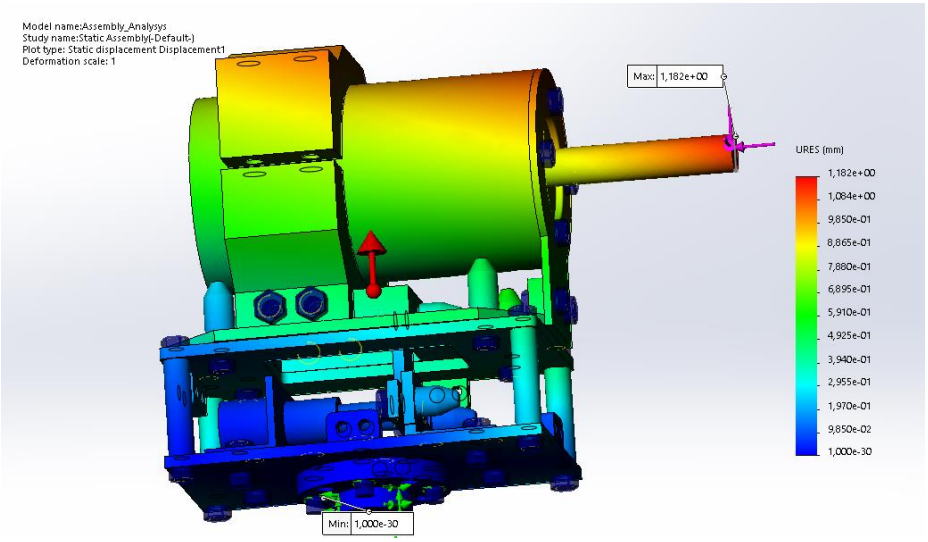

Figure 85 - Normal displacement plot (Force 3)

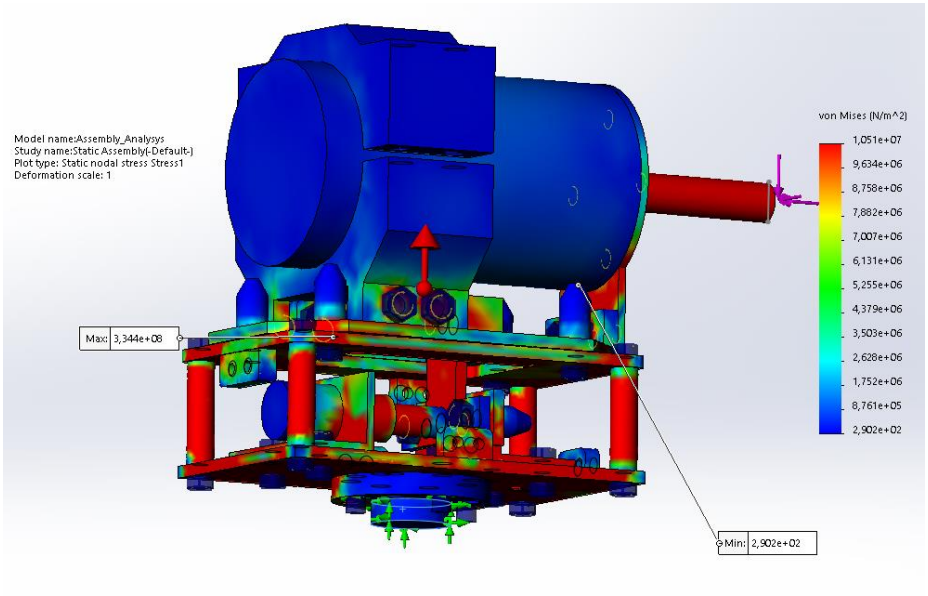

Figure 86 - von Mises stress plot (Force 3)

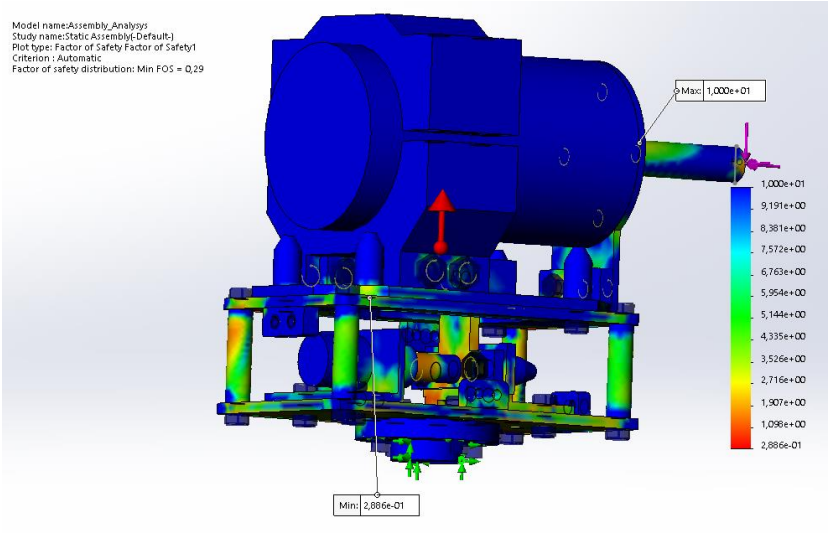

Figure 87 - von Mises factor of safety plot (Force 3)

To improve these results, several parts were reinforced with larger thickness and/or area. This will result in more material resisting the solicitations and reduce the displacement occurred in the critical parts of the assembly. The following parts were altered:

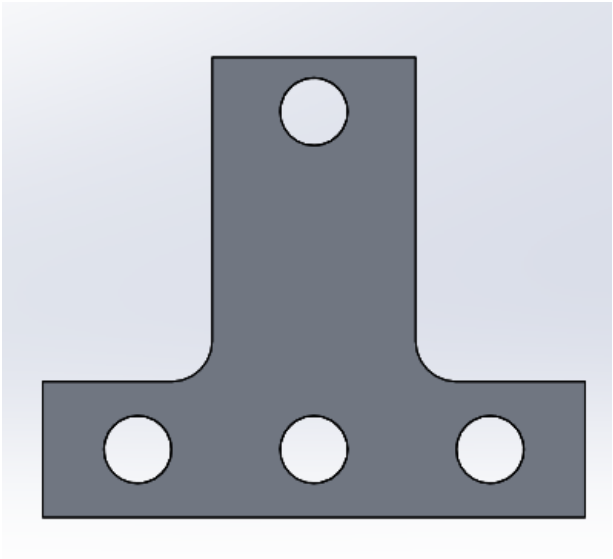

Figure 88 - RH/LM connector

This connector was modified in the thickness that went from 3 to 4mm and the addition of 1mm in radius fillet in the stress concentration area.

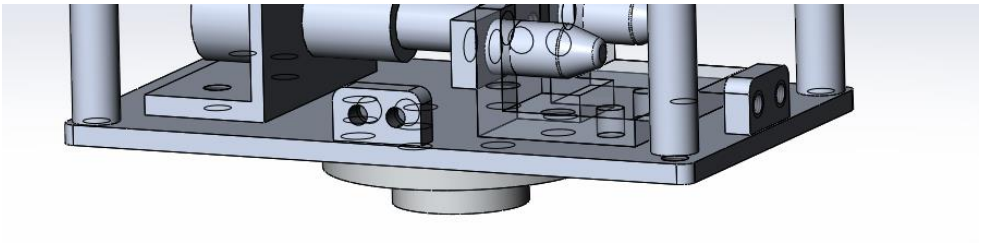

Figure 89 - LM bottom plate

As this component is the holding block of the whole structure, its thickness was increased from 3mm to 4mm.

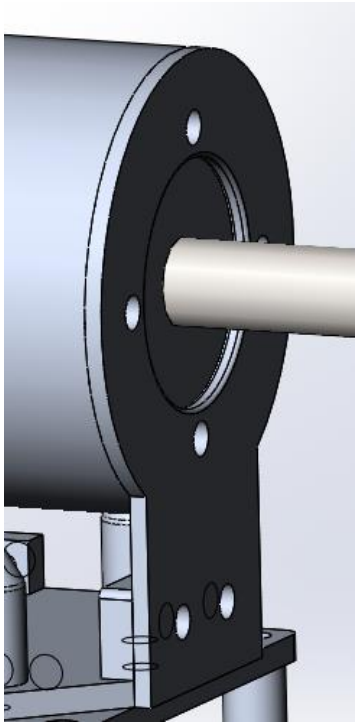

Figure 90 - Spindle motor front shield

The spindle motor front shield had a 2mm thickness which is not adequate for the component that will hold a structural position. To reduce internal stress of this component, the thickness was increased to 3mm.

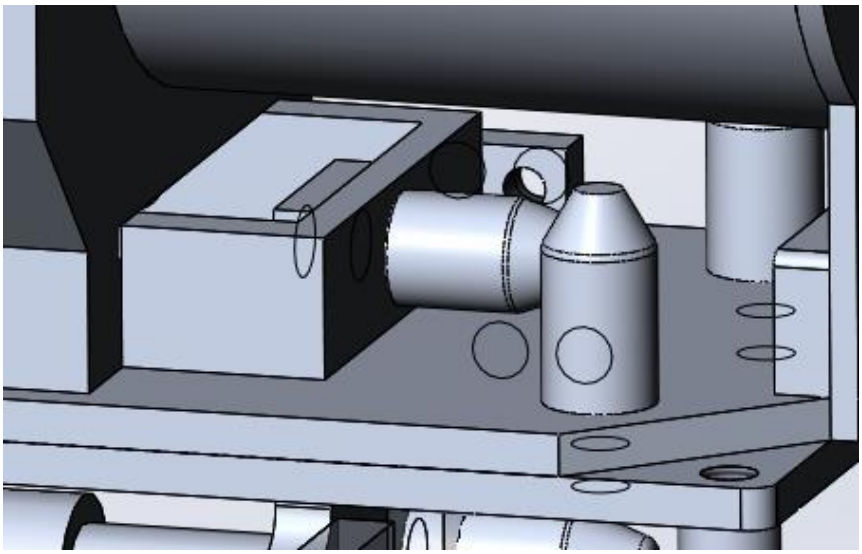

Figure 91 - MH connector receptacle

The thickness of the MH connector receptacle was increased from 3mm to 4mm. The objective is to reduce rotation of the MH in relation to LM and increase contact area of the connector pin and the MH receptacle.

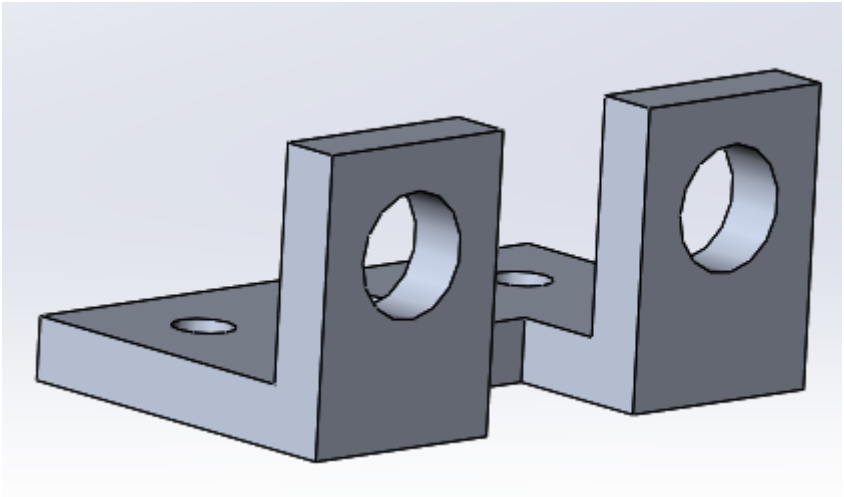

Figure 92 - LM connector receptacle

The initial design for the receptacle was changed to the one represented. This change is aimed at the rigidity of the receptacle, which must support most of the solicitations. The design was changed to accommodate 3 M4 bolts instead of 2 and the thickness was increased from 3mm to 4mm.

After performing these changes, the studies were repeated, and these were the results:

Modified results for the first set of forces (1)

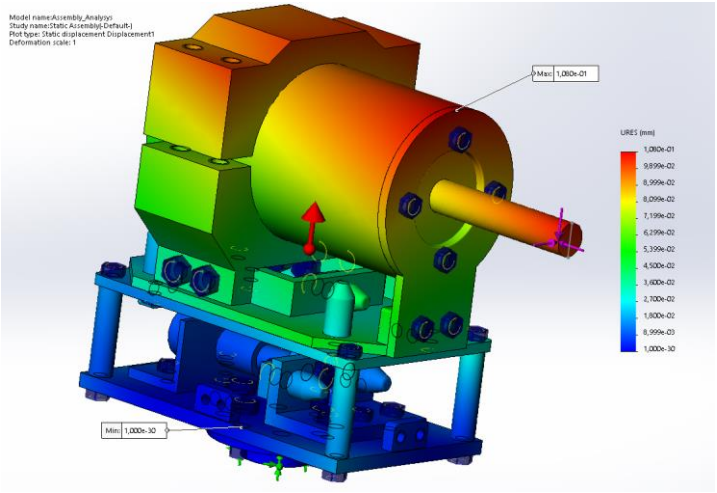

Figure 93 - Modified normal displacement results (Force 1)

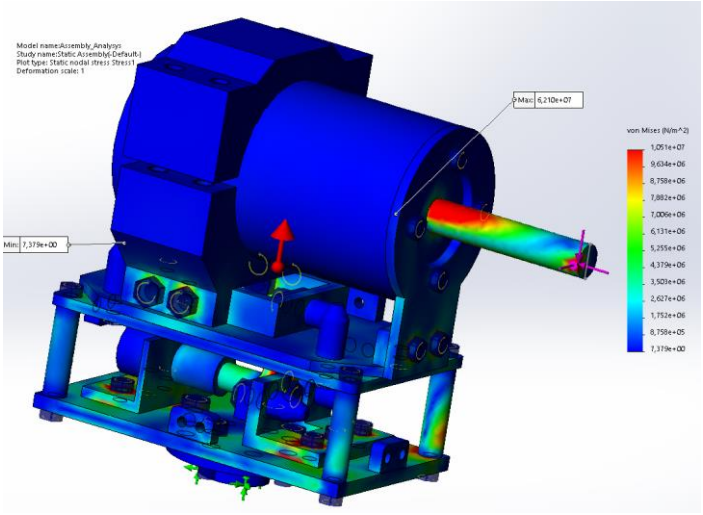

Figure 94 - Modified von Mises stress (Force 1)

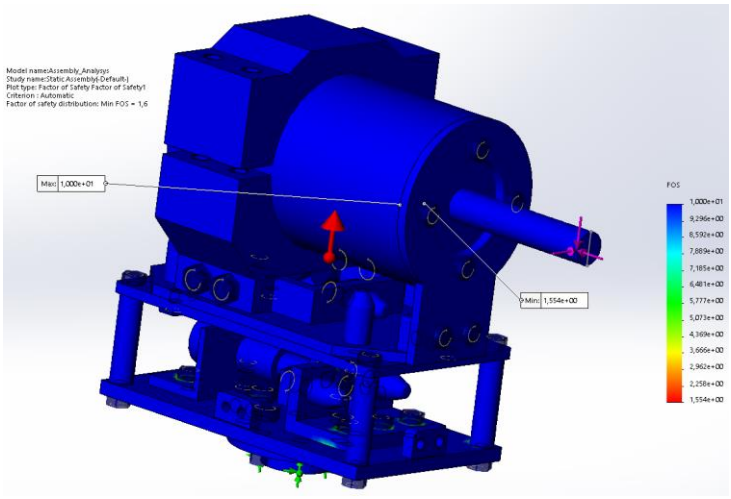

Figure 95 - Modified von Mises stress factor of safety (Force 1)

Modified results for the second set of forces (2)

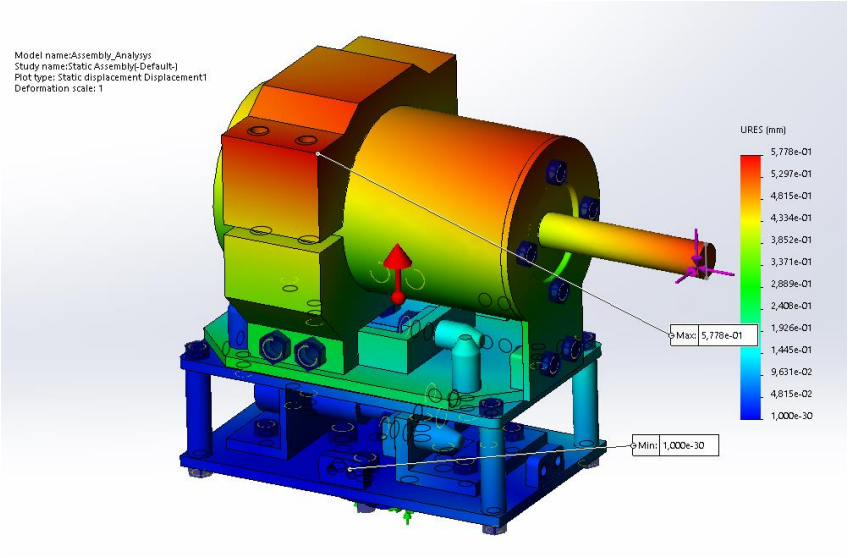

Figure 96 - Modified normal displacement results (Force 2)

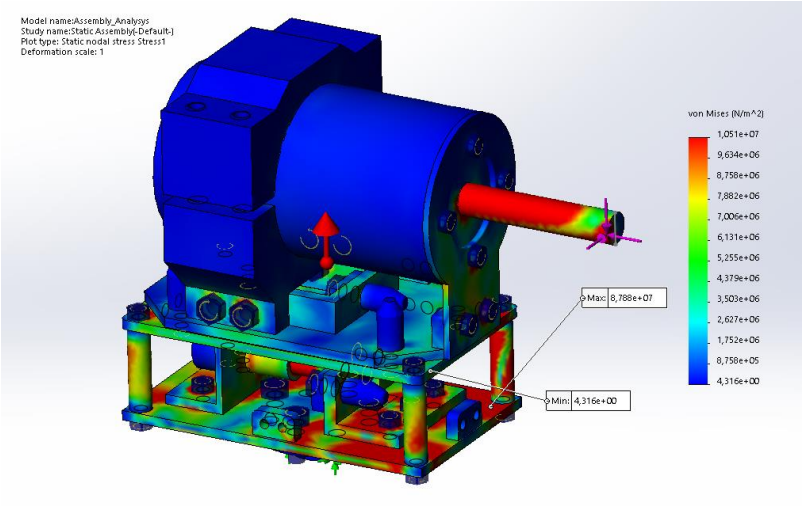

Figure 97 - Modified von Mises stress results (Force 2)

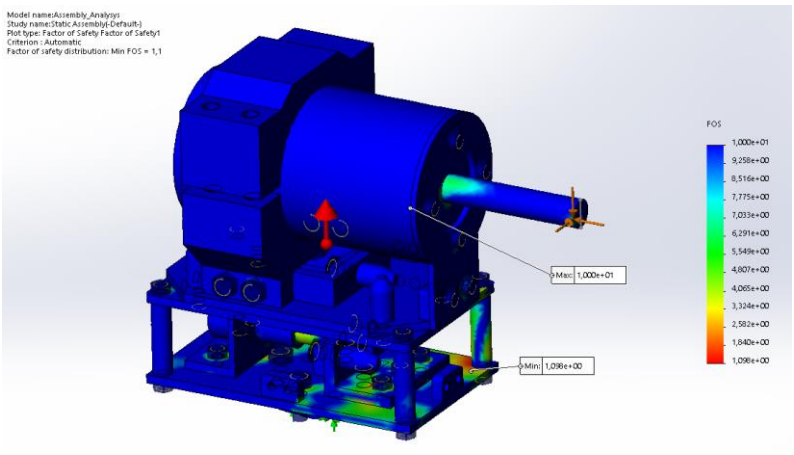

Figure 98 - Modified von Mises Stress results (Force 2)

Modified results for the third set of forces (3)

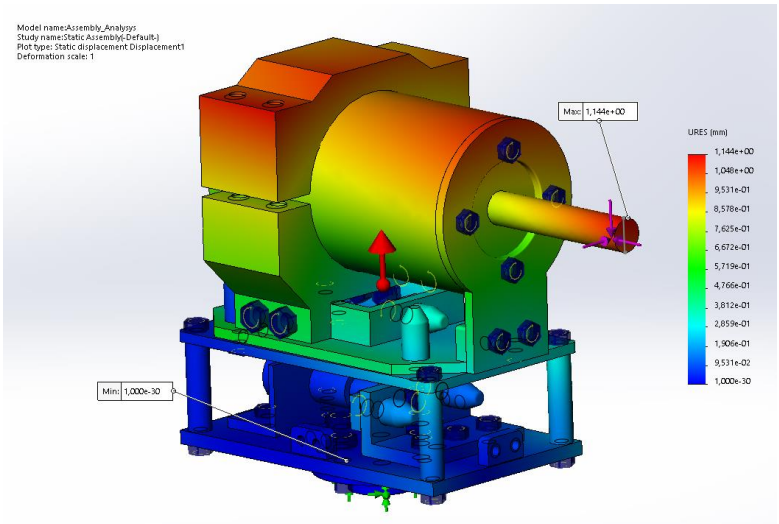

Figure 99 - Modified normal displacement results (Force 3)

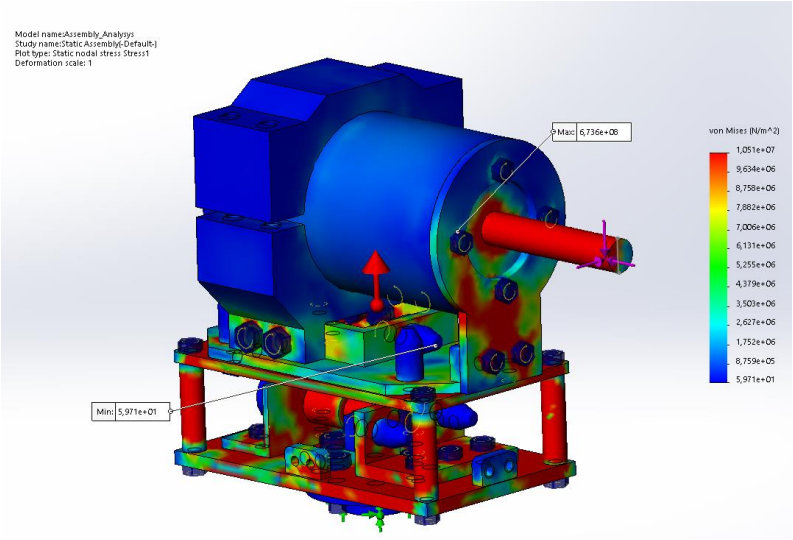

Figure 100 - Modified von Mises stress results (Force 3)

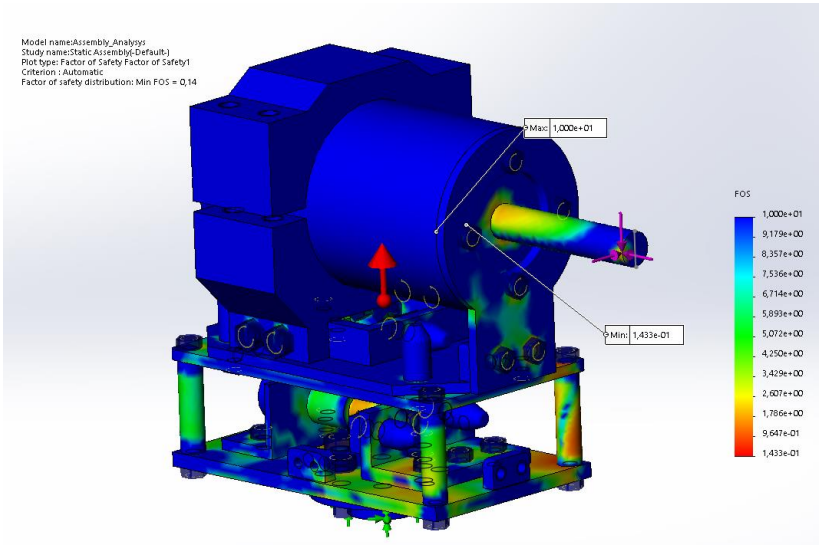

Figure 101 - Modified von Mises stress safety factor (Force 3)

The following table resumes the results obtained from the modifications.

Table 13 - Static results table

	Force 1		**Force 2**		**Force 3**	
Results	Initial	Final	Initial	Final	Initial	Final
Max. Normal Disp. [mm]	0.183	0.108	0.455	0.578	1.18	1.14
Max. von Mises Stress [MPa]	42.5	62.0	93.3	87.8	334.4	673.3
Min. FOS	2.23	1.554	1.034	1.1	0.29	0.14

These results show that the increased solicitation produce larger displacements and stresses, as expected. But from their interpretation, the maximum stress value is always in the same spot in the interior of the motor/shaft interface. As the real configuration is composed of other components like bearings and coils, this result should be ignored. The rest of the results are consistent and show a decrease of stresses with the rigidity modification (less vibrant colors).

4.2 Frequency Analysis

The frequency analysis is needed to ensure that the dynamic loading and motor rotational frequency does not interfere with the natural frequency of the assembly, as this could potentially influence the accuracy of the cutting or even harm the structure and its components.

The fixtures and loading for this study were the same used for the static analysis. Some differences reside in the use of modeled bolts and nuts for the connections instead of virtual ones, the transformation of some components in remote forces to simplify the analysis and detailing of the analyzed parts. Some lighter components were not used as they would not change substantially the natural frequency of the system. The motor used in this analysis is solid because it is the component with the largest mass of the assembly.

4.2.1 Components

The components used were the same as in the static study except for the bolts and nuts. These were selected via Toolbox and fixed in their respective locations.

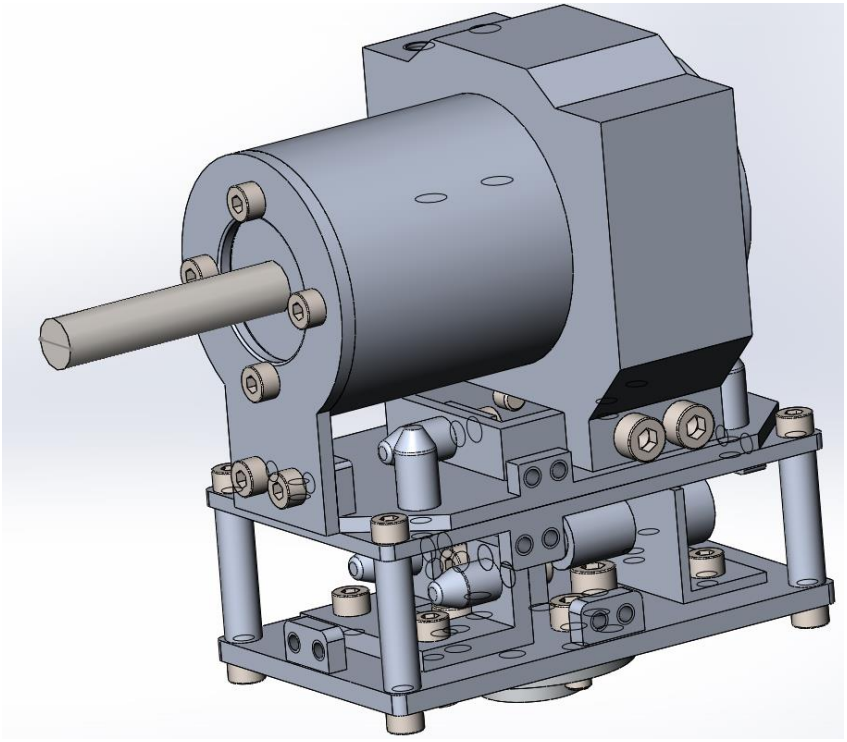

4.2.2 Frequency analysis setup

The fixtures used in this study was the same as in the static study. The contacts between components are “bonded”. The solicitations from the static study were replicated in the frequency study.

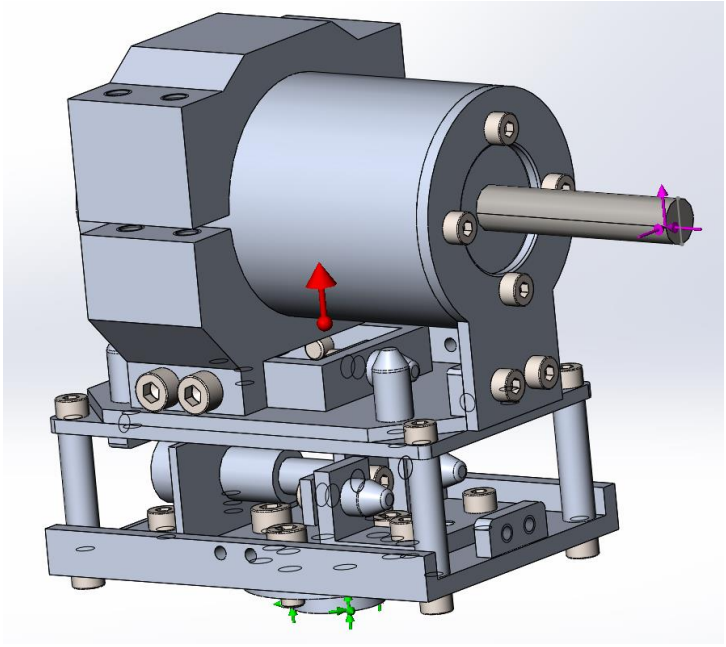

Figure 102 - Frequency study setup representation

4.2.3 Results

The results show that the first two natural frequencies of the assembly are 268 Hz. This value must be distant from the frequency of the spindle motor. The maximum spindle speed is 12000 rpm, and this translates it to 200 Hz.

Study name:Frequency 1

Mode No.	Frequency(Rad/sec)	Frequency(Hertz)	Period(Seconds)
1	1 684,6	268,12	0,0037297
2	1 685,9	268,31	0,003727
3	3 918,9	623,71	0,0016033
4	6 074,6	966,81	0,0010343
5	7 646,4	1 217	0,00082172

Figure 103 - Resultant natural frequencies

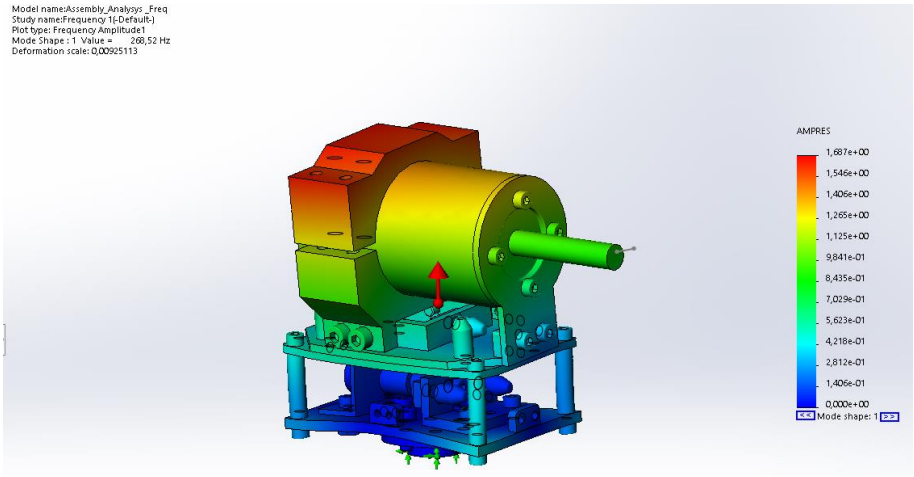

Figure 104 - First mode of vibration

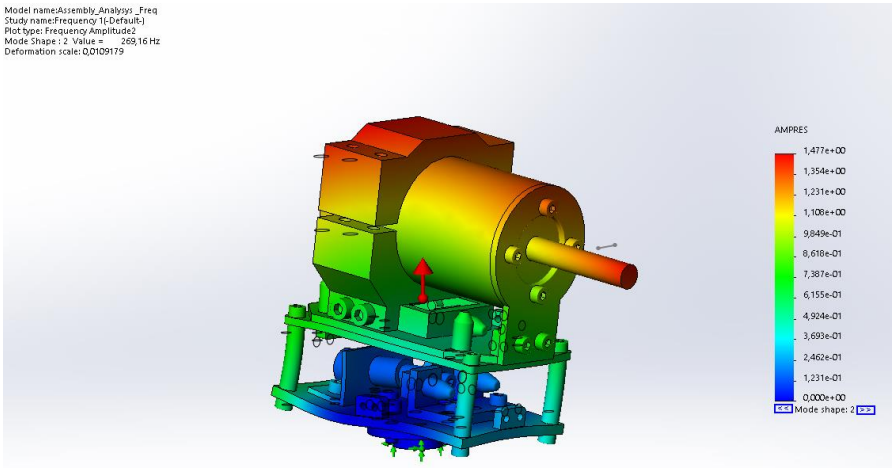

Figure 105 - Second mode of vibration

The first two resonant frequencies have some distance from the system maximum frequency, but the mode of their vibration is harmful for the structure and could harm the machining results. To ensure safety, the aim of disparity between frequencies was 100 Hz. This could be achieved by removing mass from the system or improving its rigidity.

The system was modeled with weight reduction in mind so further significant weight reduction is not possible. The increased rigidity strategy was adopted.

There are several possibilities in increasing system rigidity like higher thickness in structural components and reinforcing features. For this specific case due to the modes of vibration, the latter was chosen. For this feature a bend in the base plate of the LM was implemented.

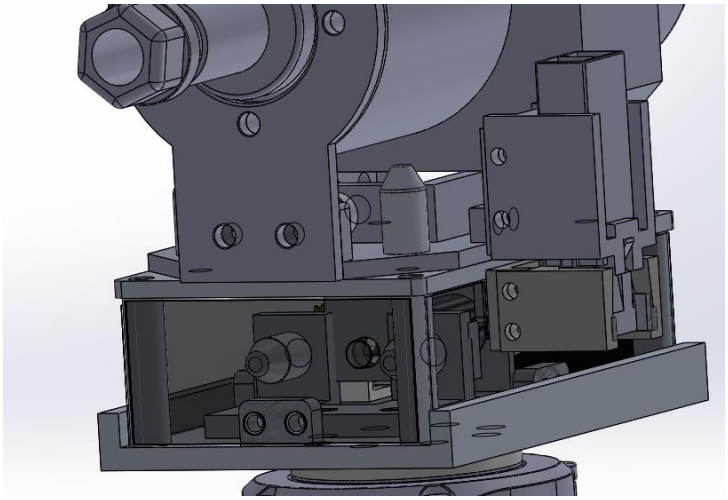

Figure 106 - LM base plate reinforcement bend

This will increase the material that is bending and thus increase bending resistance. The modification will increase slightly the weight, but the benefits are superior. After running the modified study, the following results were obtained:

Study name:Frequency 1

Mode No.	Frequency(Rad/sec)	Frequency(Hertz)	Period(Seconds)
1	1 841,5	293,08	0,003412
2	1 894,3	301,49	0,0033169
3	4 159,6	662,02	0,0015105
4	6 504,4	1 035,2	0,00096599
5	7 902,2	1 257,7	0,00079512

Figure 107 - Resultant natural frequencies after modifications

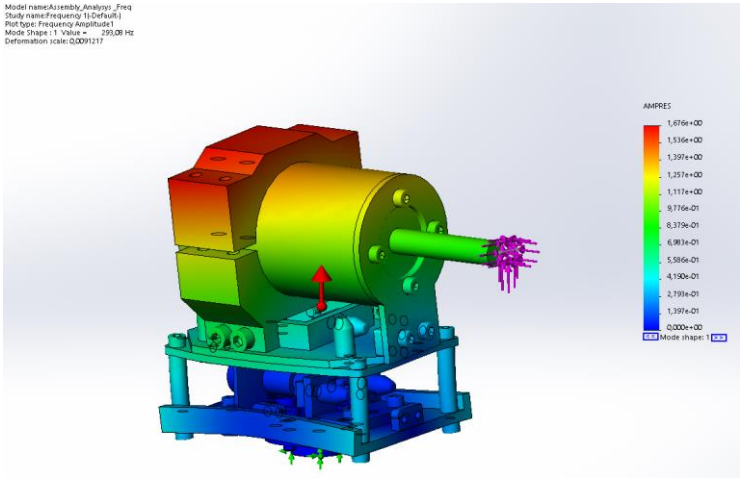

Figure 108 - Modified first mode of vibration

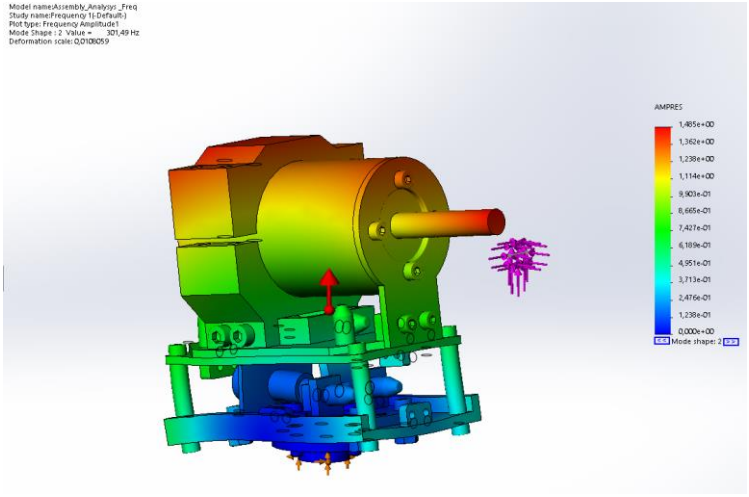

Figure 109 - Modified second mode of vibration

The natural frequencies of the assembly changed accordingly and now are almost at the desired value. As this action is merely a safety precaution on an already over dimensioned structure, this modification will be set as final.

4.3 Weight Analysis

The final analysis is the weight of the structure. This analysis verifies the objective weight of the system and if it reaches the target that was set earlier in the development. This analysis will divide each module of the project and evaluate its weight. The first module is the LM.

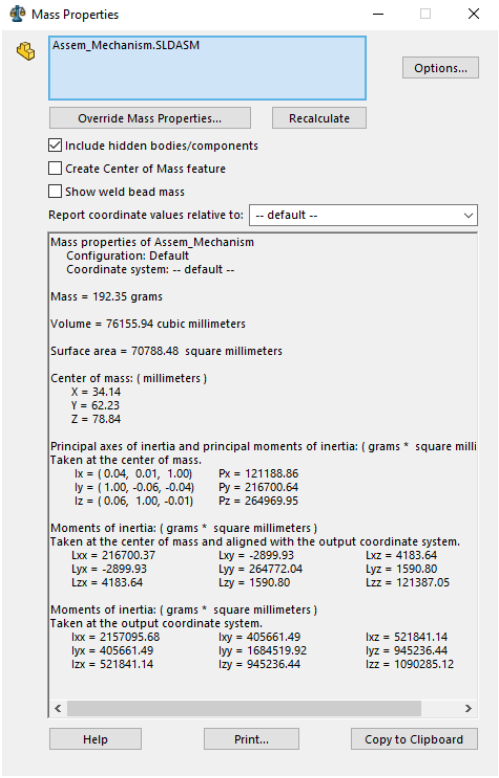

Figure 110 - LM total weight (without selected components)

The second figure represents the weight of the machining head without selected components.

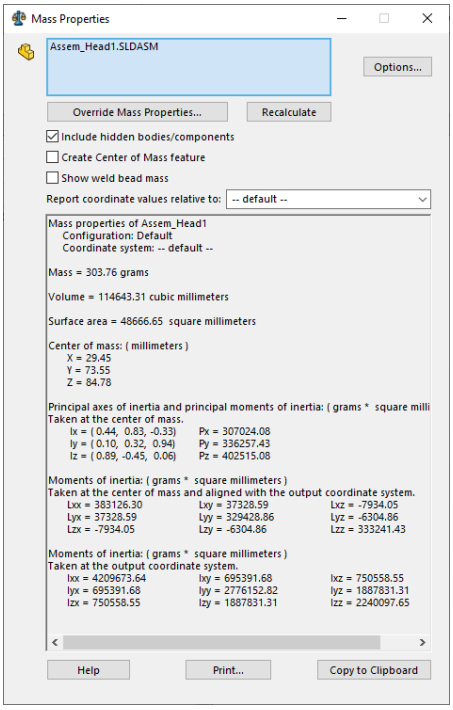

Figure 111 - MH total weight (without selected components)

The following table represents the weight distribution of the equipment.

Table 14 - Component weight distribuition

Component	Weight [kg]
Spindle Motor	0.800
Stepper Motor	0.028
Stepper Driver	0.002
Photoelectric Sensor	0.008
Structure	0.496
Total	1.334

The total weight of the structure and the selected components present in the 3D representation, with their respective materials, is 1.334kg which is under the defined maximum limit of 2kg.

5 Discussion

This dissertation provides a proposed solution for a machining head of a robot to improve surface quality of 3D FFF printed parts. Research was made on the previous works regarding similar implementations and using some of the gathered ideas, the initial model was designed.

To select the correct spindle for the MH an attempt at finding research on ABS and PLA machining forces was made. No study was found on this specific topic, so the next best approach mas made. Studies of machining forces on similar material were analyzed instead. Most of the information found was on plastics and reinforced plastics. As the data provided by these studies were detailed, they were selected for use in spindle selection. From the machining forces, a cutting torque was calculated, and this value was used in spindle selection. Other criteria were used in spindle selection like size, weight and maximal speed.

The first objective of this MH project was to have the possibility of automatically attach to the robot flange without external intervention. It was decided the use of electrical actuation in opposition to the pneumatic. For the actuation, a linear stepper motor was selected. This motor was made to control a connection claw that will connect the lower mechanism and the machining head, making both subassemblies a unit. The control for both motors was selected according to motor specification. The driver unit for the stepper was mounted in the LM and the driver for the spindle, due to size constraints, was left out of the assembly along with the controller of both units. To ensure correct feedback for the spindle speed control, a photoelectric sensor was mounted in the lower mechanism.

The lower mechanism and the machining head were built around the selected components but always allowing modifications. The main structural material that was used is aluminum to ensure that the weight objective is achieved. The lower mechanism has a cage like structure with an opening for the claw actuation while the MH uses a modified clamping solution from the spindle supplier.

Initial concept for the assembly was tested in a simulation environment for frequency and static force distribution. In the static study two sets of forces were tested, one with ABS and PLA in account and other set of forces was used to verify the system response when other materials are machined. The initial set of forces resulted in overall reduced stress concentrations and minimal displacements for lower forces. When higher forces were applied the system was starting to function under desired requirements. To resolve these

issues some modifications to the initial components were made. After the modifications, it was discovered that for the ABS and PLA forces, the structure handles better than before. As for the other set of forces the result are varied. Some conditions reduce displacement while others increase von Mises Stresses. The maximal stress results were influenced by the simplification because the higher stress value was in the interior of the motor representation, which is different in real conditions. Representation plots of the stress distribution shows a reduction in stresses while the structural rigidity is increased.

During frequency analysis it was discovered that the natural frequency of the assembly is to the maximum spindle frequency of 200 Hz. To increase safety, a reinforcement to the LM base plate, was made. This change increased the difference between natural frequency and the system functional frequency and reduced the severity of the first vibration modes.

This solution was developed to machine ABS and PLA but used reinforced plastic machining forces in account so, it could machine other stronger materials in theory but as it is mostly theoretical, several experiments are needed to verify functionality. Other assessments are needed in some areas like thermal management and component distribution. Thermal studies to discover how the components behave under load and interact with each other and component distribution to take in account for control units that were left out of the main assembly but were selected.

Some of the components need adjustment in order to make them easier to manufacture as that was one of the limitation of this concept. Production requirements were not implemented in the design of the assembly.

For future work it is recommended to test a prototype with most of the features of this assembly and verify how it behaves and if the tolerances are achieved.

6 Conclusion

The objective of this dissertation is the project of an automatically exchangeable machining head for a robot. This equipment needs to enhance the finish of 3D FFF printed parts made from filaments of ABS and PLA with cutting and grinding operations.

Connecting mechanism is composed of a claw and a linear stepper motor. The stepper motor will position the claw inside the fixation holes in the upper and lower machine head. The cutting is made by a spindle motor with an adjustable chuck for milling cutters and other accessories.

Initial objectives included reduced weight, that was achieved by using aluminum in the structural components, cutting tolerance, that was optimized for ABS and PLA but can be applied for some other materials without significant tolerance reduction and automatic actuation of the connecting mechanism, which was achieved using a stepper actuated claw.

Results for static and frequency studies demonstrate that the theoretical model is adequate for its application and the stability of the system is obtainable. Other applications require modification or further structural enhancement.

Nonetheless, the results need to be confirmed with prototypes and the forces that were used to design components verified as the current models use forces of stronger materials which can mean that the current iteration is over engineered.

The robot model used is for illustrative purposes so an adapted robot needs to be used in this solution or a custom made, which possibly is the patch that will be taken.

For future work is recommended to adjust the designed parts to be more manufacturing friendly, verify ABS and PLA actual cutting forces and according to the results, modify the current components. Furthermore, it is necessary to test the actuation of the connection mechanism and evaluate if the theoretical tolerances are met.

7 References

[1] A. Bandyopadhyay and S. Bose, Additive Manufacturing, Boca Raton: CRC Press, 2019.

[2] M. Ghazy and M. Hossam, "Effect of SLA Process Parameters on Part Build-Time," in *The 25th International Conference on Computer Theory and Applications*, Alexandria – Egypt, 2015.

[3] N. Martelli, C. Serrano, H. v. d. Brink, J. Pineau, P. Prognon, I. Borget and S. E. Batti, "Advantages and disadvantages of 3-dimensional printing in surgery: A systematic review," *Surgery*, vol. 159, pp. 1485-1500, 2016.

[4] V. Petrovic, J. V. Haro, O. Jordá, J. Delgado and J. R. Blasco, "Additive Layer Manufacturing: State of the art in industrial applications through case studies," *International Journal of Production Research*, 2010.

[5] M. Saffarzadeh, G. Gillispie and P. J. Brown, "SELECTIVE LASER SINTERING (SLS) RAPID PROTYTPING TECHNOLOGY: A REVIEW OF MEDICAL APPLICATIONS," in *Rocky Mountain Bio-engineering Symposium*, Denver, Colorado, 2016.

[6] S. Yuan, D. Strobbe, X. Li, J.-P. Kruth, P. V. Puyvelde and B. V. d. Bruggen, "3D printed chemically and mechanically robust membrane by selective laser sintering for separation of oil/water and immiscible organic mixtures," *Chemical Engineering Journal*, vol. 385, 2020.

[7] M. Beecroft, "Digital interlooping: 3D printing of weft-knitted textile-based tubular structures using selective laser sintering of nylon powder," *International Journal of Fashion Design, Technology and Education*, vol. 12, pp. 218-224, 2019.

[8] N. Roy, C. S. Foong and M. Cullinan, "Design of a Micro-Scale Selective Sintering System," in *27th Annual International Solid Freeform Fabrication Symposium*, Austin, Texas, 2016.

[9] M. Ghazy and M. Hossam, "Effect of SLA Process Parameters on Part Build-Time," in *The 25th International Conference on Computer Theory and Applications*, Alexandria, Egypt, 2015.

[10] W. Chen, F. Wang, K. Yan, Y. Zhang and D. Wu, "Micro-stereolithography of KNN-based lead-free piezoceramics," *Ceramics International*, vol. 45, pp. 4880-4885, 2019.

[11] J. P. Davim, Additive and Subtractive Manufacturing Emergent Technologies, De Gruyter, 2020.

[12] C. Schmidleithner, S. Malferrari, R. Palgrave, D. Bomze, M. Schwentenwein and D. M. Kalaskar, "Application of high resolution DLP stereolithography for fabrication of tricalcium phosphate scaffolds for bone regeneration," *Biomedical Materials*, vol. 14, 2019.

[13] N. Guo and M. C. Leu, "Additive manufacturing: technology, applications and research needs," *Frontiers of Mechanical Engineering*, vol. 8, pp. 215-243, 2013.

[14] R. Singh and H. K. Garg, "Fused Deposition Modeling – A State of Art Review and Future Applications," in *Reference Module in Materials Science and Materials Engineering*, 2016.

[15] J. Guo and J. Zhang, "Study of Environment Maintenance Feasibility of Polyvinyl Alcohol," in *International Conference on Information Computing and Applications*, 2011.

[16] C. Reyes, R. Somogyi, S. Niu, M. A. Cruz, F. Yang, M. J. Catenacci, C. P. Rhodes and B. J. Wiley, "Three-Dimensional Printing of a Complete Lithium Ion Battery with Fused Filament Fabrication," *ACS Applied Energy Materials*, vol. 1, pp. 5268-5279, 2018.

[17] E. Prasad, M. T. Islam, D. J. Goodwin, A. J. Megarry, G. W. Halbert, A. J. Florence and J. Robertson, "Development of a hot-melt extrusion (HME) process to produce drug loaded Affinisol™ 15LV filaments for fused filament fabrication (FFF) 3D printing," *Additive Manufacturing*, vol. 29, 2019.

[18] M. Leite, J. Fernandes, A. M Deus, M. Vaz and L. Reis, "STUDY OF THE INFLUENCE OF 3D PRINTING PARAMETERS ON THE MECHANICAL PROPERTIES OF PLA," in *3rd International Conference on Progress in Additive Manufacturing (Pro-AM 2018)*, Singapore, 2018.

[19] L. Novakova-Marcincinova and J. Novak-Marcincin, "Testing of Materials for Rapid Prototyping Fused Deposition Modelling Technology," *World Academy of Science, Engineering and TechnologyInternational Journal of Industrial and Manufacturing Engineering*, vol. 6, no. 10, pp. 2082-2085, 2012.

[20] Plastics Europe, "Thermoplastics," [Online]. Available: https://www.plasticseurope.org/en/about-plastics/what-are-plastics/large-family/thermoplastics. [Accessed 1 12 2020].

[21] A. Y. Khan, S. Talegaonkar, Z. Iqbal, F. J. Ahmed and R. K. Khar, "Multiple Emulsions: An Overview," *Current Drug Delivery*, vol. 3, no. 4, pp. 429-443, 2006.

[22] T. Rogers, "Creative Mechanisms," 13 7 2015. [Online]. Available: https://www.creativemechanisms.com/blog/everything-you-need-to-know-about-abs-plastic. [Accessed 15 6 2020].

[23] Omnexus, "Glass Transition Temperature," [Online]. Available: https://omnexus.specialchem.com/polymer-properties/properties/glass-transition-temperature. [Accessed 20 12 1].

[24] R. J. Gutierrez, "PLA Plastic/Material: All You Need to Know in 2020," All3DP, 11 1 2020. [Online]. Available: https://all3dp.com/1/pla-plastic-material-polylactic-acid/. [Accessed 18 6 2020].

[25] M. Leite, J. Fernandes, A. M Deus, M. Vaz and L. Reis, "STUDY OF THE INFLUENCE OF 3D PRINTING PARAMETERS ON THE MECHANICAL PROPERTIES OF PLA," in *3rd International Conference on Progress in Additive Manufacturing (Pro-AM 2018).*, Singapore, 2018.

[26] M. Attaran, "The rise of 3-D printing: The advantages of additive manufacturing over traditional manufacturing," *Business Horizons*, vol. 60, pp. 677-688, 2017.

[27] V. P. Filipovic, J. V. Haro, O. Jordá, J. Delgado, J. R. B. Puchades and L. Portoles, "Additive Layer Manufacturing: State of the art in industrial applications through case studies," 2010.

[28] S.-H. Ahn, S. R. And, P. K. Wright, M. Montero, D. Odell and S. Roundy, "Anisotropic material properties of fused deposition modeling ABS," *Rapid Prototyping Journal*, vol. 8, p. 248–257, 2002.

[29] All3DP, "FDM 2.0: Reinforced Layer Adhesion with Kai Parthy," 26 3 2019. [Online]. Available: https://all3dp.com/4/fdm-2-0-reinforced-layer-adhesion-kai-parthy/. [Accessed 15 3 2020].

[30] K. Gunaydin and H. S. Türkmen, "Common FDM 3D Printing Defects," in *International Congress on 3D Printing (Additive Manufacturing) Technologies and Digital Industry*, Antalya, Turkey, 2018.

[31] MiT, 2012. [Online]. Available: http://fab.cba.mit.edu/classes/863.12/people/laia.mogassoldevila/projects/p7.html. [Accessed 20 1 2020].

[32] M. T. University, 8 9 2018. [Online]. Available: https://web.archive.org/web/20180908030836/http:/www.mfg.mtu.edu/cyberman/machining.html. [Accessed 5 2 2020].

[33] J. J. Ph.D., "Abrasive Cutting Pros & Cons," Metal Cutting Corporation, 7 6 2018. [Online]. Available: https://metalcutting.com/knowledge-center/abrasive-cutting-pros-and-cons/. [Accessed 10 3 2020].

[34] Engineering Articles, "Machining Operation and Types of Machining Tools," 26 08 2015. [Online]. Available: http://www.engineeringarticles.org/machining-operation-and-types-of-machining-tools/. [Accessed 16 01 2021].

[35] BlogMech, "Drilling Machine Operations | Functions of a Drilling Machine," 15 04 2020. [Online]. Available: https://blogmech.com/drilling-machine-operations-functions-of-a-drilling-machine/. [Accessed 16 01 2021].

[36] Wilhelm Bauer GmbH & Co. KG, "Turning," [Online]. Available: https://www.wilhelm-bauer.de/drehen.php. [Accessed 16 01 2021].

[37] B. M. C. Centers. [Online]. Available: http://www.belotti.com/de-DE/milling-process.aspx. [Accessed 6 3 2020].

[38] Market Prospects, "What Is a Bridgeport Milling Machine? The Background of Bridgeport Mill," 04 08 2020. [Online]. Available: https://www.market-prospects.com/articles/bridgeport-milling-machine. [Accessed 16 01 2021].

[39] M. Theias, "What Is CNC Milling? – Simply Explained," All3D, 11 1 2019. [Online]. Available: https://all3dp.com/2/what-is-cnc-milling-simply-explained/. [Accessed 12 9 2020].

[40] R. H. Todd, D. K. Allen and L. Alting, in *Manufacturing Processes Reference Guide*, Industrial Press Inc., 1994, pp. 43-48.

[41] Modern Machine Shop, "Three Face Milling Myths & Truths," 19 07 2019. [Online]. Available: https://www.mmsonline.com/articles/three-face-milling-myths-truths. [Accessed 17 01 2021].

[42] Cusack Manufacturing, "Milling, Drilling, and CNC," [Online]. Available: https://cusackmanufacturing.com/pages/milling. [Accessed 17 01 2021].

[43] CGSTool, 26 7 2016. [Online]. Available: https://www.cgstool.com/blog/what-is-end-milling/. [Accessed 6 3 2020].

[44] Custompart.net, "Milling Speed and Feed Calculator," [Online]. Available: https://www.custompartnet.com/calculator/milling-speed-and-feed. [Accessed 17 01 2021].

[45] D. A. Dixit, "Types of Milling Cutters Used in Machining Process," Department of Mechanical Engineering, [Online]. Available: https://madhavuniversity.edu.in/types-of-milling-cutters.html. [Accessed 20 4 2020].

[46] "Milling formulas and definitions," Sandvik Coromat, [Online]. Available: https://www.sandvik.coromant.com/en-gb/knowledge/machining-formulas-definitions/pages/milling.aspx?_sm_au_=iVVRndBM7s0SJStsJB2VjKtqv28G6. [Accessed 5 2 2020].

[47] Mitsubishi Materials, "Cutting Power for Face Milling," [Online]. Available: http://www.mitsubishicarbide.com/en/technical_information/tec_rotating_tools/face_mills/tec_milling_formula/tec_milling_power_formula. [Accessed 18 01 2021].

[48] Sandvik Coromat, "Specific cutting force," [Online]. Available: https://www.sandvik.coromant.com/en-gb/knowledge/materials/pages/specific-cutting-force.aspx. [Accessed 18 01 2021].

[49] M. V. K.P., G. C. and C. E., "Cutting Force Modeling," in *CIRP Encyclopedia of Production Engineering*, Berlin, Heidelberg, Springer, 2014.

[50] Y. Patel, *The Machining of Polymers*, London, 2008.

[51] L. Sorrentino and S. Turchetta, "Cutting Forces in Milling of Carbon Fibre Reinforced Plastics," *International Journal of Manufacturing Engineering*, vol. 2014, 2014.

[52] F. Su, J. Yuan, F. Sun, Z. Wang and Z. Deng, "Modeling and simulation of milling forces in milling plain woven carbon," *The International Journal of Advanced Manufacturing Technology*, vol. 95, pp. 4141-4152, 2018.

[53] M. Sortino, K. E and G. Totis, "Advanced Manufacturing Systems and Technology - AMST'08," in *Vibrations and Chatter in Machining: State of the Art and New Approaches*, Udine, 2008.

[54] C. YUE, H. GAO, X. LIU, S. Y.LIANG and L. WANG, "A review of chatter vibration research in milling," *Chinese Journal of Aeronautics*, vol. 32, pp. 215-242, 2019.

[55] D. Cowan and L. Najafi, "Robotics," in *Handbook of Electronic Assistive Technology*, Academic Press, 2019, pp. 311 - 345.

[56] K. Tai, A.-R. El-Sayed, M. Shahriari, M. Biglarbegian and S. Mahmud, "State of the Art Robotic Grippers and Applications," *Robotics*, vol. 5, 2016.

[57] A. Grau, M. Indri, L. L. Bello and T. Sauter, "Industrial robotics in factory automation: From the early stage to the Internet of Things," in *IECON 2017 - 43rd Annual Conference of the IEEE Industrial Electronics Society*, Beijing, China, 2017.

[58] "What Are The Main Types Of Robots?," RobotWorx, [Online]. Available: https://www.robots.com/faq/what-are-the-main-types-of-robots#:~:text=There%20are%20six%20main%20types,are%20referred%20to%20as%20axes.. [Accessed 15 3 2020].

[59] D. COLLINS, "What is a Cartesian robot?," Linear Motion Tips, 5 9 2018. [Online]. Available: https://www.linearmotiontips.com/what-is-a-cartesian-robot/. [Accessed 15 9 2020].

[60] "SCARA ROBOTS MITSUBISHI MELFA RH-10AH85," Eurobots, [Online]. Available: https://www.eurobots.com.br/Scara-Robots-robots-Mitsubishi-Melfa-RH-10AH85-p68-pt.html. [Accessed 15 9 2020].

[61] X. Lu and M. Liu, "Optimal Design and Tuning of PID-Type Interval Type-2 Fuzzy Logic Controllers for Delta Parallel Robots," *International Journal of Advanced Robotic Systems*, vol. 13, 2016.

[62] YRG Robotics, "Multi-axis Articulated Robot," [Online]. Available: https://www.yrginc.com/products/details/?product=6-axis. [Accessed 02 02 2021].

[63] "6 Axis Industrial Pick and Place Robot for Boxes,Carton," Alibaba, [Online]. Available: https://www.alibaba.com/product-detail/6-Axis-Industrial-Pick-and-Place_60670353776.html. [Accessed 20 4 2020].

[64] M. P. Groover, "Industrial Robotics," in *Automation, Production Systems, and Computer-Integrated Manufacturing (3rd Edition)*, Prentice Hall, 2007, p. Chapter 8.

[65] B. Greenway, "Robot Accuracy," *Industrial Robot: An International Journal*, vol. 27, pp. 257 - 265, 2000.

[66] A. Sirinterlikci, M. Tiryakioğlu, A. Bird, A. Harris and K. Kweder, "Repeatability and Accuracy of an Industrial Robot: Laboratory Experience for a Design of Experiments Course," *Technology Interface Journal*, vol. 9, 2009.

[67] T. M. Anandan, "Why Robots Are Taking It Off," Robotics Industry Association , 11 6 2013. [Online]. Available: https://www.robotics.org/content-detail.cfm/Industrial-Robotics-Industry-Insights/Why-Robots-Are-Taking-It-Off/content_id/4502. [Accessed 20 3 2020].

[68] "What Is A Robot Cell?," Robot Worx, [Online]. Available: https://www.robots.com/faq/what-is-a-robot-cell. [Accessed 13 4 2020].

[69] M. Pollák, M. Telišková, M. Kočiško and P. Baron, "Application of industrial robot in 5-axis milling process," *MATEC Web of Conferences*, vol. 299, 2019.

[70] "Robot machining solutions," CNC Robotics, [Online]. Available: https://www.cncrobotics.co.uk/applications/machining/. [Accessed 25 6 2020].

[71] A. Dinea and G.-C. Vosniakos, "On the development of a robot-operated 3D-printer," *Procedia Manufacturing*, vol. 17, pp. 6-13, 2017.

[72] I. B. Ishak, J. Fisher and P. Larochelle, "ROBOT ARM PLATFORM FOR ADDITIVE MANUFACTURING USING MULTI-PLANE," in *ASME 2016 International Design Engineering Technical Conferences and Computers and Information in Engineering Conference*, Charlotte, North Carolina, 2016.

[73] X. Zhang, M. Li, J. H. Lim, Y. Weng, Y. W. D. Tay, H. Pham and Q.-C. Pham, "Large-scale 3D printing by a team of mobile robots," *Automation in Construction*, vol. 95, pp. 98-106, 2018.

[74] E. Barnett and C. Gosselin, "Large-scale 3D printing with a cable-suspended robot," *Additive Manufacturing* , vol. 7, pp. 27-44, 2015.

[75] W.-c. Lee, C.-c. Wei and S.-C. Chung, "Development of a hybrid rapid prototyping system using low-cost fused deposition modeling and five-axis machining," *Journal of Materials Processing Technology*, vol. 214, pp. 2366-2374, 2014.

[76] S. Keating and N. Oxman, "Compound fabrication: A multi-functional robotic platform for digital design and fabrication," *Robotics and Computer-Integrated Manufacturing*, vol. 29, pp. 439-448, 2013.

[77] "Robotic Tool Changers," ATI Industrial Automation, [Online]. Available: https://www.ati-ia.com/products/toolchanger/robot_tool_changer.aspx. [Accessed 15 2 2020].

[78] M. Babcinschi, *Automatic Tool Changer on Collaborative Robots*, Coimbra, 2018.

[79] "Can-Stack Stepper 15000 15mm," Haydonkerkpittman, [Online]. Available: https://www.haydonkerkpittman.com/products/linear-actuators/can-stack-stepper/15mm-15000. [Accessed 20 9 2020].

[80] "MP6500 Stepper Motor Driver Carrier, Digital Current Control," Polulu Robotics and Electronics, [Online]. Available: https://www.pololu.com/product/2968. [Accessed 20 9 2020].

[81] "ARDUINO UNO REV3," Arduino, [Online]. Available: https://store.arduino.cc/arduino-uno-rev3. [Accessed 20 9 2020].

[82] "7.50mm Pitch Super Sabre Plug Crimp Housing, UL 94V-2, Glow-Wire Capable, 2 Circuits," Molex, [Online]. Available: https://www.molex.com/molex/products/part-detail/crimp_housings/1726733002. [Accessed 25 9 2020].

[83] "7.50mm Pitch Super Sabre Receptacle Crimp Housing, UL 94V-2, Glow-Wire Capable, 2 Circuits," Molex, [Online]. Available: https://www.molex.com/molex/products/part-detail/crimp_housings/1726723002. [Accessed 25 9 2020].

[84] ABB, "IRB 120 CAD Models," [Online]. Available: https://new.abb.com/products/robotics/industrial-robots/irb-120/irb-120-cad. [Accessed 20 5 2020].

[85] Curbell Plastics, *Machining Recommendations for Semi-Finished Engineering Plastics.*

[86] R. G. Pămărac and R. Petruse, "Study Regarding the Optimal Milling Parameters for Finishing 3D Printed Parts from ABS and PLA Materials," *Acta Universitatis Cibiniensis. Technical Series*, vol. 70, pp. 66 - 72, 2018.

[87] Ali Express, "XINHUANGDUO AUTOMATION Store," [Online]. Available: https://pt.aliexpress.com/store/117324?spm=a2g0o.detail.1000002.2.65d8248casIIPV. [Accessed 23 4 2020].

[88] "RobotShop," Cytron, [Online]. Available: https://www.robotshop.com/eu/en/cytron-25a-7-58v-single-brushed-dc-motor-driver.html. [Accessed 16 6 2020].

[89] "RobotShop - Grove Infrared Reflective Sensor v1.2," SeeedStudio, [Online]. Available: https://www.robotshop.com/en/grove-infrared-reflective-sensor-v12.html?gclid=Cj0KCQjws536BRDTARIsANeUZ5_Uy_uKV9mzJejHVPc7-p-fFOSxmy275SoiHoAw_F8nY-WSFmyhMSoaAqQuEALw_wcB. [Accessed 29 9 2020].

[90] Banggood, "7Pcs ER11 Colantes de mola de 1-7mm com ER11A Roda de extensão do suporte do eixo de motor de 5mm," [Online]. Available: https://www.banggood.com/pt/brands-MACHIFIT-b-702.html. [Accessed 20 6 2020].

[91] "AliExpress," OOTDTY, [Online]. Available: https://www.aliexpress.com/i/32958431712.html. [Accessed 2 10 2020].

[92] Dormer Pramet, "Dormer Selector," [Online]. Available: http://selector.dormertools.com/web/prt/pt-pt/mm. [Accessed 20 5 2020].

[93] BOSSARD, "Technical Information - Preload and Tightening torques," [Online]. Available: https://media.bossard.com/-/media/bossard-group/website/documents/technical-resources/en/f_047_en.pdf. [Accessed 5 11 2020].

[94]

[95] MatWeb, MatWeb, [Online]. Available: http://www.matweb.com/search/DataSheet.aspx?MatGUID=3a8afcddac864d4b8f58d40570d2e5aa&ckck=1. [Accessed 10 7 2020].

[96] MatWeb, MatWeb, [Online]. Available: http://www.matweb.com/search/DataSheet.aspx?MatGUID=ab96a4c0655c4018a8785ac4031b9278. [Accessed 10 7 2020].

[97] E. C. Sherbrooke and G. Coleman, "High Performance Multi-axis Milling". United States of America Patent US 10,022,833 B2, 7 11 2013.

[98] Roland, "Modela Pro MDX-650 3D Milling Machine," [Online]. Available: https://www.rolanddga.com/es/soporte/products/milling/modela-pro-mdx-650-3d-milling-machine. [Accessed 5 2 2020].

[99] "Orion 5D milling machine," [Online]. Available: https://ua.all.biz/en/orion-5d-milling-machine-g7303715. [Accessed 2 3 2020].

[100] A. Sharma, P. Zanotti and L. P. Musunur, "Enabling the Electric Future of Mobility: Robotic Automation for Electric Vehicle Battery Assembly," *IEEE Access*, vol. 7, pp. 170961 - 170991, 2019.

[101] "IRB 120," ABB, [Online]. Available: https://new.abb.com/products/robotics/pt/robos-industriais/irb-120. [Accessed 20 9 2020].

8. APPENDIX A

Selected components data sheets